Coordinated Control and Management of Multiple Electric Ships forming Seaport Microgrids

Mutarraf, Muhammad Umair

DOI (link to publication from Publisher):
10.54337/aau494411892

Publication date:
2022

Document Version
Publisher's PDF, also known as Version of record

COORDINATED CONTROL AND MANAGEMENT OF MULTIPLE ELECTRIC SHIPS FORMING SEAPORT MICROGRIDS

BY
MUHAMMAD UMAIR MUTARRAF

DISSERTATION SUBMITTED 2022

AALBORG UNIVERSITY
DENMARK

Coordinated Control and Management of Multiple Electric Ships forming Seaport Microgrids

Ph.D. Dissertation

by

Muhammad Umair Mutarraf

AAU Energy, Aalborg University

E-mail: mmu@energy.aau.dk

Dissertation submitted May 31, 2022

Dissertation submitted: May 31, 2022

PhD supervisor: Josep M. Guerrero, Professor
Aalborg University

PhD Co-supervisors: Juan C. Vasquez, Professor
Aalborg University

Yajuan Guan, Assistant Professor
Aalborg University

PhD committee: Associate Professor Zhenyu Yang (chairman)
Aalborg University, Denmark

Associate Professor Nursyarizal Mohd Nor
Universiti Teknologi PETRONAS, Malaysia

Associate Professor Muzamir Isa
Centre of Excellence for Renewable Energy, Malaysia

PhD Series: Faculty of Engineering and Science, Aalborg University

Department: AAU Energy

ISSN (online): 2446-1636
ISBN (online): 978-87-7573-889-2

Published by:
Aalborg University Press
Kroghstræde 3
DK – 9220 Aalborg Ø
Phone: +45 99407140
aauf@forlag.aau.dk
forlag.aau.dk

Printed in Denmark by Stibo Complete, 2022

Curriculum Vitae

Muhammad Umair Mutarraf received his bachelor of science in electrical engineering from the University of Engineering and Technology, Lahore, Pakistan in 2013, and the Maser of engineering in Control Theory & Control Engineering from Xidian University, China in 2017. He is currently working towards the doctorate degree with thesis entitled "Coordinated Control and Management of Multiple Electric Ships forming Seaport Microgrids" with the AAU Energy Department, Aalborg University, Denmark. His research interests include control of power electronics, coordination control of energy storage systems in AC, DC, and hybrid architecture interfaced seaport and shipboard Microgrids, electric ships and their charging technologies.

Curriculum Vitae

Abstract

Climate change is among the major environmental concerns on the earth these days where greenhouse gases (GHG) emissions are the key cause of this climate change, resulting in environmental and health-related effects. The major sources of these emissions come from heating, fossil fuel for the generation of electricity, and the transportation sector. Among the transportation sector particularly the maritime sector is a significant contributor to such emissions, which are expected to increase further due to an increase in demand for the transportation of goods and people by sea knowing the fact that it is one of the cheapest sources. To mitigate or minimize emissions caused by the maritime sector, conventional fossil fuel-based power generation sources need to be replaced partially or fully with renewable energy sources (RES) along with energy storage systems (ESS) at ports as well as in the shipboard microgrids (SMGs).

Besides environmental issues, the main technical challenge in conventional SMGs are the long-term and short-term power fluctuations caused by the dynamic loads and environmental changes in the sea exacerbate onboard generators wear and tear. Among other challenges, the operational and maintenance cost for such ships is higher. The integration of ESS devices is found out to be an alternative solution but their sole integration with several types of ships is challenging especially longer route ships due to cost, lifecycle, energy, and power density concerns. Therefore, the use of a single ESS device may result in an increase in weight, cost, size, which leads to the hybridization of two or more ESS devices as a single ESS device either can provide high energy or high-power density benefits only. Therefore, the potential ESS device and its hybrid combination need to be analyzed. Further, ESS in the maritime sector is relatively new, hence, different benefits that can be achieved using them on board along with different architectures need to be explored.

The first part of this thesis, therefore, highlights these concerns by reviewing the architecture of different types of SMGs, several types of ESS devices, and optimal selection based on comparative analysis and their benefits that can be achieved in the maritime sector.

In SMGs, synchronous generators onboard operate under varying load profiles due to the environmental changes in the sea resulting in low loading and high loading operation, which results in declining the efficiency of an engine. To tackle this problem, a droop-based adaptive power management system for hybrid SMG is proposed to achieve quasi load-leveling, a trade-off between utilization of battery and operating diesel generators at their optimal point, where during low-loading and high loading conditions, ESS is utilized to absorb and supply power respectively. Further, RES and battery-equipped ships could be used to support seaport, grid, etc., particularly beneficial for smaller islands with limited sources of energy referred to as Ship-to-X or Ship-to-grid (S2G).

The last part addresses the benefit of ESS in SMGs that can be achieved by its use for cold-ironing purposes. One of the major effects of the maritime sector is the emission of ships at ports, as when fossil fuel-powered ships arrive at ports their auxiliary engines are turned on to power the auxiliary loads. One solution to reduce emissions at some major ports is addressed by powering ships through a shore connection, which is connected to the national grid also referred to as cold-ironing. The major obstacle in using such an approach is the lack of availability of cold-ironing facilities at most of the ports. Alternatively, we propose multiple electric ship-based seaport microgrid to provide a mobile cold-ironing facility to power auxiliary loads of fossil fuel-powered ships during their port stays. This sort of strategy will minimize emissions from ports and is particularly useful for ports that are far from the national grid such as remote islands. To share power among various SMGs autonomously, an adaptive multi-mode decentralized control based on V-I and I-V droop control is proposed for proportional power-sharing among different SMGs.

Resumé

Klimaændringer er blandt de største miljøproblemer på jorden i disse dage, hvor drivhusgasemissioner (GHG) er hovedårsagen til denne klimaændring, hvilket resulterer i miljø- og sundhedsrelaterede effekter. De vigtigste kilder til disse emissioner kommer fra opvarmning, fossilt brændstof til produktion af elektricitet og transportsektoren. Blandt transportsektoren forårsager især den maritime sektor til emissioner, som forventes at stige yderligere på grund af en stigning i efterspørgslen efter transport af varer og mennesker ad søvejen, da det er én af de billigste kilder. For at mindske eller minimere emissioner forsaget af den maritime sektor, skal de konventionelle fossile brændstofbaserede elproduktionskilder erstattes helt eller delvist med vedvarende energikilder (RES) sammen med energilagringssystemer (ESS) i havne såvel som i skibe mikrogrids (SMG'er).

Udover miljøproblemer er den største tekniske udfordring i konventionelle SMG'er de langsigtede og kortsigtede effektudsving forårsaget af de dynamiske belastninger og miljøændringer i havet, hvilket forværrer slid på generatorer ombord. Udover dette er operationelle og vedligeholdelsesomkostninger for sådanne skibe store. Integrationen af ESS-enheder har vist sig at være en alternativ løsning, men alene dennes integration med flere typer af skibe udfordrer især skibe pålængere ruter pågrund af de forbundne omkostninger, livscyklus, energi og bekymringer relateret til effekttæthed. Derfor kan brugen af en enkelt ESS-enhed resultere i en stigning i vægt, omkostninger, størrelse, hvilket fører til hybridisering af to eller flere ESS-enheder, da en enkelt ESS-enhed kun kan give høj energi eller høj effekttæthed. Derfor skal den potentielle ESS-enhed og dens hybridkombination analyseres. Yderligere er ESS relativt ny i den maritime sektor, og derfor er der forskellige fordele, der kan opnås ved at bruge dem sammen med forskellige arkitekturer, hvilket skal udforskes.

Den første del af denne afhandling fremhæver derfor disse bekymringer ved at gennemgåarkitekturen af forskellige typer af SMG'er og ESS-enheder, og dernæst udvælge en optimal løsning baseret påen komparativ analyse og fordele, der kan opnås i den maritime sektor.

I SMG'er fungerer synkrone generatorer ombord under varierende belast-

ningsprofiler pågrund af de miljømæssige ændringer i havet, der resulterer i lav belastning og høj belastningsdrift, hvilket resulterer i faldende effektivitet af en motor. For at løse dette problem er et droop-baseret adaptivt strømstyringssystem til hybrid SMG foreslået for at opnånæsten belastningsudjævning, som er en afvejning mellem udnyttelse af batteri og drift af dieselgeneratorers optimale punkt, hvor ESS under lav- og højbelastningsforhold udnyttes ved henholdsvis at optage og levere strøm. Derudover kan RES og batteriudstyrede skibe bruges til at understøtte havne, grid osv., især gavnligt for mindre øer med begrænsede energikilder benævnt Ship-to-X eller Ship-to-grid (S2G).

Den sidste del omhandler fordelen ved ESS i SMG'er, der kan opnås ved dets anvendelse til cold-ironing formål. Én af de store effekter af den maritime sektor er emissionen af skibe i havne, som når fossilt brændstofdrevne skibe ankommer til havne, tændes deres hjælpemotorer for at drive hjælpemotoren belastninger . En løsning til at reducere emissionerne i nogle større havne behandles ved at drive skibe gennem en landforbindelse, som er forbundet til national grid ogsåkaldet cold-ironing. Den største hindring i brugen af sådan en tilgang er manglen påtilgængelighed af cold-ironing faciliteter påhavnene. Alternativt foreslår vi flere elektriske skibsbaserede havne mikrogrid til at give en mobil cold-ironing facilitet til at forsyne hjælpebelastninger til fossilt brændstofdrevne skibe under deres havneophold. Denne form for strategi vil minimere emissioner fra havne og er især nyttig for havne, der ligger langt fra det nationale elnet såsom fjerntliggende øer. For at kunne dele strøm mellem forskellige SMG'er selvstændigt er en adaptiv multi-mode decentral styring baseret på V-I og I-V droop kontrol foreslået til proportional strømdeling mellem forskellige SMG'er.

Publications

Parts of the doctoral study have been published in or submitted to peer-reviewed scientific journals and international conference.

1. **M. U. Mutarraf**, Y. Terriche, K. A. K. Niazi, J. C. Vasquez, and J. M. Guerrero, "Energy storage systems for shipboard microgrids—A review," *Energies*, vol. 11, no. 12, 2018, p.3492.

2. **M. U. Mutarraf**, Y. Terriche, K. A. K. Niazi, F. Khan, J. C. Vasquez, and J. M. Guerrero, "Control of hybrid diesel/PV/battery/ultra-capacitor systems for future shipboard microgrids," *Energies*, vol. 12, no. 18, p. 3460, 2019.

3. **M. U. Mutarraf**, Y. Terriche, M. Nasir, Y. Guan, C. L. Su, J. C. Vasquez, and J. M. Guerrero,"A Decentralized Control Scheme for Adaptive Power-Sharing in Ships based Seaport Microgrid," In *IECON 2020 The 46th Annual Conference of the IEEE Industrial Electronics Society, Singapore*, October, 2020, pp. 3126-3131, IEEE.

4. **M. U. Mutarraf**, Y. Terriche, M. Nasir, Y. Guan, C. L. Su, J. C. Vasquez, and J. M. Guerrero," A Communication-less Multi-mode Control Approach for Adaptive Power-Sharing in Ships-based Seaport Microgrid," *IEEE Transactions on Transportation Electrification*, vol. 7, no. 4, 2021.

5. **M. U. Mutarraf**, Y. Guan, C. L. Su, Y. Terriche, M. Nasir, J. C. Vasquez, and J. M. Guerrero," A Modified Hierarchical Control-based Adaptive Power Management System for Hybrid Shipboard Microgrids," *IEEE Access*, vol. 10, 21397–21411, 2022. IEEE.

6. **M. U. Mutarraf**, Y. Guan, C. L. Su, J. C. Vasquez, and J. M. Guerrero, "Electric Cars, Ships, and their Charging Infrastructure – A Comprehensive Review," *Sustainable Energy Technologies and Assessments*, vol. 52, 102177, 2022, Elsevier.

7. **M. U. Mutarraf**, Y. Terriche, K. A. K. Niazi, C. L. Su, J. C. Vasquez, and J. M. Guerrero, "Battery Energy Storage Systems for Mitigating Fluctuations Caused by Pulse Loads and Propulsion Motors in Shipboard

Microgrids," *2019 IEEE 28th International Symposium on Industrial Electronics (ISIE)*, 1047–1052, 2019, IEEE.

8. **M. U. Mutarraf**, Y. Terriche, M. Nasir, K. A. K. Niazi, J. C. Vasquez, and J. M. Guerrero,"Hybrid energy storage systems for voltage stabilization in shipboard microgrids," *2019 9th International Conference on Power and Energy Systems (ICPES)*, 1–6, 2019, IEEE.

9. Y. Terriche, **M. U. Mutarraf**, S. Golestan, C. L. Su, J. M. Guerrero, J. C. Vasquez, and D. Kerdoun, "A hybrid compensator configuration for VAR control and harmonic suppression in all-electric shipboard power systems," *IEEE Transactions on Power Delivery*, vol. 35, no. 3, pp. 1379–1389, 2019.

10. Y. Terriche, **M. U. Mutarraf**, A. Laib, C. L. Su, J. M. Guerrero, J. C. Vasquez, and S. Golestan, "A Resolution-Enhanced Sliding Matrix Pencil Method for Evaluation of Harmonics Distortion in Shipboard Microgrids," *IEEE Transactions on Transportation Electrification*, vol. 6, no. 3, pp. 1290–1300, 2020.

11. Y. Terriche, C. L. Su, A. Lashab, **M. U. Mutarraf**, M. Mehrzadi, J. M. Guerrero, and J. C. Vasquez, "Effective Controls of Fixed Capacitor-Thyristor Controlled Reactors for Power Quality Improvement in Shipboard Microgrids," *IEEE Transactions on Industry Applications*, vol. 57, no. 3, pp. 2838–2849, 2021.

12. Y. Terriche, C. L. Su, A. Lashab, **M. U. Mutarraf**, M. Mehrzadi, J. M. Guerrero and J. C. Vasquez, "Design of Cost-Effective Compensators to Enhance Voltage Stability and Harmonics Contamination of High-Power More Electric Marine Vessels," *IEEE Transactions on Industry Applications*.

13. M. Sadiq, S. W. Ali, Y. Terriche, **M. U. Mutarraf**, M. A. Hassan, K. Hamid, Z. Ali, J. Y. Sze, C. L. Su, and J. M. Guerrero, "Future Greener Seaports: A Review of New Infrastructure, Challenges, and Energy Efficiency Measures," *IEEE Access*, 2021.

14. S. W. Ali, M. Sadiq, Y. Terriche, S. A. R. Naqvi, **M. U. Mutarraf**, M. A. Hassan, G. Yang, C. L. Su, and J. M. Guerrero, "Offshore Wind Farm-Grid Integration: A Review on Infrastructure, Challenges, and Grid Solutions," *IEEE Access*, 2021.

Contents

List of Figures

Acknowledgments

This Ph.D. project "Coordinated Control and Management of Multiple Electric Ships forming Seaport Microgrids" is carried out at at AAU Energy under the supervision of Prof. Dr. Josep M. Guerrero, Prof. Dr. Juan C. Vasquez, and Assistant Professor Dr. Yajuan Guan. This project was supported by AAU Energy, Aalborg University, Denmark, Otto Mønsted Fond, and Higher Education Commission of Pakistan. I would like to thank all the funding agencies for their financial support and kindness.

I would also like to express my sincere acknowledgement to my supervisor Prof. Josep M. Guerrero for his guidance and support during the Ph.D. studies. Additionally, I would also like to commend my co-supervisors Prof. Juan C. Vasquez, and Assistant Professor Yajuan Guan for their assistance, advice, guidance, and encouragement. I also acknowledge the continuous support from Prof. Chien-lien Su and thankful for inviting me for study abroad at National Kaohsiung University of Science and Technology (NKUST) in Taiwan.

I would also like to appreciate the guidance provided by my colleagues and friends during my stay at Aalborg University. I would like to mention few of them: Dr. Mashood Nasir, Dr. Yacine Terriche, Dr. Kamran Ali Khan Niazi, Dr. Abderezak Lashab, Noor Hussain, Sadiq Baloch, Syed Wajahat Ali, Yaqoob Baloch, Dr. Muzaidi othman, Dr. Fawad Khan, and Dr. Nor Baizura Bintiahmad. I would like to further enlighten and acknowledge efforts and support of my family. Lastly, I would extend my gratitude to all the Centre of Research on Microgrids (CROM) members for their support.

Muhammad Umair Mutarraf
Aalborg University, May 31, 2022

Part I

Extended Summary

Chapter 1

Introduction

This chapter describes the background and the objectives of the Ph.D. thesis. In the end, a contribution list is enlisted, which is accomplished during the three years of research work.

1.1 Background

Worldwide countries are moving from conventional fossil fuel-based generation sources (natural gas, coal, and petroleum) that produce a huge amount of emissions to renewable energy sources (RES) such as wind power, photovoltaic (PV), etc. With an increased RES particularly the integration of a vast amount of wind energy, several coal-fired power plants have already been shut down with a target of closure of rest power plants by 2030 [1]. Where there is a reduction in emissions from the energy sector observed but still there are some challenges in reducing emissions from the transportation sector particularly from the maritime sector. In recent years, growing concerns regarding greenhouse gas (GHG) emission from the transportation sector and depletion of fossil fuels along with their fluctuating prices have gained attention. Hence, electrification of ships particularly commercial ships such as ferries has been a trend in the last decade or so such that to minimize emissions and to enhance overall efficiency [2]. The contribution of GHG emissions from the different transportation sectors in the European Union (EU) is shown in Figure 1.1 illustrating that emissions from the maritime sector contribute to a major extent [3].

The international marine organization (IMO) states in the third IMO study that the global NOx and SOx emissions from the whole shipping exhibit approximately 15% and 13% respectively, which in recent few years have been minimized by the utilization of alternative fuels along with scrubbers in the exhaust gases [4]. The latest study of IMO, i.e., fourth study, states that CO_2

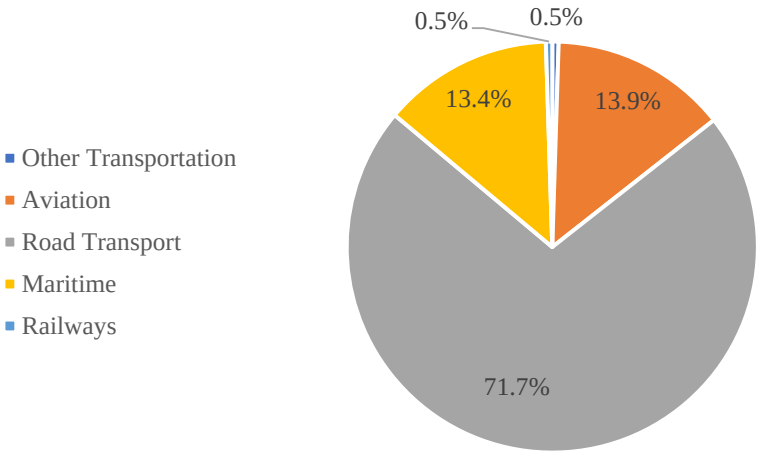

Figure. 1.1. Emissions from different transportation sector in EU [3].

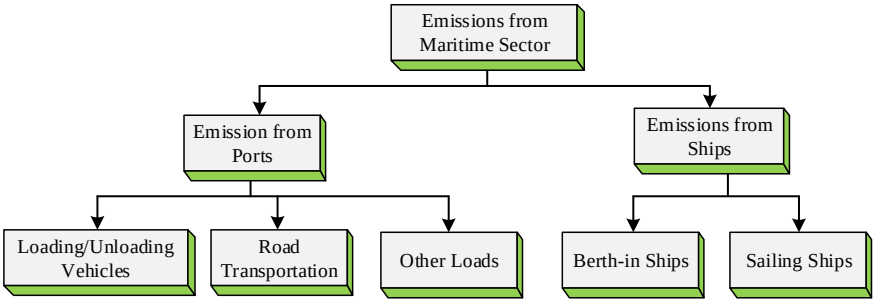

Figure. 1.2. Categorization of maritime emissions.

emission from domestic, fishing and international shipping has increased up to 9.6% comparing to the levels of 2012 [5]. Whereas talking about the share of shipping emissions in overall global emissions, these have increased from 2.76% to 2.89% compared to the levels in 2012. Further, IMO forecasts that these emissions could rise about 90-130% if alternative solutions are not considered [5]. The emissions from the maritime sector can be categorized into two main categories as shown in Figure. 1.2, which are emissions produced by the ships when they are at the port and while they are sailing in the sea/ocean. Another categorization is the equipment placed at the port such as loading/unloading machinery, road transportation, and other critical loads.

1.2 Shipboard Microgrids

Microgrids are defined as locally based energy grids comprising of their own generation, energy storage, and critical loads that can be operated in islanded mode as well as grid-connected mode [6]. Hence, the shipboard microgrids (SMGs) these days somewhat behaves like a conventional microgrid, which operates in an islanded mode while cruising and grid-connected mode while berth-in time. Moreover, the increased use of power electronic converters (AC and DC drives) along with the converters needed to integrate RES and ESS-based sources makes it more like a conventional microgrid. The major distinction between these microgrids is the involvement of dynamic loads (propulsion motors), which accounts for the major part, i.e., more than 70% of the overall loading along with the continuous movement of the ship. The similarities and dissimilarities between these microgrids are illustrated in Table. 1.1 [7].

The sources in SMGs evolved in the last century from steam turbine-based plants to gas-turbine followed by the diesel engine. These traditional ship power systems were segregated in nature such that a separate generation system for both propulsion and service loads. With an increase in load demand, and concerns over reliability, fuel efficiency, emissions, and the development in power electronics (variable speed drives) urged to move towards the all-electric ship (AES) concept. Hence, a breakthrough from mechanical to electric propulsion along with an integrated power system (IPS) concept helped to minimize the number of prime movers on board thus bringing benefits in terms of fuel and space savings. Queen Elizabeth II, an ocean liner exemplifies an AES concept, it was originally a steam-powered vessel, which was later on retrofitted with diesel-electric propulsion bringing savings in terms of fuel cost, i.e., 35% at a speed of 28.5 knots [8].

The surge in the integration of ESS and RES in SMGs bring twofold benefits such as minimization of emission, operational cost and noise pollution from transportation sector as well may help in aiding remote islands. The bi-directional power flow between grid and the SMGs may provide resiliency and stability to such remote islands, which are equipped with RES. The Ærø-island in Denmark exemplifies such a kind that is equipped with onshore wind turbines, biomass, and solar-based resources covering more than 55% islands need along with interconnection with the mainland. Hence, energy sector in the island is responsible for zero emissions. To become self-sustaining in resources for remote islands far from the mainland, stationary battery banks and electric ships could be an alternative solution. The future perspective is illustrated in Fig. 1.3 where power-sharing between ship-to-ship (S-S) and ship-to-grid (S2G) can bring several benefits.

Table 1.1. Comparison between shipboard and terrestrial microgrids.

	Features	Shipboard Microgrid	Terrestrial Mircrogrid
Resemblance		Increased use of RES Bi-directional flow of power Integration of ESS for applications such as peak shaving Finite Inertia Grid-connected and islanded mode of operation AC, DC, and hybrid AC/DC types of architectures	
Dissimilarities	Sources	Internal combustion engine dominated sources and RES (fuel cell and PV)	Conventional hydropower plants and RES (Solar and Wind).
	Loads	Propulsion motors, pulsating loads, and auxiliary loads	Conventional household and commercial loads
	Load profile	Highly varying load profile	Not so much variations
	Energy storage devices	Batteries with the possibility of using high power density devices such as ultra-capacitors and flywheels	Battery packs with already installed flywheel for frequency regulation
	Equipment Footprints	Highly important	Not so crucial
	Environmental effects	Moisture, vibrations, and harsh sea conditions	Relatively lesser impact
	Maneuvering	Steady and in motion	Steady

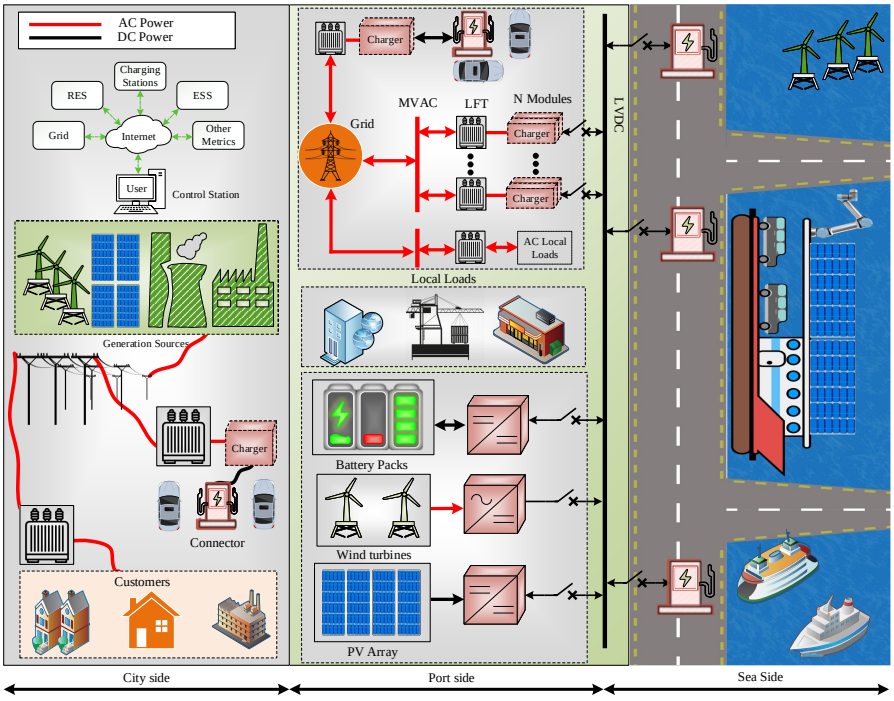

Figure. 1.3. Integration of electric ships in remote islands with grid–A future perspective.

1.3 Challenges in Conventional Shipboard Microgrids

The strict regulations from IMO's International Convention for the Prevention of Pollution from Ships (MARPOL)–Annex VI regarding NOx, SOx, and particulate matters emissions lead the governments and shipowners to move towards exhaust gases after treatment methods, alternative fuels, full battery, or partial battery-based solutions. Further, although AES, IPS concepts along with an onboard DC brings fuel savings and minimizes operational cost, there are still some challenges that need to be addressed, among them few are described below:

- The power fluctuations caused by propulsion motor due to the continuous movement of the ship along with harsh weather conditions need to be catered through innovative ways. During the islanded mode operation of SMG, the conventional fossil fuel-equipped SMGs during their voyage operate under varying load profiles due to the presence of dy-

namic loads such as propulsion motor loads. As a consequence, several generators are turned on and off manually during the whole voyage. These variations are mainly occurred due to the occurrence of environmental changes in the sea/ocean. As a result, onboard generators do not function at their optimal loading condition, which enhances the fuel consumption. To measure fuel efficiency, the specific fuel oil consumption (SFC) curve is utilized to recognize the optimal operating point of diesel generators. During low-loading operations of diesel generators, the fuel economy is poor knowing the fact that total fuel is not used for the combustion process. The leftover fuel dilutes oil resulting in wear to the walls of the cylinder, which leads to leakage from slip joints. Therefore, it is advised by the manufacturers not to operate less than 30% of the rated power [9]. Further, the manufacturers also insist to operate diesel generators above 50% loading [10] or 60 to 100% loading conditions [11]. In order to cope with the aforementioned challenges, the integration of energy storage systems (ESS) and the coordination between different sources can help to mitigate these concerns. The conventional studies rely on coordination control for hybrid sources interfaced with DC distribution systems. For instance, the authors in [11] exploit battery banks, diesel generators, and fuel cells to share the load current while operating diesel engines in a range of 60 to 100% of the rated power. Such a method has the disadvantage of undesirable load sharing with generators during variations in load, which leads to uncertainty problems. The study in [12] tries to resolve this problem by employing master-slave control such that maintaining battery voltage constant through DC/DC converter, thus any fluctuations in the load will instantly be catered to by the ESS. Hence, the operating point of the diesel generators remains constant. The hierarchical control with a hybrid energy storage system (HESS) proposed in [13], where inverse droop is utilized for power-sharing between diesel generators and ESS where higher frequency oscillations are handled by ultra-capacitors and lower frequency oscillations are tackled by the battery banks. The traditional approaches mostly are based on DC-based architecture operating in an islanded mode whereas the coordination between grid and SMG during on port operation is neglected. In addition, none of the aforementioned methods taken into account the operation for the hybrid AC/DC architecture, which is attaining much attention in rendering traditional ships. The only relevant methodology for hybrid SMG is considered in [14] in which fixed-frequency operation is adapted, thus, supplying the fixed amount of power for the optimal operation of diesel generators. Such an approach will lead to continuous charge and discharge of the battery bank, which may result in overcharging or over-discharging. Further, such an approach did not consider the use of

SMG for supporting the grid or exporting power back to the grid. The proposition to the aforementioned problem is addressed in Chapter 3 by proposing an adaptive power management system (PMS) for an islanded operation of a hybrid SMG and a hierarchical control scheme for importing and exporting power to and from the grid.

- Another challenge is the inclusion of pulsating loads such as high-power radar systems and rail guns in future warships, which draw high power leads the ship's power system to instability. Normally, the gas-turbine generators have a ramp rate falling between 35 to 50 MW/min whereas the pulsating loads require 100MW/s [15]. Therefore, one solution is to interface ESS devices with complementary features of high energy and high power density such as battery energy storage and ultra-capacitor energy storage respectively. The coordination control scheme to mitigate sudden load changes and pulsed loads is presented in Chapter 3.

- The lack of availability of shore power facilities at most of the seaports is among main challenge these days. When the fossil fuel-based ships berth at the ports, the auxiliary engines are kept online to power their auxiliary loads, which include cooling, heating, lighting, refrigeration, and emergency equipment. In order to cope with this challenge, providing power to ships during their berth-in time from the national grid is being used at some larger ports, which is also referred to as cold-ironing [16]. Although, such an approach minimizes emission and noise pollution from the ports but upsurges demand of power on the national grid. Additionally, providing power to such ports that are considerably far from the grid may require enormous investments, which include infrastructural costs such as substations, transmission lines, transformers, and so on, and therefore, not seemed like a viable solution for remote ports. The majority of the existing literature has focused on either seaport microgrids [17] or SMGs [18], [19] where a coordination control scheme between SMG and grid is considered in [20], which highlights the ship-to-grid (S2G) concept for electrifying a remote island. However, none of the existing works considered the operation of SMG for mobile cold-ironing facilities. Alternatively, the solution of the aforementioned problem for the seaports that are considerably far from the grid is proposed in Chapter 4 where an SMG equipped with ESS and RES having the capability to share power among nearby ships during their berth-in time by providing mobile cold-ironing facilities. A local grid is formulated using multiple ships thus allowing power-sharing using decentralized multi-mode adaptive droop control scheme. The multi-mode scheme operates on the basis of V-I and I-V droop methods for proportional power-sharing among different SMGs.

1.4 Research Questions

1. What are the main differences between SMGs and terrestrial microgrids and what are the benefits that can be achieved by the integration of ESS in SMG applications?
2. How to attain coordinated control between battery banks and diesel generators onboard in a hybrid AC-DC architecture during its islanded and grid-connected operation–S2G and Grid-to-Ship (G2S)?
3. How to tackle with sudden load changes and pulsed load demands during SMG voyage mode using hybrid energy storage systems?
4. How to provide cold-ironing facilities to SMGs during on-port operation for smaller seaports that are far from the grid and what is the suitable architecture?
5. How to autonomously share power among different SMGs interfaced to each other via islanded DC microgrid formed using multiple SMGs.

1.5 Thesis Objective

As mentioned above the challenges in conventional SMGs during their voyage and on port operation desires to be addressed to achieve better performance in terms of fuel efficiency and reliability along with limitations by following the guidelines set by the maritime authorities. The specific objectives of this project are:

1. To study about shipboard microgrids, their evolution, suitable energy storage devices, and benefits that ESS brings to ships along with their charging infrastructure.
2. Development of an adaptive PMS for hybrid shipboard microgrids for power-sharing among diesel generators and battery banks to achieve quasi-load leveling.
3. To develop a hierarchical control scheme to transmit or export power from SMG to grid or seaport loads referred to as Ship-to-X operation.
4. To develop a coordinated control scheme for HESS interfaced to a SMG in order to deal with pulsed load demands.
5. To develop RES and ESS-equipped multi-ships interfaced seaport microgrid to deal with cold-ironing issues at ports that are far from the grid and electrifying such ports from the national grid does not seem like a viable solution.

6. To develop an autonomous decentralized control scheme to share power among different SMGs interfaced with each other during their port stays and to validate it experimentally.

1.6 Thesis Organization

The outcome of this Ph.D. study is written in the thesis as a collection of journal and conference papers where three journal papers and a conference paper are already published and two journal papers are under review.

Chapter 1: Presents an introduction regarding emission problems and how SMGs can be a viable solution for cutting down emissions from the transportation sector. This chapter also presents the challenges, objectives, and the organization of this thesis.

Chapter 2: Presents state-of-the-art on SMGs, classify different architectures on the basis of distribution, network configuration, and propulsion types. This chapter also highlights energy storage devices that are suitable for SMG application and benefits that can be achieved by the integration of ESS for SMG application. Further, the classification of SMGs on the basis of energy storage device are also part of this chapter. To charge such ESS equipped ships, the categorization is presented along with possible ways to charge higher capacity battery banks. This chapter also exhibit state-of-the-art on cold-ironing and existing approaches utilized for providing cold-ironing such as using seaport microgrids and so on.

Chapter 3: Demonstrate an adaptive PMS for autonomous power-sharing among diesel generators and battery banks. For the implementation, a multi-mode control scheme considering islanded and grid interfaced operation is presented. Moreover, coordination control scheme employing low pass filter (LPF) to split low and high frequency components is part of this chapter.

Chapter 4: Presents a novel solution to provide a cold ironing facility using multiple ships forming seaport microgrid. A multi-mode decentralized control scheme is presented for autonomous power-sharing among different SMGs. The verification of the proposed scheme is validated in MATLAB/Simulink and experimentally using hardware-in-the-loop.

Chapter 5: The contribution of this Ph.D. study is summarized along with the future work.

Chapter 2

Shipboard and Seaport Microgrids–State of the Art and Ambitions

This chapter summarizes the evolvement of conventional SMGs and provides classification. The progress beyond the state-of-the-art and ambitions for the work carried out under this work are briefly summarized. A further detailed explanation can be found at the papers section in Paper I.

2.1 Classification based on Distribution

Like a conventional microgrid, SMGs can be categorized into AC, DC, and hybrid AC/DC architectures. The benefits and drawbacks of these types of architectures are discussed below:

2.1.1 AC-based Shipboard Microgrids

The traditional ships are dominated by fossil fuel-equipped generators and are interfaced with AC-based distribution architecture operating at a fixed frequency either 50 Hz or 60 Hz with an exception where 400 Hz frequency is utilized for some military ships equipment [21]. The typical architecture of the AC shipboard power system is illustrated in Fig. 2.1 where several generators are interfaced with two buses referred to as a starboard side and port side buses interlinked together using a bus tie switch. The typical low voltage (LV) levels are less than 1000 V (380, 400, 440, 690 V, etc.) and high voltage (HV) side levels used onboard are 3.3, 6.6, 10, 11, and 13.8 kV, fed to propulsion motor and auxiliary loads using step-down transformers [22]. Among

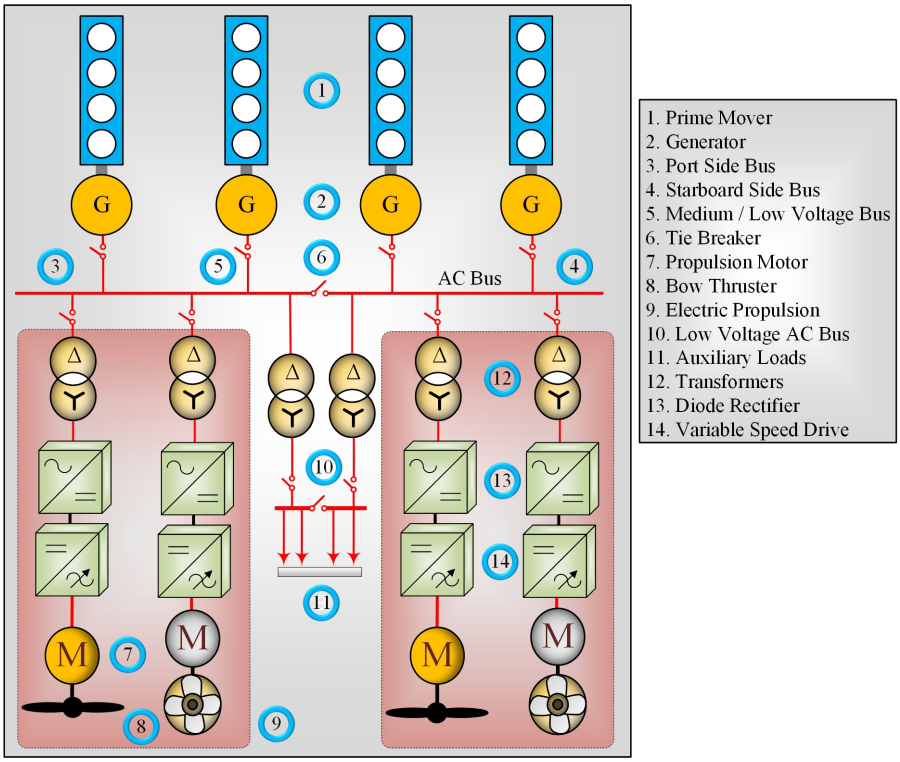

Figure. 2.1. Typical AC gird-based SMG.

the main challenges for the AC-based distribution is that generators on board are forced to operate at a fixed speed, as a result, any further enhancement in the fuel efficiency is limited. Further, the increased use of diode-based rectification in variable speed drives (VSD) results in power quality issues such as harmonic distortions, unbalanced currents, and flow of reactive power. To cope up with this challenge, passive filters are being integrated conventionally with the possibility of the use of active filters, ultimately increasing the cost and space onboard [23].

2.1.2 DC-based Shipboard Microgrids

The DC-based grids are attaining popularity again in the terrestrial microgrids as well as in SMGs bearing in mind that most of the RES and energy storage devices are inherently DC-driven. This leads to lesser conversion stages and ultimately increases overall efficiency [24], [25]. On the other hand, in terms of controllability, both frequency, and voltage need to be tracked in an AC while only voltages in DC. Further, major sources are still generators,

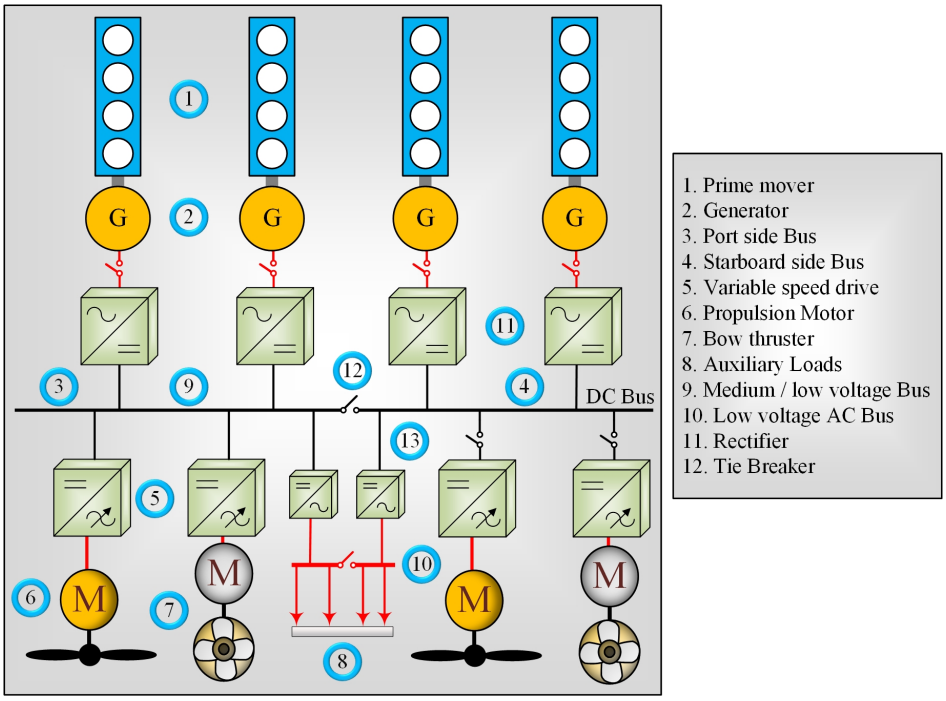

Figure. 2.2. Typical DC gird-based SMG.

hence, for synchronization in AC, frequency, voltage, phase angle need to be matched while only voltage in terms of DC provides an ease in the parallel connection among several sources. The rectification stage in VSDs is also eradicated knowing the fact that a major part of the load is propulsion motor, hence, resulting in minimization of losses involved in conversion along with the elimination of harmonics issues interlinked with it. The typical architecture of a DC-based SMG is illustrated in Fig. 2.2. Moreover, the fixed speed operation of generators linked to frequency restrictions in AC is not a problem in DC, and hence, generators can be operated in a varying frequency range, thus operating diesel generators close to their optimal point bringing benefits in terms of emissions and fuel consumption. Among onboard DC-grid configurations, multi-drive and fully distributed approaches are being adopted by ABB, in the former approach all converting modules are placed at a single place occupying the space of the AC switchboard. The latter approach distributes all converters closer to their respective loads and sources, hence, each load is fed by a separate inverter [26]. In both approaches, line frequency bulky transformers and AC switchboard are removed and the auxiliary and critical loads are fed by separate inverters.

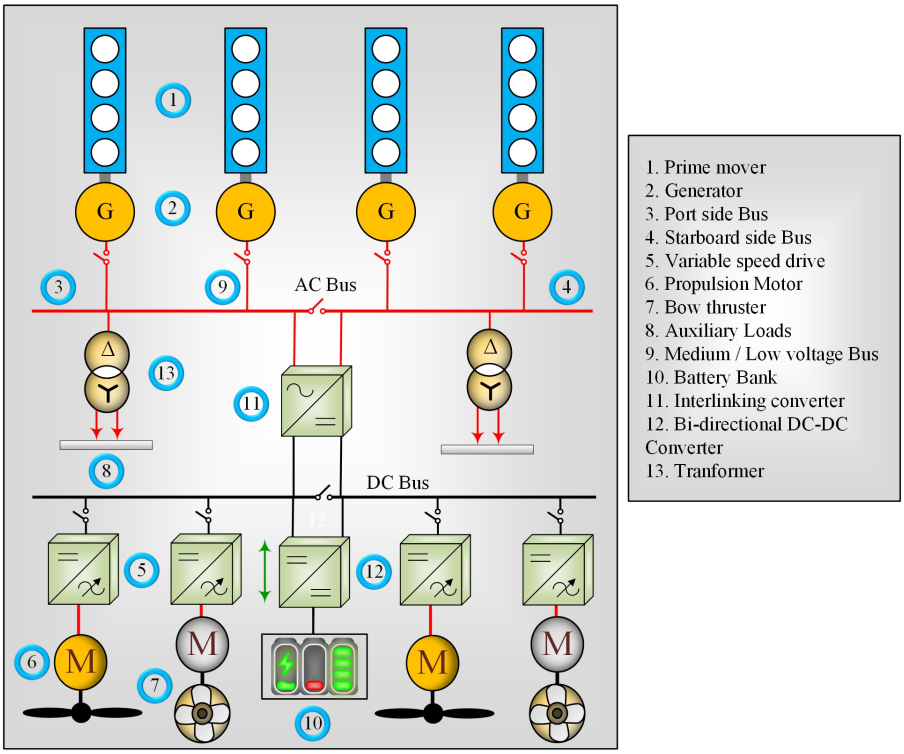

Figure. 2.3. Hybrid AC/DC grid-based SMG.

2.1.3 Hybrid AC/DC-based Shipbaord Microgrids

Even though DC has clear benefits but most conventional ships are AC interfaced, and hence retrofitting them completely to DC requires a vast investment cost, which is quite challenging for a shipowner. Hence, hybrid AC/DC-based SMGs could be one of the possible solutions, a trade-off between investment and operational cost. AC-based sources (generators) and loads (auxiliary loads) are interfaced with the AC bus whereas DC-based sources (energy storage) and loads (propulsion motor) are connected with the DC bus, and for coordination between both buses interlinking converter is integrated as shown in Fig. 2.3 [27].

2.2 Classification based on Network Configuration

In terms of network configuration, SMGs are classified into radial, zonal, and ring-based configurations whereas mostly traditional SMGs follow radial configuration.

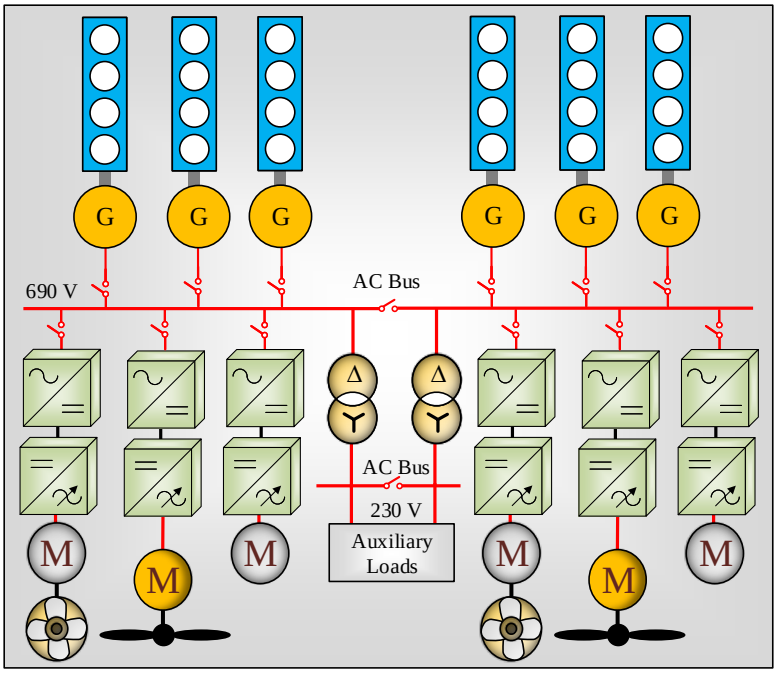

Figure. 2.4. Typical radial network configuration in conventional AC ships.

2.2.1 Radial Network Configuration

The most common network configuration in ships is based on a radial network with the uni-directional power flow as shown in Fig. 2.4. The onboard generators are fed by diesel engines, which are separated into port and starboard side main buses using bus tie switches. The major loads such as propulsion motor, pump motors, and bow thruster are fed from the main buses using variable frequency converting units. The auxiliary loads are then fed using a sub-bus supplied from the main bus using step-down transformers. Similar to AC configuration, ABB multi-drive onboard DC configuration [28] exemplifies a typical radial DC configuration as shown in Fig. 2.5 where each onboard generator is rectified and is interfaced to the DC bus. Therefore, the rectification stage in propulsion load is eradicated, while ultimately aiding to minimize space onboard. The auxiliary or AC consumers are fed by separate inverters to provide power to sensitive loads. These typical radial configurations have the drawback of single-point failure at the load or the source side, which may lead to loss of several crucial loads, particularly propulsion motor. Hence, affecting the reliability and survivability of the SMG thus may result in loss of power and ultimately may cause accidents.

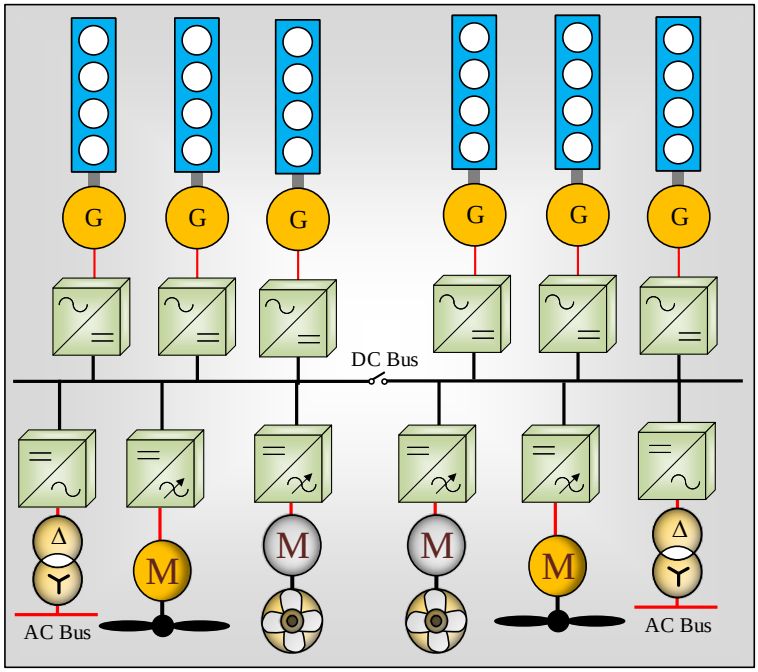

Figure. 2.5. Typical radial network configuration in conventional DC ships.

2.2.2 Zonal Network Configuration

Though the radial architecture has been widely adopted in several ships, there is an utmost need for a system that can provide better efficiency, higher reliability, and survivability. AC and DC-based zonal electric distribution (ZED) has emerged as a possible solution to attain the aforementioned benefits [29]. Typically, in a zonal system, critical loads are fed by alternative generation sources via switching devices fed from two buses where these buses are interconnected at the bow and the stern as shown in Fig. 2.6. The distribution system is separated into several zones with independent sources of generation so that any fault does not propagate to other zones. Moreover, the fault at one of the buses leads to the shift of loads to the second bus, thus continuity of supply. The long feeder cables used in radial systems are replaced with shorter feeders in ZED that helps to minimize the weight and cost [21]. For the last many years, AC and DC-based radial network configuration with main and sub-buses with either generator as the main source, ESS (battery) or RES (fuel cell) are being used in most ships. The advancement of power electronics and the problems radial network has urged the need for AC or DC-based ZED adopted in some navy ships such as DDG 1000 [30]. Among AC and DC-based ZED, DC-based ZED is preferred as most ESS

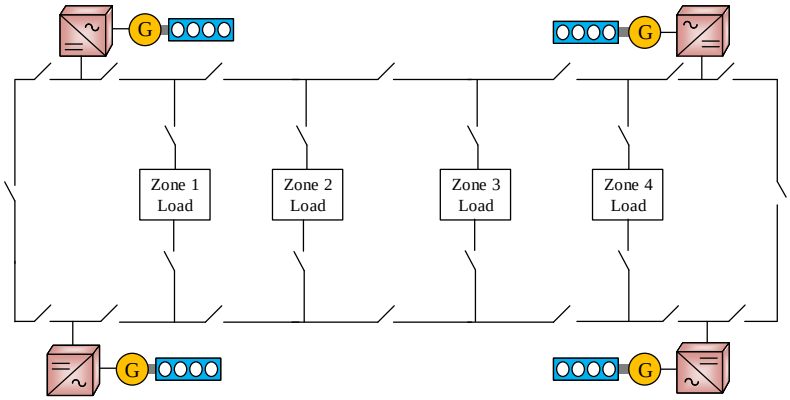

Figure. 2.6. Typical zonal network configuration in conventional DC ships.

and RES output is a DC system, hence, it helps to minimize the conversion stages and ultimately increases the efficiency of the overall system. Further, a zonal system with IPS brings a reduction in the number of prime movers, shortens the length of onboard cables, and supporting high power pulsating loads are further benefits of such an architecture [31]. Although zonal architecture provides resilience and redundancy, complex control, protection, and coordination are the key challenges.

2.3 Classification based on Propulsion system

The traditional ships were based on a segregated distribution system where there are separate generating units for propulsion motors and auxiliary loads and are mainly based on mechanical propulsion as shown in Fig. 2.7(a). Such type of propulsion has lesser components such as prime mover, gearbox, and propeller resulting in minimal conversion stages and ultimately lesser conversion losses suitable for nearly constant speed application such as cargo ships [32]. It is considered as highly efficient upon its operation between 80 to 100% of the designed speed [33]. Hence, low speeding or low-loading operation of a ship decreases the overall efficiency, increases fuel consumption, and emissions [18]. To achieve faster response, minimize weight and space of mechanical equipment between diesel engine and propeller, ease in maneuverability, minimal noise, and automation are the fringe benefits to move from mechanical propulsion interfaced ships to electric-driven propulsion system where propulsion and auxiliary loads are fed by separate generators [8]. However, these segregated conventional mechanical and electrical

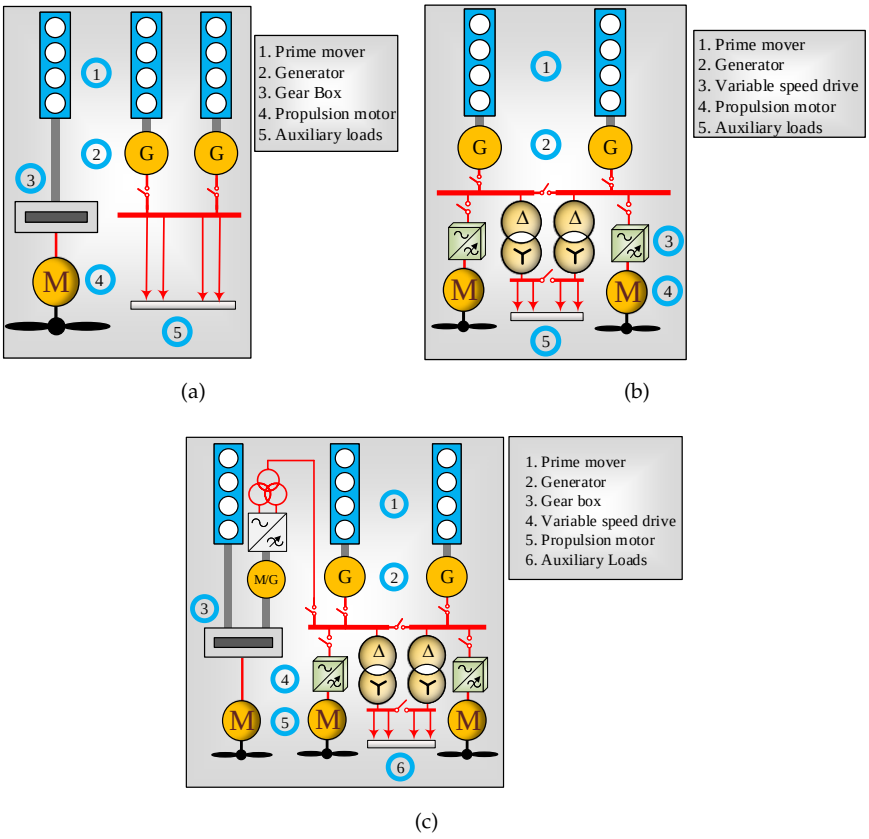

Figure. 2.7. Different types of propulsion, (a) Mechanical, (b) Electrical, (c) Hybrid.

propulsion have a drawback that any failure in the components of the drive train results in the loss of propulsion, which is quite dangerous for a ship during its voyage. In addition, the use of sole power systems for propulsion brings a disadvantage that power from each generator can not be used for other loads [34].

The developments of power electronic drives in the late last century gave birth to an IPS as shown in Fig. 2.7(b), which delivers electrical power to both propulsion and auxiliary loads. IPS along with electric propulsion brings benefits in terms of lower operational cost (lower maintenance and fuel consumption), hence, increasing the efficiency along with a lesser number of prime movers needs to be kept online. Where there are benefits of adopting an electrical propulsion system, the complete retrofitting of conventional mechanical ships might not be a cost-effective approach. Hence,

Table 2.1. Energy and power density of different energy storage devices [38–40]

Devices	**Power Density (W/kg)**	**Energy Density (Wh/kg)**	**Response Time**	**Life cycle**
Lead Acid (PbA)	180-200	30-50	ms	<1000
Nickel Cadmium (NiCd)	150-300	50-75	ms	<1500
Sodium Sulphur (NaS)	150-240	150-240	ms	1000-3000
Lithium-ion (Li-ion)	150-315	100-250	ms	>4500
Flywheel	400-1500	Up to 100	ms-mins	10,000 - 100,000
Ultra-capacitors	Up to 10000	2.5-15	ms-mins	100,000 +
Fuel Cell	500+	800-10000	mins	20000+

hybrid propulsion showed in Fig. 2.7(c) adopting both mechanical and electrical propulsion functionalities is proposed for navy applications (DDG-51), relatively suitable for low-speed shipping [35], where during low speeding operating conditions electrical propulsion is utilized. Besides this, abundant power generated by the main engine can be supplied by operating the motor/generator in the generation mode to the grid [36]. In addition, ships such as tugs, fishing vessels, and RoPax that have a flexible operation and varying power demand also get benefits in terms of fuel efficiency, silent operation, and reliability [37].

Although the evolvement of the SMG from mechanical to electrical propulsion and from the segregated distribution system to IPS and then to zonal brings improvement in terms of reliability, survivability, fuel savings, and improved efficiency. Yet operating diesel generators at their most optimal point, minimal noise and smooth operation needs to be catered along with managing highly dynamic loads such as propulsion motors and pulsating loads, integrating ESS devices could be one of the feasible solutions to do so.

2.4 Energy Storage Technologies

An energy storage system mainly consists of an energy storage device and a converting unit for its connection to either an AC or DC-based system [39]. They are mainly stored in the form of electrical (superconducting magnetic energy storage (SMES), Ultra-capacitor), chemical (fuel-cell), electro-chemical

(batteries), and mechanical ways (flywheel, pumped-hydro). These devices vary from each other in the form of charge/discharge rates, life cycle, efficiency, energy, and power density as illustrated in Table 2.1. Among batteries, three kinds of battery chemistry are frequently used in the literature for several applications, which are Nickel-based, Lead-acid, and Lithium-based [41]. The former two have nominal voltage less than or close to 2V and lower energy density in comparison with lithium chemistry with a typical nominal voltage level above 3V. Lead-acid (PbA) and Nickel Cadmium (NiCd) are used in several ships for UPS purposes to supply critical loads onboard with typical voltage level (12 or 24V) [42]. Among different secondary batteries, batteries that are frequently being used for electric cars and ships for propulsion purposes are Lithium-iron-phosphate ($LiFePO_4$) and Lithium nickel manganese cobalt oxide (NMC). The latter chemistry is being used in the transportation sector comparatively more in comparison to the former one due to its higher energy density [43, 44]. Among other lithium chemistry's, Lithium titanate oxide (LTO) provides faster charge capability with a relatively higher number of cycles (up to 20000), however, it has lower energy density comparable to other competitors (60-110 Wh/kg) [45]. Although batteries can provide higher energy density, the lack of their ability to deal with high power fluctuations caused by the pulsating loads leads to a need for a high power density device such as ultra-capacitor and flywheel. Ultra-capacitor has lower power and energy density in comparison with the flywheel by weight whereas in terms of volume it has lesser power density but higher energy density than the flywheel [46]. In terms of the life-span flywheel has a superior characteristic in comparison with its competitor ultra-capacitor. At the current moment, there is not a single device that has both the features of higher energy and higher power density that leads to the hybridization of two or more devices. Among these, battery-ultra-capacitor [47–49] and battery-flywheel [50–52] are among the most utilized hybridization combination with complementary characteristics used in the literature [39]. The comparison between different energy storage devices is enlisted in Table 2.2.

Among various energy storage devices available in the market, only batteries, fuel-cell, flywheel, and ultra-capacitors are among the devices which have the potential to be used in the SMG application. Large units of flywheel have already been implemented in terrestrial power systems by Beacon Power such as 20 MW (200 flywheels) for frequency regulation by responding operator within 2s in the Hazle, USA [53] and the largest 400 MW Joint European Torus with the capability to supply 400 MW for the 30s. In transportation applications (railways), ABB has installed 40 MJ of ultra-capacitors to store energy from decelerating of metro cars in Warsaw, Poland aiding to minimize operational cost and increasing energy efficiency [54]. In addition, flywheel ESS was integrated into Los Angeles Metro in order to save energy, and sev-

Table 2.2. Advantages and Disadvantages of different ESS devices [39], [45]

Battery type	**Advantages**	**Disadvantages**
PbA	Inexpensive ´	Low energy density
	World wide adopted	Short life cycle
	Easily recyclable	Lower nominal voltage (2.1 V)
NiCd	Lower cost	Lower nominal voltage (1.2V)
	Higher energy density than PbA	Cadmium toxicity
	Higher peak discharging rate (up to 20C)	
Li-ion	Higher nominal voltage (2.6-3.85)	Higher cost
	Higher cycle count	Life cycle affected by deep discharge
	Low maintenance	Overcharge protection requirement
Fuel cell	Higher efficiency even at low-loading	Lack of availability of refueling infrastructure
	Higher reliability	Hydrogen storing
	Minimal noise	Lower energy density than HFO
Flywheel	Faster response time	Higher cost
	Higher cycle count	Safety issue upon failure of rotor
	Higher power density	Low-energy density
	Higher efficiency (above 90 %)	Heat and noise concerns
Ultra-capacitor	Higher charge and discharge rate	Low cell voltage (2.3-2.75V)
	Higher cycle life	Higher self discharge
	Higher energy efficiency	Low energy density
	Higher efficiency (above 90 %)	

eral examples for ultra-capacitors installation are found for voltage regulation and energy savings [46]. On the other hand, the commercial integration of high power density devices (ultra-capacitor) in marine application is barely reported. The only claim reported for a commercial ferry with an installation of 128 ultra-capacitors by a company "Nidec" [55].

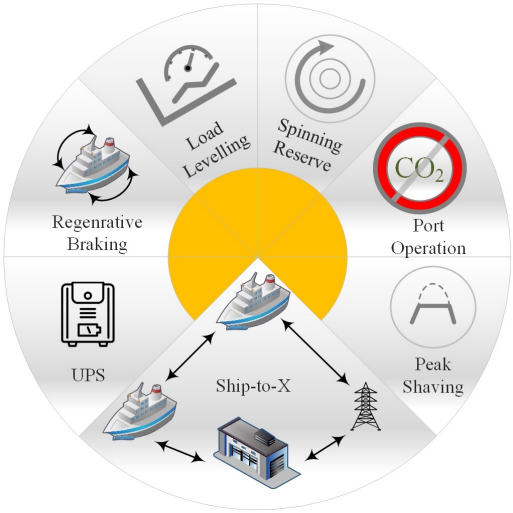

Figure. 2.8. Benefits energy storage systems brings to shipboard microgrids [7].

2.4.1 Benefits/Advantages Energy Storage Systems brings to Shipboard Microgrid

The integration of ESS (especially batteries) to ships is not new as it is being widely used in the past for emergency purposes to supply crucial loads. In fact, the first PbA interfaced boat (Eureka) exist from the late 19th century built by a French Gustave Trouve with quite a limited range due to the lower energy density characteristics of PbA [56]. With the advancement in the last couple of decades in battery chemistries particularly lithium that after successful utilization in land-based transportation, it is being integrated these days with SMGs. Lithium with chemistries that are frequently installed are $LiFePO_4$ and NMC due to their higher energy density, lower self-discharge, higher efficiency, minimal maintenance, and higher nominal voltage. Among the benefits that can be achieved using battery banks onboard are enlisted below:

1. The first benefit that can be achieved by the integration of the battery is its use for the emergency purposes such as during blackout situations for feeding emergency lightening, navigational devices, and other critical devices onboard, the capacity of such batteries is quite low, and are of low-voltage category [47].

2. The regenerative braking phenomenon is frequently being applied in modern electric cars, in which instead of wasting energy during braking, energy is sent back to recharge batteries. Although it is beneficial in

cars as brakes are applied frequently whereas in ships brakes are not so frequently applied and hence are not that suitable. It may bring some benefit to short route ships like ones those sailing on river crossings.

3. The third benefit is its use for load-leveling purposes, which during low-speeding operation of a ship stores power whereas during high speed or high loading conditions it injects or supplies back the power, which helps to improve the fuel consumption of the onboard ship.

4. The spinning reserve is another benefit where the emergency generator is replaced by the battery banks such that during an outage of the main source of generation or at the distribution side, ESS takes over the load within milliseconds to supply the load until the main generation source is brought online.

5. Further, auxiliary loads of fossil fuel-based or electric ship during their port staying time needs to be fed either through a shore connection or using onboard auxiliary generators. Due to the lack of shore connection facilities at most of the ports, ESS onboard could be used for feeding auxiliary loads whereas for ferries the port stays varies from a few minutes to several minutes (5 to 30 mins).

6. Peak shaving, which is somewhat similar to load-leveling but the purpose of it is to reduce the peaks rather than improving fuel consumption, which is mainly caused by the pulsating loads onboard where high power density devices such as ultra-capacitors and flywheels could be useful.

7. It enhances the stability of hybrid sources-based SMG that occurs due to the slow response of onboard engines to varying load demands.

8. Lastly, knowing the fact that most of the modern ships (especially ferries) are equipped with a battery bank with a capacity in a span of several kilowatt hour to a few megawatt hour range and RES, hence, they can support peer ships by either providing power to their auxiliary load, charging their battery banks upon deep discharge situations or even feeding back power to the grid upon need, particularly useful for RES equipped remote islands by bringing resiliency to the grid, can be referred as Ship-to-X operation.

2.4.2 Types of Battery-equipped Shipboard Microgrids

The ESS particularly lithium-ion batteries have developed to that extent in the last decade along with extensive curtailment in its prices that it is now

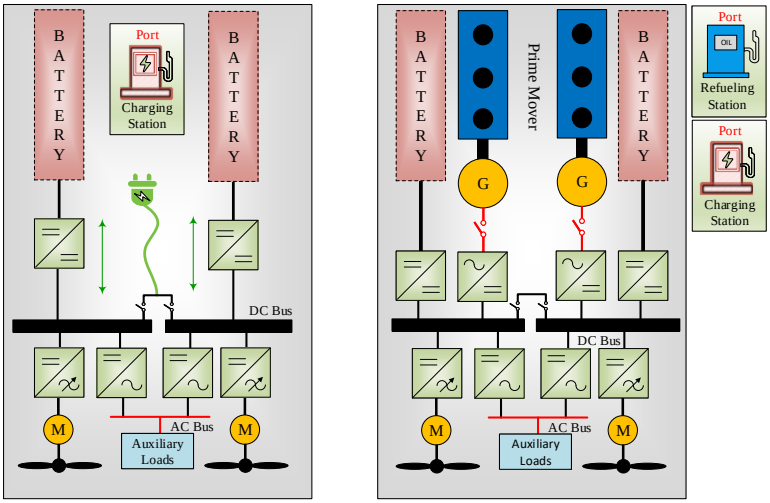

Figure. 2.9. Different types of battery equipped ships, (a) BES, (b) HES & PHES.

being integrated into ships. In addition, the strict regulations from IMO and emissions from conventional shipping have led the shipping industry to move towards minimal local emission solutions. To address these concerns, integrating batteries partially or entirely based solutions have been implemented where Ampere ferry that sails in the seas of Norway was the first to utilize 100% battery banks [57]. Hence, similar to electric cars, electric ships can be classified as battery-electric ships (BESs), hybrid-electric ships (HESs), and plug-in hybrid electric ships (PHESs). The characteristics of these types of SMGs are summarized in Table 2.3. Several strings of batteries are connected using converting units to either AC or DC bus where each string is interfaced with several modules connected in series and parallel fashion to form the required voltage and power level. In addition, failure in one of the strings does not impact the overall system. Further, at least two battery systems placed at two different places are recommended in accordance with the guidelines set by Det Norske Veritas (DNV), one at the port side and the other at the starboard side [58]. The use of BES shown in Fig. 2.9(a) brings several advantages over conventional ICE-based ships, for instance, it is cheaper to run these ships as the cost of diesel fluctuates and the threat involved in prices uncertainty will also be diminished. The minimal use of mechanical parts by the replacement with electric motors will minimize the maintenance

cost. Moreover, smooth operation and higher efficiency are some other advantages compared to ICE-based SMGs. However, despite having several benefits of using BES, the charging of several kWh to MWh capacity battery banks is time-consuming comparable to refueling gasoline. In addition, several BES charging at the same moment may have a negative impact on the existing grid. Apart from these concerns, convincing ship companies/owners to move towards BES to a larger extent in the market with the high capital cost is quite challenging. The limited number or lack of charging infrastructure at seaports is among the main obstacles in the vast implementation of BES. Moreover, the sole use of battery banks as a source is limited for short-route ships only. Due to this, they are being used especially in short route ferries only such as Ampere and Ellen ferries where the capacity of ESS varies from several kW to a few MW range. On the other hand, HES and PHES shown in Fig. 2.9(b) are among the other types where the former is charged only using ICE-based engines placed onboard whereas the latter one can be charged using onboard generators as well as charging infrastructure installed onshore, where another major difference is the installed capacity of battery banks. Happiness Ferry is an example of the latter type, which can charge using shore connection at the port as well as during the ship's islanded operation using onboard generators [59]. Such hybrid sources-based SMGs overcome the short-range drawback of BES and help in range extension. In addition to it, better fuel economy and higher efficiency are some of the benefits that hybrid ships provide. However, complex control, cost, and management of multiple sources are some of the major concerns for such kinds of ships. In terms of ESS coupling with AC or DC bus, DC coupling is preferred over AC due to lesser conversion stages as inherently batteries are DC driven.

The HES and PHES can be further categorized based on either integration of battery with electrical or hybrid propulsion types. In the former case, multiple sources, i.e., battery banks and ICE-based sources mechanically interfaced with a generator. These sources are then coupled with power electronic units to drive electric motors using either or both sources. Hence, there is no mechanical coupling between engine and propulsion motor ultimately enhances flexibility, minimizes complexity and weight onboard. Moreover, battery banks can be charged using onboard generators. Another configuration where battery banks are interfaced to power electronic unit while powering electric motor whereas there is a mechanical coupling between ICE-based engine and the propulsion motor termed as hybrid propulsion. Such a configuration reduces weight by minimizing the use of the generator but ultimately brings complexity. The operation principle for such a configuration is based on utilizing battery-electric propulsion at lower speed operation while operating only ICE-based mechanical propulsion at higher speed.

Table 2.3. Characteristics of types of electric ships.

Features	**Hybrid electric ships and Plug-in hybrid electric ships**	**Battery equipped ships**
Source of Energy	Battery banks	Battery banks
	MGO/MDO/LNG	Photovoltaic
	Flywheel and Ultra-capacitor (Possibility of its use in future)	Flywheel and Ultra-capacitor (Possibility of its use in future)
Propulsion System	Electric propulsion	Electric propulsion
	Hybrid propulsion	
Onshore source	Gasoline refuelling station	Charging station
	Charging station	
Major concerns	Sizing of battery	Requirement of huge battery banks (MWh range)
	Thermal management	Lack of availability of fast-charging infrastructure on-shore
	Energy and power management	Charge and discharge C-rate
	Increased number of compo-nents	Short stays at ports
	Maintenance of ICE	Oversizing to meet emergency demands.
		Short range
Battery Capacity	Happiness Ferry (105 kWh)	Ellen (4300 kWh)
	Silent 80 (207-429 kWh)	Future of the Fjords (1800 kWh)
	MS Color Hybrid (5000 kWh)	MV Ampere (1000 kWh)

Note: MGO=Marine gas oil ; MDO= Marine diesel oil; LNG= Liquefied natural gas

2.4.3 Categorization of Charger

Battery-equipped ships can be charged either through ICE-based sources or RES (fuel cell, PV) integrated onboard or through charging infrastructure placed onshore. The charging can be performed either through an onboard or offboard type where the onboard type of a category is generally considered as slow charging due to weight, space, and cost limitations. The offboard classification can either be grid-connected or a mobile charger (interfaced with stationary battery packs and RES) as shown in Fig. 2.10. These classifications can either be AC or DC-based categorized into different levels such as slow

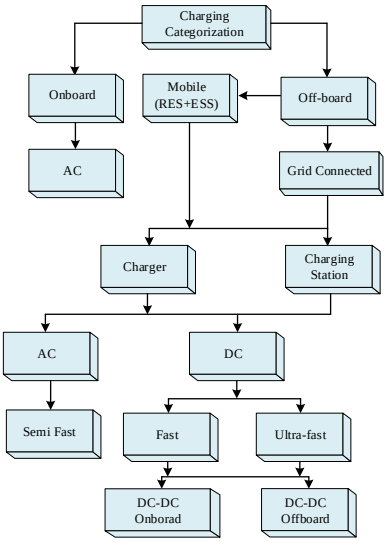

Figure. 2.10. Categorization of charger/charging stations for ships [60].

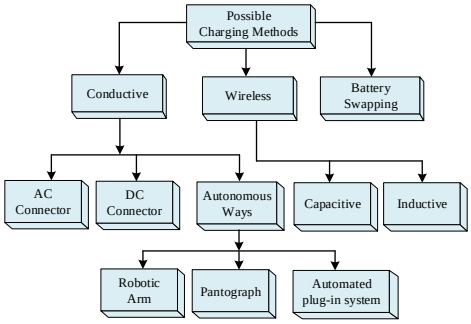

Figure. 2.11. Possible charging methods for SMGs [60].

(Level 1) semi-fast (Level 2), fast (Level 3), and ultra-fast (Level 4) types. The level 1 category is suitable for electric cars only whereas the rest of the levels are suitable for both electric cars and SMGs. The DC-DC conversion stage in case of fast and ultra-fast charging can be performed either as onboard or offboard where the charger for the Ellen ferry exemplifies the latter category.

2.4.4 Possible Charging Methods

BES and PHES can be charged either by interfacing with charging infrastructure placed onshore by using conductive (manual or automatic connectors) and wireless (inductive and capacitive) ways or using battery swapping methods. The battery swapping process may take much lesser time, in contrast, to even fast or ultra-fast charging categorizes in the case of ships due to the higher capacity of the battery banks. The additional battery banks may be located at either or both ends reliant on the short or long route of the SMG resulting in minimization of layover time at the seaport, hence, increasing the number of voyages, as knowing the fact that battery banks are mostly installed in passenger ferries and cruise ships where layover time is very short particularly in the former category. Further, in contrast to electric cars, installing batteries to ships is relatively new, hence, battery installing ways can be standardized in terms of their installation way and capacity. The conductive way of charging with manual connectors either AC or DC is quite common in electric cars in which the connectors are connected with the charging infrastructure by a human being. This process is time-consuming, hence, it may increase the overall charging process time if implemented in battery-equipped ships [61]. Therefore, autonomous ways such as robotic arm, pantograph, and automated plug-in systems (tower) are among the frequent types being used for cold ironing and charging battery-equipped ships as enlisted in Table 2.4. To minimize connection time, bulky connectors and cables can be replaced with wireless power transfer methods. It can be attained either using inductive or capacitive coupled plates. The inductive way utilizes magnetic fields in order to transfer power and is considered relatively safer. Wärtsilä introduced the world's first inductive charging for a hybrid ferry (MF Folgefonn) with a power rating of 2.5 MW operating at an efficiency of 95% eliminating the need for galvanic isolation. The wireless charging methodology has relatively more challenges for ships application comparable to cars and trucks due to the movement of the ship relative to onshore charging infrastructure [62]. To tackle the movement of the ship, an automated vacuum mooring system helps in this regard, bringing more safety and efficient way rather than using thrusters onboard.

2.5 Seaport Microgrid for Cold-ironing

The conventional seaports only provide logistics services such as cargo handling where onboard auxiliary generators are kept online during the whole process. The strict regulations from IMO regarding SOx emissions from Sulphur emission-controlled areas (SCEA) such as the Baltic Sea, North Sea, parts of Caribbean Sea, and North American coasts have been lowered down

Table 2.4. Autonomous connectors for SMGs for cold-ironing and charging purposes.

Ship Name	**Connector type**	**Battery Capacity (MWh)**
MS Color Hybrid	NG3 Plug	5
MF Tycho Brahe	ABB Robotic Arm	4.16
Ellen Ferry	Mobimar Nector	4
MF Ampere	Cavotec Automatic Plug-in System	1

to 0.1% from 2015 [63]. To comply with the regulations at ports, it is mandatory to use alternative fuel such as liquified natural gas (LNG), dual fuel, scrubbers (exhaust gas after treatment), batteries, or providing power through the national grid [64]. Cold ironing, shore connection, and alternative marine power are some of the terms used for supplying power to ships auxiliary loads during their berthed in time instead of utilizing auxiliary generators placed onboard. At present, only a few larger ports are equipped with cold-ironing facilities whereas for smaller ports still auxiliary generators are being used. Although even if the cold-ironing facility is available, the electricity generated by auxiliary generators onboard are exempted from taxes and hence is more favorable for shipowners in terms of cost whereas electricity purchased from the national grid is subject to taxes, which is another bottleneck in its implementation [65]. Therefore, the exemption in taxes and reduction in electricity prices could be a path towards the transition.

Another challenge in the interface with the grid is a difference in the frequency (50 Hz or 60 Hz), voltage (380 V, 400 V, 440 V, 690 V, etc) [66, 67], and power levels of different ships along with the safety and power quality-related concerns. The standard being utilized for high voltage shore connection (HVSC) is IEEE 80005-1 with a typical onboard voltage level (6.6 kV to 11 kV) comprising of two variants for low power requirement ($\leq$ 5 MVA) and high-power requirement ($\geq$ 5 MVA) whereas for low voltage shore connection (LVSC) it is IEEE 80005-3 providing power up to 1 MVA with voltage levels (400, 440, 690 V) [68]. Hence, the main components required to comply with these standards are a high voltage connection from the main grid, a frequency converter, a shore-side transformer (for providing galvanic isolation and step-down voltage level), a berth-side switchboard, and a cable management system. Several configurations are opted in the literature based on centralized, distributed, and dc-based cold-ironing configurations [69]. The configurations presented here are based on LVSC as for smaller ports the auxiliary load requirements for the ship are far less such as for Ellen

(55 kW), LMG-50 (30 kW) [70], and Happiness ferry (peak power 35 kW). In the centralized configuration shown in Fig. 2.13(a), the frequency converter is centralized with transformers at the input and output sides. The voltage level at the AC bus is kept higher to cope up with losses involved in the distribution, hence the voltage level could be in the medium voltage range (10-20 kV). The voltage and frequency level of different ships such as inland ferries will be the same for a specific country (50 Hz, 400 V) whereas vessels coming from different parts of the world could be 440 or 690 V. Therefore, each ship is interfaced to medium and low voltage switchgear along with medium to low voltage transformer. Although the centralized approach has a benefit with a reduced number of converting units but upon failure at the converter side will lead to a complete blackout. Hence, distributed-based cold ironing illustrated in Fig. 2.13(b) with frequency converting units at each terminal could be a possible option, a trade-off between resiliency and the number of converters. Another possibility is to have a DC-based cold-ironing configuration shown in Fig. 2.13(c) where a centralized rectification stage is performed and each terminal is interfaced with its inverters. Such an approach has a benefit in the way that RES and ESS can be interfaced easily with the DC bus to aid the cold-ironing process. Lastly, knowing the fact that modern ESS-equipped ships are interfaced with the DC bus, hence, a DC-based cold-ironing facility is needed where a central rectification stage is performed along with isolated DC-DC converting units to provide galvanic isolation with the required voltage level demand as shown in Fig. 2.12(d).

The main challenge is that conventional ports are not capable to deal with fluctuating demand from several ships docking at the same time and an increase in demand from shipping may require further cost requirements linked to retrofitting ports. Further, smaller seaports with inland ferries and cargo ships that are far away from the national grid will require huge investment costs, and for cold-ironing purposes investing this much may not be a viable approach. Hence, seaport microgrids are an emerging solution to meet the fluctuating demand requirements. The study in [16] considered RES (PV, wind turbine) and ESS (stationary battery banks and flywheel) to meet the power demand requirements from ships. To reduce the burden on the national grid, alternative fuel such as LNG is considered in [71] knowing the fact that it is among the most cleaner generation source with lesser footprints of particular matters and Sulphur emissions, which are considered a major health risk. Another approach utilized in [72], which proposes a floating platform comprising of a hybrid system with a battery and fuel cell stacks acting as a mobile power station to deal with a large number of ships at the port with a limited number of shore connections and berth points. To meet the auxiliary demands of the ship a seaport microgrid with a hybrid combination by fulfilling 75% of demand from offshore wind turbines and 25% by PV operating in an islanded and grid-connected modes for the port

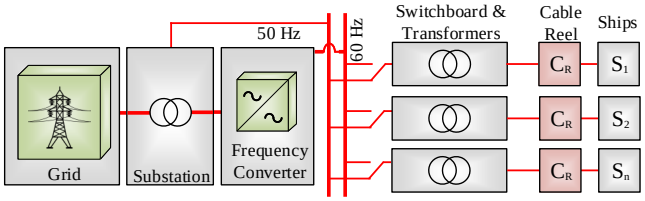

(a)

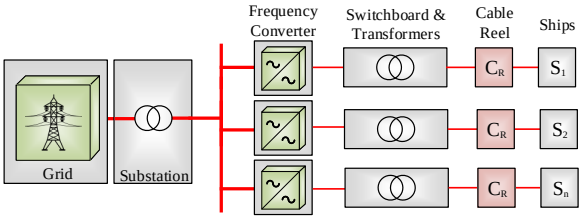

(b)

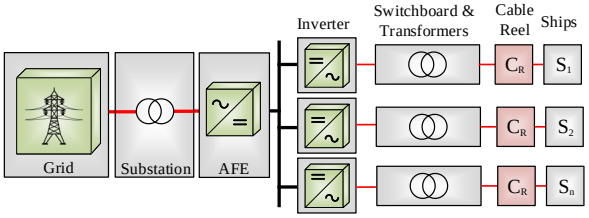

(c)

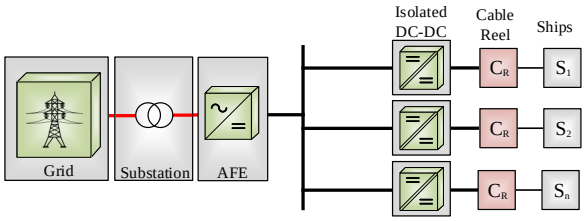

(d)

Figure. 2.12. Cold ironing topologies, (a) Centralized AC, (b) Distributed AC, (c) Centralized DC for AC ships, (d) Centralized DC for DC ships.

of Barcelona is proposed in [69]. To deal with the intermittent nature of RES, grid-connected operation is opted during nighttime. All aforementioned authors focused on the sizing of RES and ESS to aid the existing grid to provide cold-ironing facilities but fails to provide a solution for the smaller ports where grid connection requires huge investment costs. Further, the coordination control between both microgrids is ignored in these studies. The only study linked to coordination control between SMG and seaport microgrid is portrayed in [73] where authors use a hierarchical control scheme with the tertiary layer responsible to import power from the seaport microgrid.

2.6 Coordination Control Strategies for Shipboard Microgrids

The main target of coordination control strategies utilized in the literature for SMG application aims for minimization of fuel consumption and emissions by operating diesel generators close to their optimal point, economically dispatching of available resources, controlling the flow of power among different buses, power balancing between sources and loads, and mitigating power fluctuations caused by dynamic and pulsating loads onboard. As opposed to TMG loads, most power in SMG is consumed by the propulsion motors and the presence of pulsed loads such as radar and electromagnetic guns further enhances the complexity of the system.

The approaches adopted for coordination among different sources and loads for SMG applications in the literature are mainly categorized into centralized, master-slave, and decentralized methods. The study in [74] adopted a centralized technique intending to maintain the voltage deviation limit within an allowable range in a medium voltage direct current (MVDC) SMG using proportional-integral (PI) and fuzzy logic controllers [75]. The operation principle is designed considering power balancing in steady-state conditions and HESS for mitigating power fluctuations in transient conditions using an LPF. In addition, the control system takes into account the state of charge (SOC) and avoids ESS from deep discharging and overcharging. In [76], with the aim to minimize fuel economy for a tugboat, a coordinated control strategy is presented. A 150 kWh battery ESS is integrated to compensate for the power imbalance between the diesel generator and the load. Similarly, in [77] using LPF performs power-sharing between diesel generators and battery banks. The low-frequency components of load current are handled by the diesel generator whereas high-frequency components are tackled by the battery banks. Another study in [78] utilized the master-slave approach for power-sharing among different converting units where master control is a voltage controller generating reference current for the slave mod-

ules. However, the reliability of slave modules upon the master and single point of failure are some of the drawbacks of such an approach. The modified hierarchical control-based approach adopted in [12] where primary control is based on master-slave control; secondary and tertiary controllers are responsible for voltage restoration and power flow management respectively.

Although centralized approaches are beneficial in a way that they provide optimal performance, proper voltage regulation, and accurate power-sharing. However, control complexity and communication link between different sources and loads are prone to cyberattacks and single point of failure. One popular control approach without communication for power-sharing is based on droop control. It avoids control complexity, provides ease in an expansion of the system, and reduction in cost. In [11], power-sharing between diesel generators and ESS based on droop control is utilized for low voltage direct current (LVDC) distribution network by supplying fixed power from the fuel cell. To mitigate the voltage deviation caused by the primary control upon variation in load demand, a voltage compensation term is added. The operation principle is designed based on different speed operations (high, moderate, low) and operating diesel engines within a specific range, i.e., 60 to 100% of the rated power. In addition, during low speeding operation, the fuel cell and the battery are operated to achieve minimal noise and emission operation. However, such a coordination technique has a drawback that upon operation of pulsating loads, power fluctuations will also be shared with diesel generators impacting on its stable operation. Most of the aforementioned coordination control approaches were based on battery banks along with ICE-based sources. However, the limitation of the lower power density of battery and inability to deal with pulsating loads leads to hybridization of two energy storage devices with complementary features.

The study in [79] utilizes coordination control for MVDC ships with the aim of mitigating the effect of pulsating loads using HESS comprising of battery and ultra-capacitor banks. The intelligent algorithm differentiates between transient and steady-state conditions based on frequency division using a high pass filter. Further, the study based on voltage deviation acts the need for the type of ESS device injection or removal from the system. The traditional approaches mostly rely on AC or DC distribution interfaced coordination control schemes. Although DC distribution is gaining popularity, however, retrofitting existing ships requires extensive cost. Therefore, hybrid AC/DC architecture could be an alternative approach where AC and DC interfaced loads are connected to their respective buses. In order to coordinate between both buses, an interlinking converter is integrated for the bi-directional flow of power. Such an approach brings two-fold benefits, firstly, upon failure of diesel generators power can still be fed from ESS interfaced with DC bus. Secondly, the number of converters can be minimized ultimately minimizing conversion losses and cost. The relating approach for

a hybrid AC/DC architecture-based ferry is proposed in [14] where fixed power is fed from diesel generators thus operating at an optimal point (85% of the rated power). To balance the mismatch of power between load and diesel generators, battery ESS is integrated such that surplus power will be absorbed by the energy storage device. The capability to export power back to the grid is neglected in this study. Further, the all-electric port operation (AEPO) is ignored in the aforementioned approaches. The progress beyond state of the art is covered in Chapter 3.

2.7 Power-sharing Schemes for DC microgrids

To share power among different parallel interfaced converting units, several approaches are utilized in the literature such as centralized, distributed, and decentralized schemes as shown in Fig. 2.13. The centralized approach where the central control unit provides a reference to each converting unit, which has a drawback upon failure of central controller resulting in failure of the whole system. Another approach, master-slave control, and its variants [80]–[81], which guarantees slave modules following the reference current of the master. In such a method, one of the converters is working in a voltage control mode generating current reference for the slave modules. Yet another approach used in literature is based on circular chain control (3c) [82], which has a circuit configuration such that forming a ring. In such an approach, modules are in the circular chain such that each converting unit generates reference current for the preceding one where the current reference for the first unit is fed from the last module. However, these conventional approaches pivot mostly on a communication link between several converting units that compromise the redundancy and reconfigurability of the system. Further, single point of failure, lack of plug and play functionality are among the main drawbacks. To deal with it droop-based power-sharing methods based on decentralized control are adopted [83] without any communication resulting in lower cost and complexity. Conventional power-sharing methods rely on equal power-sharing that may consequence in deep discharging battery with lower state of charge (SOC), as a consequence is not that efficient.

To deal with it, power-sharing on the basis of droop control concept is proposed in [84] that is accomplished by altering the droop coefficient in accordance with the SOC of the battery banks. In [85], a proportional power-sharing scheme was proposed for DC microgrids to accomplish balancing of power between distributed units with different SOC. Such schemes have a tradeoff between voltage regulation and power-sharing accuracy. To tackle it, the SOC balancing method where the droop coefficient is taken to be inversely proportional to SOC^n whereby altering exponent term "n" proposed in [86] such that to regulate the speed of balancing SOC and equalization

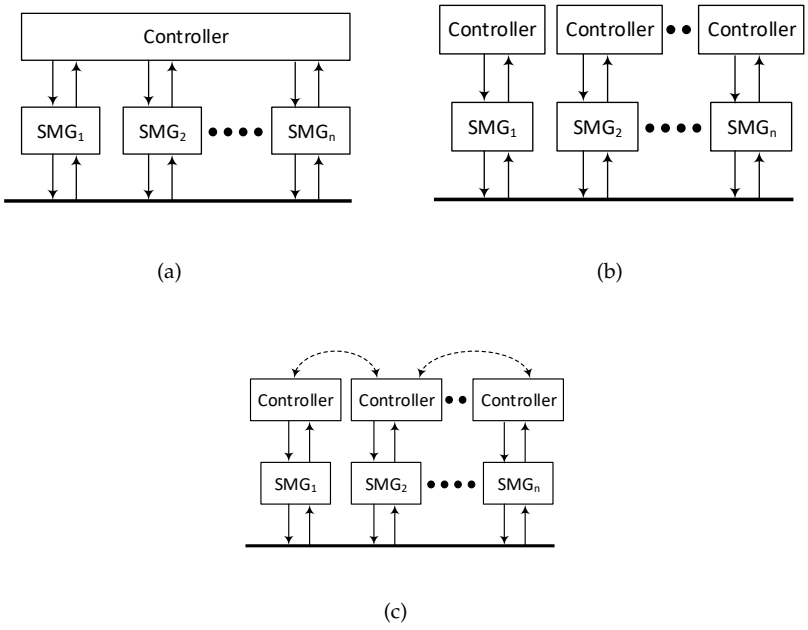

Figure. 2.13. Control approaches, (a) Centralized, (b) Decentralized, (c) Distributed.

of power. Such an approach accomplishes balancing of resources during the discharging mode but fails to deliver proportionate power-sharing in the charging mode. Moreover, by using a single-mode droop control scheme will result in needless power-sharing, which ultimately will result in undesirable distribution losses. To attain a proportionate power-sharing in both discharging and charging modes, a multi-mode droop method based on I-V droop is proposed in [87], which although has a better transient performance incomparable to V-I droop but stability margins are comparatively smaller, which ends up in instability issues [88], [89]. Further, variants of multi-mode droop control are proposed in the literature [90] but extreme scenarios were not undertaken resulting in the destabilizing whole system. The progress beyond state of the art is covered in Chapter 4.

Chapter 3

Coordination Control Scheme for Power-sharing among Multi-Sources interfaced Shipboard Microgrids

This chapter summarizes the contribution made in the submitted paper (Paper V), which can be found in the papers section. A further detailed explanation along with results and outcomes can be found in the appendix section.

3.1 Introduction

Strict regulations from maritime authorities such as IMO enforced shipowners to move towards novel solutions such as changing fuels, partially or fully retrofitting conventional sources with ESS. Although efficiencies of diesel generators have improved in the last many year's resulting in reducing SFC and exhaust gases, yet the wide range of operational situations bound the overall efficiency. As marine diesel generators operate under fluctuating load profiles during the ship's whole voyage causing generators to work under low-loading and high-loading circumstances. The low-loading operation causes low pressure in the cylinder causing poor combustion resulting in the formation of soot particles in the cylinder along with the leakage of oil from the exhaust. Hence, increased operation at the low load will damage the generator, increasing the overall operational cost. Conventionally, several generators are turned on and off during the whole voyage to cater to the situation whereas in shorter route ships such as river crossing, due to lesser

power requirements, all generators (two or three), are kept online operating much below their optimal points. Another challenge is due to the lack of cold-ironing facilities at the ports forces onboard generators to be kept online to feed auxiliary demands of the ship while keeping in mind that the auxiliary loads are far less (20 to 30% of total loading). To cope with the aforementioned challenges, a hybrid solution is needed, where the integration of battery banks is the possible candidate to solve these concerns. As it aids in optimizing the energy consumption by operating engines at their optimal load thus reducing the size of the generator. Several researchers tried to utilize ESS for different purposes such as minimizing operational cost, maximizing efficiency and reliability, tackling with a higher power ramp-rate needs of pulsating loads, prevention from blackout, power balancing, load leveling, and so on. This chapter introduces a multi-mode hierarchical control scheme for adaptive power-sharing between diesel generators and ESS to achieve quasi-load-leveling along with the Ship-to-X (S2X) operation during on port operations. To accomplish this, a piecewise function is integrated with the conventional *P-Q* droop control strategy for a fixed and varying frequency operation during SMG's islanded operation. During the operation of generators under light loading conditions, ESS will absorb power while delivering during high loading conditions. Whereas ESS remain idle or share the least amount of power during the operation of diesel generators in between minimum and maximum loading threshold limit, This sort of strategy will help to minimize the utilization of ESS and helps to operate diesel generators close to their optimal point, thus improving the efficiency and operational cost.

3.2 Coordinated Control Strategies

The power sharing approaches for uninterrupted power supply (UPS) can be divided into communication-based and communication-less-based approaches. Although communication-based approaches adopted in the literature provide better power-sharing capabilities along with voltage regulation, the dependence of communication lines among different converting units declines the reliability of microgrid, thus limiting the expansion and flexibility. The communication-based approaches for power control are categorized into central control, master-slave [91], circular chain [82], average current sharing, consensus-based droop control [92], and angle droop based methods. On the other hand, communication less approaches such as the droop control are used at the primary control level. Such an approach brings a reduction in cost, ability for a plug-and-play operation, reduced complexity, and higher reliability. The conventional *P-f* droop approach for synchronous machines upon an increase in active load demand results in a drop of the rotational

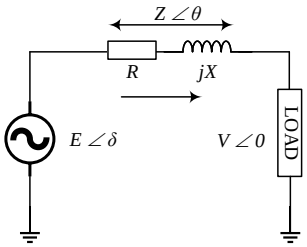

Figure. 3.1. Power flow from source to load.

speed of the generator thus drooping in frequency. However, in converter interfaced micogrids due to lack of inertia, the droop strategy is dependent on the characteristics of the transmission line.

The current flowing from source through an impedance can be expressed using (3.1).

$$I = \frac{E\angle\delta - V\angle 0}{Z\angle\theta} \tag{3.1}$$

The active and reactive power flow can be expressed using (3.2)–(3.3).

$$P = \left(\frac{E.V}{Z}\cos\theta\cos\delta - \frac{V.V}{Z}\cos\theta\right) + \left(\frac{E.V}{Z}\sin\theta\sin\delta\right) \tag{3.2}$$

$$Q = \left(\frac{E.V}{Z}\cos\delta\sin\theta - \frac{V.V}{Z}\sin\theta\right) + \left(\frac{E.V}{Z}\sin\delta\cos\theta\right) \tag{3.3}$$

For an inductive distribution line θ is considered to be 90°, hence, equations (3.2)–(3.3) can be rewritten as:

$$P = \left(\frac{E.V}{Z}\sin\delta\right) \tag{3.4}$$

$$Q = \left(\frac{E.V}{Z}\cos\delta - \frac{V.V}{Z}\right) \tag{3.5}$$

Assuming δ to be very small, i.e., $\delta \simeq 0$.

$$P \simeq \left(\frac{EV}{Z}\delta\right) \tag{3.6}$$

$$Q \simeq \left(\frac{V}{Z}(E - V)\right) \tag{3.7}$$

Hence, it can be inferred from (3.6)–(3.7) that active power-sharing is dependent on the phase angle while reactive power-sharing on the terminal voltage. Generally, frequency is utilized for active power rather than phase angle due to the lack of angle information of other converting units, as power angle is dependent on frequency.

The droop control principle can be expressed as follows:

$$\begin{aligned} \theta &= \theta^* - K_P(P^* - P_{ref}) \\ E &= E^* - K_Q(Q^* - Q_{ref}) \end{aligned} \tag{3.8}$$

where $\theta = \omega t$, E^*, P^*, and Q^* are the measured active and reactive power. On the other hand, P_{ref}, and Q_{ref} are the references for the active power and reactive power respectively, generally P_{ref} and Q_{ref} are set as zero in an island operation of microgrid. K_P, K_Q are the droop coefficients.

$$K_{\mathrm{P}} = \frac{\delta\omega}{P_{max}} \tag{3.9}$$

$$K_{\mathrm{Q}} = \frac{\delta V}{Q_{max}} \tag{3.10}$$

where $\delta\omega$ and δV are the maximum allowable deviation in frequency and voltage, P_{max} and Q_{max} are the maximum allowable active and reactive power.

3.3 Architecture of a Hybrid Shipboard Microgrid

The architecture taken into consideration is shown in Fig. 3.15 comprising of two diesel generators interfaced with AC bus using P-f droop control for active power-sharing. Each interfaced generator is of 88kW power with 60Hz frequency. The coordination between both generators is based on communication less control, thus providing ease in plug and play operation and power balancing between both generators. By allowing frequency droop, unbalanced power will be allocated to each generator according to droop characteristics. The auxiliary loads are interfaced with the AC bus using an onboard transformer, which in this study is taken to be 35kW constant. To connect the AC Bus with the DC bus, an Active front-end converter (AFE) is employed bringing benefits in terms of the bi-directional flow of power. In addition to it, an AFE converter also allows the elimination of higher-order harmonics thus providing low harmonic distortion [93, 94]. It helps in improving the power factor, which ultimately helps in saving costs. On the other hand, the battery bank is integrated with the DC-bus by using bi-directional DC-DC converter. Moreover, dynamic loads such as propulsion motors are interfaced with the DC bus thus mitigating the rectification stage in variable speed drives.

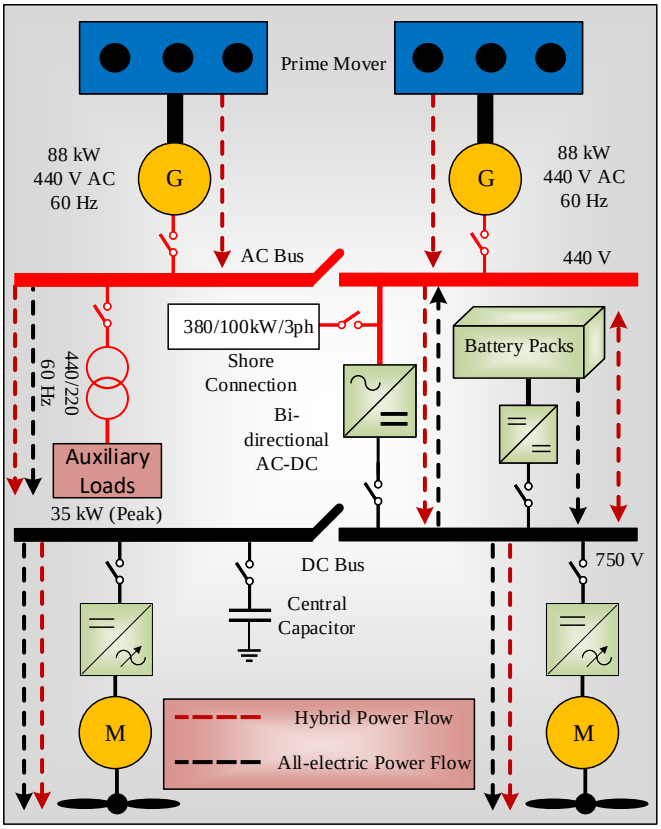

Figure. 3.2. Case study into consideration.

3.4 Modes of Operation

In a hybrid configuration, inherently AC-driven sources and loads such as diesel generators and auxiliary loads (hotel loads) are integrated with AC bus whereas DC-driven sources and loads, i.e., ESS and propulsion motors are connected with the DC bus. To have a linkage between both buses, an interlinking converter is vital to control the flow of active and reactive power. The main objective of the coordination control scheme relies on the operation of diesel generators within a specific operating range by utilizing ESS. Moreover, the coordination scheme also allows all-electric operation, which usually is missing in most of the previous studies conducted along with AEPO. The overall coordination control scheme is divided into four modes: The voyage mode indicate the islanded operation, which starts during berth out time; the second mode of operation corresponds to AEPO; the third mode refers to as

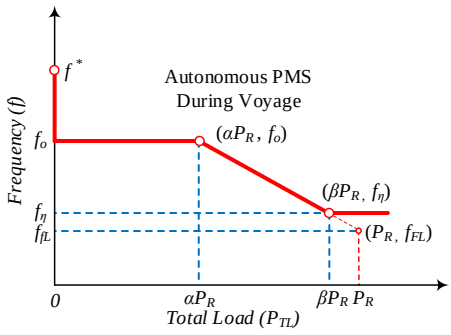

Figure. 3.3. Piece-wise function [7].

grid connection operation to provide cold-ironing facilities; lastly, the fourth mode refers to as S2G or S2X operation. Moreover, such an approach allows the continuity of operation even upon the failure of generators. The need for a multi-mode scheme not only allows operating diesel generators at their optimal point but also switching between different modes autonomously.

3.4.1 Mode 1: Voyage Mode

SMGs operating in an islanded mode is referred to here as "voyage mode", therefore, frequency and voltage requires to be controlled. Since SMG functions at varying load profiles either because of varying speed operation or because of occurrence of the environmental changes in ocean/sea. This results in the operation of diesel generators either at low-loading or high-loading. As a consequence, SFC increases under low-loading conditions and also causes soot particles and an increase in emissions ultimately resulting in increasing operational cost and decreasing the lifetime of onboard generators. Therefore, to minimize SFC and emissions, an adaptive PMS is designed in a way that diesel generators are operated within a specific range (50 to 90 % of rated power). To achieve this integration of ESS can bring two-fold benefits. Firstly, excessive power generated by diesel generators can be stored during low-loading operation whereas during high-loading conditions ESS can support. Secondly, ESS can be helpful to tackle with pulsating loads knowing the fact the ramp rate limitations of generators.

To share power among different sources, an adaptive PMS employing piece-wise function expressed in (3.11) with conventional $P - f$ droop control is utilized. This sort of strategy will help to operate diesel generators within a specific range by fixed and varying frequency operation for active power-

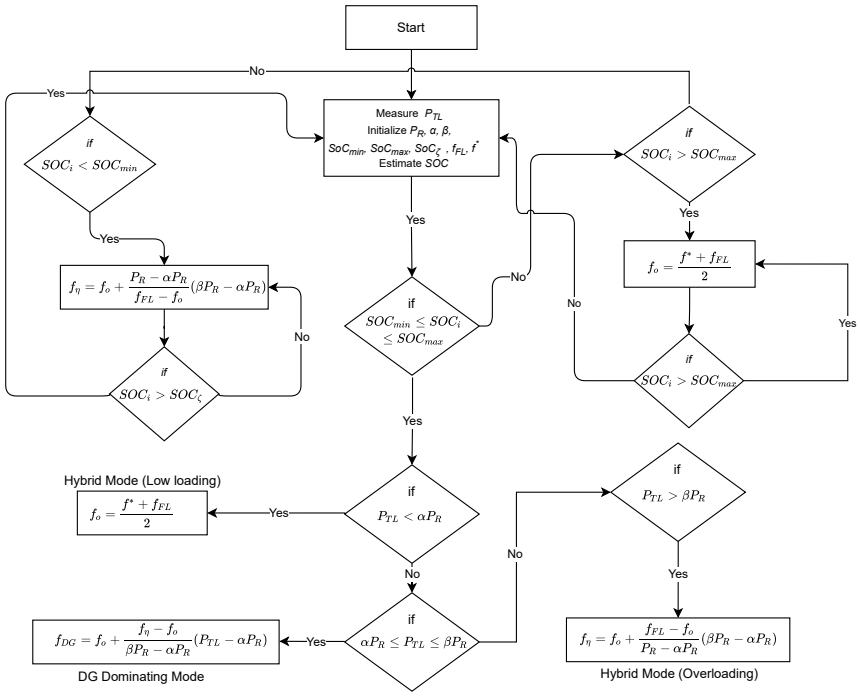

Figure. 3.4. Operation principle for adaptive power-sharing [7].

sharing among sources. The overall operation principle for voyage mode is depicted in Fig. 3.4. The allowable frequency deviation limit in ships according to different authorities are: for instance, according to DNV and American Bureau of Shipping (ABS) deviation limit is ±5% [95], on the other hand, according to IEEE standards (IEEE Std. 45.1-2017) the allowable deviation is is ±3% [96]. The maximum frequency deviation in this study is considered 1%.

$f_{PMS} =$

$$\begin{cases} f_o = \frac{f^* + f_{FL}}{2} & 0 \leq P_{TL} < \alpha P_R \\ f_{DG} = f_o + \frac{f_\eta - f_o}{\beta P_R - \alpha P_R}(P_{TL} - \alpha P_R) & \alpha P_R \leq P_{TL} \leq \beta P_R \\ f_\eta = f_o + \frac{f_{FL} - f_o}{P_R - \alpha P_R}(\beta P_R - \alpha P_R) & P_{TL} > \beta P_R \end{cases} \tag{3.11}$$

The operation principle is formulated based on following points:

1. If the SOC of the battery bank falls within the range of minimum and

maximum threshold limit:

(a) Diesel generators need to be operated above the set minimum threshold limit, i.e., αP_R. Therefore, if the total load (P_{TL}) lies below the minimum threshold value, the frequency is set to a constant value, which is f_o. It represents an average of full-load and no-load frequency as depicted in (3.11). It will allow supplying a fixed amount of power thus restraining diesel generators from operating at low loading. Thus, the excessive power in this scenario will be stored in the battery bank. Such an operation usually occurs when the vessel is operating with a lower speed, hence, it is termed in this study as a hybrid-mode operating at low loading.

(b) If the ship is operating at overloading condition that may be caused by environmental changes during the voyage in the sea, such a scenario will result in an increase in demand for power and may overload above the maximum threshold limit (βP_R). Hence, instead of overloading generators, battery banks can be utilized to supply excessive power. In order to achieve this, a fixed frequency operation is adopted such that a fixed amount of power is supplied by the generators. Hence, any mismatch in source and load will be catered by the ESS. In addition, any fluctuations caused by the propulsion motors will also be handled by the ESS.

(c) The scenario when the ship is operating at loading higher than the set minimum threshold limit and lower than the set maximum threshold limit ($\alpha P_R \leq P_{TL} \leq \beta P_R$), during such a scenario the ship operates in diesel generator dominating mode, and battery bank shares the least amount of power. This will result in a lower depth of discharge (DOD) thus enhancing the lifetime of the battery.

2. Another condition, where SOC of battery bank falls below the minimum threshold limit, i.e., $SOC_i < SOC_{min}$, the ultimate goal would be to recharge battery banks using onboard generators. In order to achieve this, generators are operated at their maximum rating such that to recharge up to a predefined limit (SOC_ζ).

3. Another condition, where SOC of battery banks is above the maximum threshold limit, i.e, SOC_{max}, the ship operates in a hybrid mode. Generally, battery banks are fully charged during nighttime using slow charging whereas during day time fast-charging is performed such that only constant current (CC) phase is considered. Hence, such a mode is only utilized during the first journey of the ship.

3.4.2 Mode 2: All Electric Port Operation

The interface of battery banks in ships allows operating all-electric during port operations. Generally, onboard generators are used to power auxiliary loads but with the restrictions from countries aiming to minimize emissions from ports and reduce noise pollution urge to move towards greener solutions. As ferries layover time is relatively quite shorter in comparison with other types of the ship such as cargo ships, therefore, either cold ironing facilities can be utilized during on port operations or battery banks can be used to power auxiliary loads. At present, only a few larger and popular ports have the capability to provide cold-ironing facilities. In some cases, particularly river crossing or routes for connecting islands with the mainland, cold ironing facilities are available at one end only, therefore, battery banks can be utilized at the other end. In order to smoothly transform from voyage mode to all-electric mode, frequency is fetched back to the normal value. Hence, the secondary loop is utilized operating as soon a total power reaches close to hotel load or propulsion motor's speed drops to zero.

$$\begin{aligned} \delta\omega_{SMG} &= K_{psf}(\omega^*_{SMG} - \omega_{SMG}) + K_{isf}\int(\omega^*_{SMG} - \omega_{SMG})dt \\ \delta E_{SMG} &= K_{pse}(E^*_{SMG} - E_{SMG}) + K_{ise}\int(E^*_{SMG} - E_{SMG})dt \end{aligned} \tag{3.12}$$

where K_{psf}, K_{isf}, K_{pse}, K_{ise} are the PI parameters for secondary controller. On the other hand, E^*_{SMG} and ω^*_{SMG} are the references for the voltage and angular frequency respectively, E_{SMG} and ω_{SMG} are the measured voltage and angular frequency.

3.4.3 Mode 3: Fast Charging Using CC-CV Method

The third mode corresponds to providing fast charging by the use of constant-current constant-voltage (CC-CV) method. Due to unavailability of a fast DC charger at the seaport, the AC shore connection needs to be rectified following a DC-DC conversion stage for full use of the onboard battery. This type of charging method is also referred to as onboard charging. The control of the AC/DC converting unit will switch from power-control mode to voltage-control mode as shown in Fig. 3.6 considering the fact that the DC-bus voltage requires to be maintained to 750 V, hence, ${V_{DC}}^*$ is compared with V_{DC} and is fed through the controller as depicted in Fig. 3.6.

3.4.4 Mode 4: Cold-ironing and Ship-to-X

The fourth mode corresponds to cold-ironing and S2X where conventional control based on *P-f* and *Q-V* droop scheme is implemented. S2G, a technology that helps energy to be supplied back to the grid from battery banks

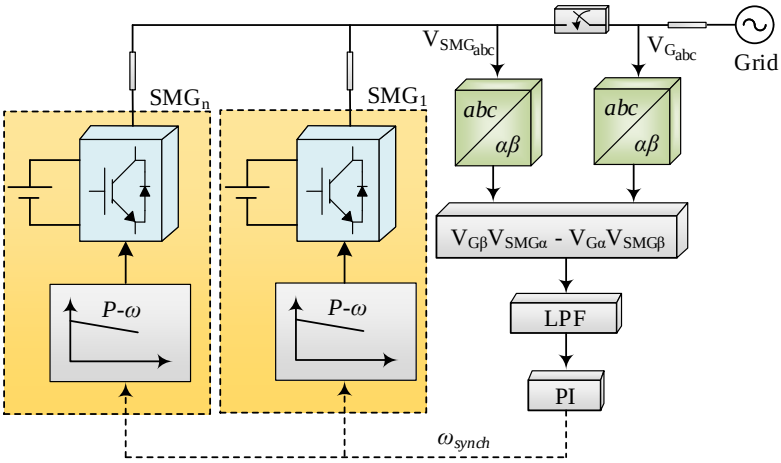

Figure. 3.5. Synchronization loop for grid-connected operation.

of an electric ship. On the other hand, S2X is mentioned to here as the ship to everything that can be ship-to-seaport, ship-to-building, ship-to-ship, or ship-to-grid. Due to the fact that, modernized ships are equipped with several kW to MW range battery banks along with a transition towards fuel cell-based shipping. Therefore, in case of an emergency or islands equipped with RES, electric ships can be utilized to import and export power. The services that can be provided by this technology include frequency response (keeping frequency within threshold limits), time-shifting, storing energy during low pricing and selling during high pricing, and acting as reserve source. Hence, the beneficiaries could be Transmission System Operator (TSO), distribution system operator (DSO), or any third party. For electric cars, around 50 projects globally while dominating in Europe region (Denmark, Netherlands, Germany, UK) are already installed, most of them with DC chargers [97]. The two mature projects include frequency services at the TSO level in Denmark (Parko project) and load shifting at the DSO level in Japan [98]. For importing and exporting power to and from the grid, the conventional $P-f$ and $Q-V$ droop control are utilized at the primary level. To switch from islanded to grid-connected mode, voltages in terms of frequency need to be synchronized as shown in Fig. 3.5, any mismatch will result in reactive power to flow, hence, synchronization is performed at the secondary control level. The synchronization loop takes the voltage components of the SMG ($V_{SMG_{abc}}$) and the grid ($V_{G_{abc}}$), the cross product of the α and β components as expressed in (3.13) needs to be zero in order to be synchronized.

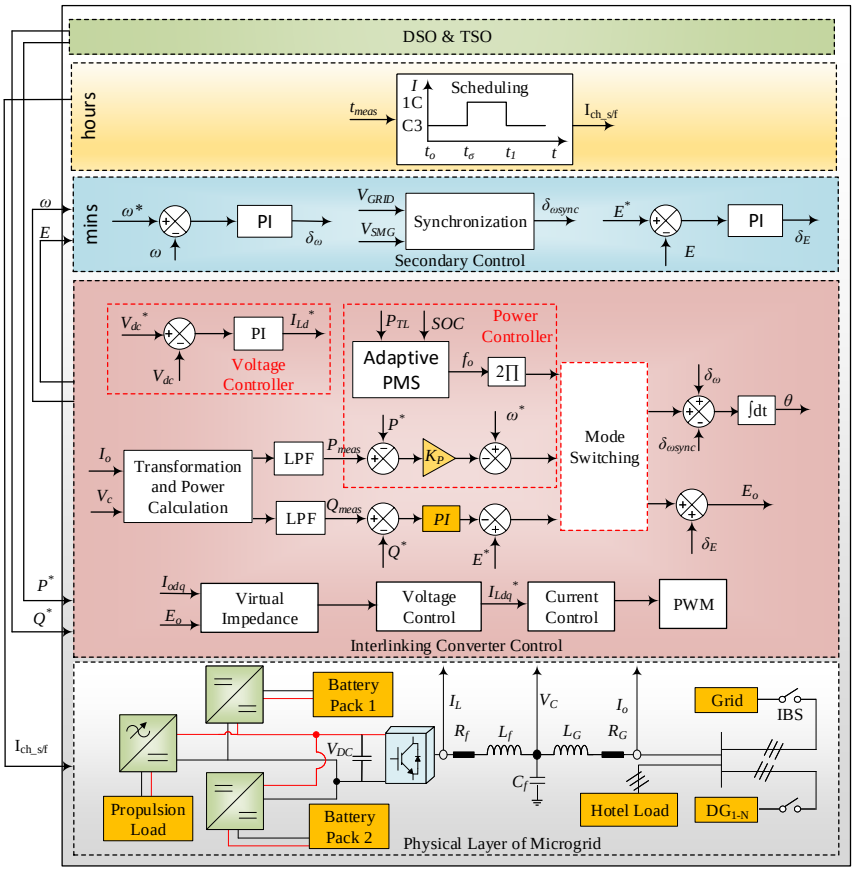

Figure. 3.6. Hierarchical control approach for hybrid shipboard microgrids [7].

$$< V_{G\beta} V_{SMG\alpha} - V_{G\alpha} V_{SMG\beta} >= 0 \tag{3.13}$$

The synchronization structure comprises of orthogonal product, LPF, and PI controller as expressed in (3.14)

$$\delta_{\omega sync} = \left(\frac{K_{psyn} s + K_{isyn}}{s} \right) \left(V_{g\beta} . V_{SMG\alpha} - V_{g\alpha} . V_{SMG\beta} \right) \left(\frac{\omega_c}{s + \omega_c} \right) \tag{3.14}$$

where K_{psyn} and K_{isyn} are the PI parameters for the synchronization loop. The cutt-off frequency for LPF is represented by ω_c, the resulting term $\delta_{\omega sync}$ is fed to the primary layer for synchronization purposes. The benefit for frequency based approach is the need for low bandwidth communication in comparison with time domain or phase information.

Table 3.1. Parameters for the hybrid electric ferry [7].

Category	Parameters	Values
Diesel generator	Electric Power	2x88 kW
	Nominal frequency	60 Hz
	RMS voltage	440 V
Battery Bank	Rated capacity	160 Ah
	Nominal voltage	650 V
Propulsion Motor	Rated power	2x112 kW
Hotel load	Nominal power	35 kW
Voltage	DC-Bus voltage	750 V
Interlinking Converter	Inner Loop	K_{pi}=13.93, K_{ii}=4875
	Outer Loop	K_{pv}=0.4586, K_{iv}=494.6
	Secondary Control	K_{pfs}=0.9, K_{ifs}=0.1 K_{pes}=0.8, K_{ies}=0.01 K_{psyn}=5e-4, K_{isyn}= 1e-3
Grid Connected Mode	Droop coefficients	$K_P = 5e-5$, $K_{QP} = 7.6e-5$, $K_{QI} = 1e-2$
Bi-directional DC-DC converter	Switching frequency	10 kHz
	DC-link capacitor	10000 μF
	Inner loop	Kpi= 5, Kii=10
	Outer loop	Kpv=2, kvi=100

For importing power from the grid and exporting power to the grid, the reference signals of active (P_G^*) and reactive power (Q_G^*) are sent by either TSO or DSO. In addition, if an energy management system (EMS) is available, the access power generated by RES (PV and fuel cell) can also be supplied. In this study, the assumption is made that reference signals (P_G^*) and (Q_G^*) are set by TSO or DSO.

3.5 Simulation Results and Discussion

The ship taken into account here is the hybrid-electric ferry known as Happiness ferry, it was originally a diesel-powered ferry that is retrofitted with

a hybrid sources-based hybrid AC/DC architecture. The ferry operates on a shorter route of 650m between Cijin and Gushan pier station. The operational duration of the ferry during its voyage is 5 minutes, where the ferry stops at each side for 5 minutes. The parameters for the ferry taken in this study are enlisted in Table. 3.1

3.5.1 Case Study 1: Hybrid Operation During Low-Loading Condition

The first scenario corresponds to when the ship is operating at a lower speed, thus the power requirement from the total load (P_{TL}) lies below the minimum threshold limit, i.e., 50% of P_R. Such a scenario will cause diesel generators to operate at low loading resulting in an increase in SFC. In order to cope with it, diesel generators are operated at a fixed power using fixed frequency operation of the interlinking converter thus supplying a fixed amount of power where the excessive power is stored in the battery bank for later use as illustrated in Fig. 3.7(a). The deviation of frequency is set to be $\pm 1\%$, hence, the minimum and maximum frequency fall between 59.4 to 60.6 Hz. The variation in torque and speed of the propulsion motor is shown in Fig. 3.7(b). As the battery bank is absorbing an excess amount of power, therefore, SOC is being raised proportionally between two battery banks as shown in Fig. 3.7(c). Additionally, the DC-bus voltage remains within the set threshold-limit and surge in bus voltage indicates battery banks are being charged.

3.5.2 Case Study 2: Hybrid Operation During High-Loading Condition

The second scenario corresponds to when the vessel is operating at a higher speed leading the power required to rise above the set maximum threshold limit, i.e., BP_R. This will cause diesel generators to operate at overloading resulting in poor performance and elimination of soot particles from the exhaust. To cope with this challenge, excessive power needs to be supplied from battery banks. To achieve this, the fixed frequency operation of the interlinking converter helps to supply a fixed amount of power (βP_R) at a frequency (f_η). It can be visualized from Fig. 3.8(a) that from till 4 to 8s, power demand lies between the minimum and maximum set threshold limit, hence, power supported by battery banks close to zero. After 8s, demand of power rises above the maximum set threshold limit, hence, the battery bank starts to contribute to the excessive demand for power. Due to the rise in power demand, the frequency drops to the value 59.52 Hz. Hence supplying the fixed amount of power (158 kW) corresponding to maximum power supplied from diesel generators. The variation in speed and torque of propulsion motor are illustrated in Fig. 3.8(b). Further, it is observed from Fig. 3.8(c) that up till 4s,

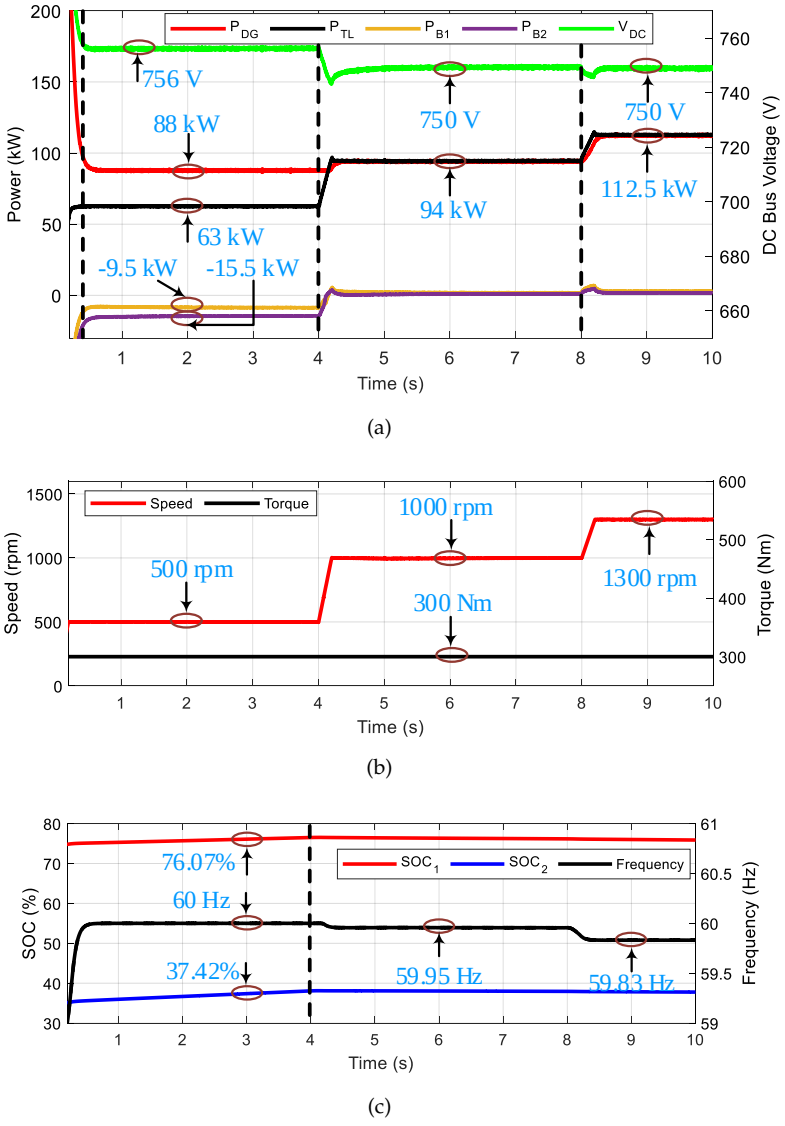

Figure. 3.7. Simulation results for low loading case study: (a) Sources and load power along with frequency, (b) Torque and speed of propulsion motor (c) state of charge of battery and DC bus voltage [7].

SOC is rising whereas, from 8s, SOC of battery bank starts to fall knowing the fact that it is contributing towards the load.

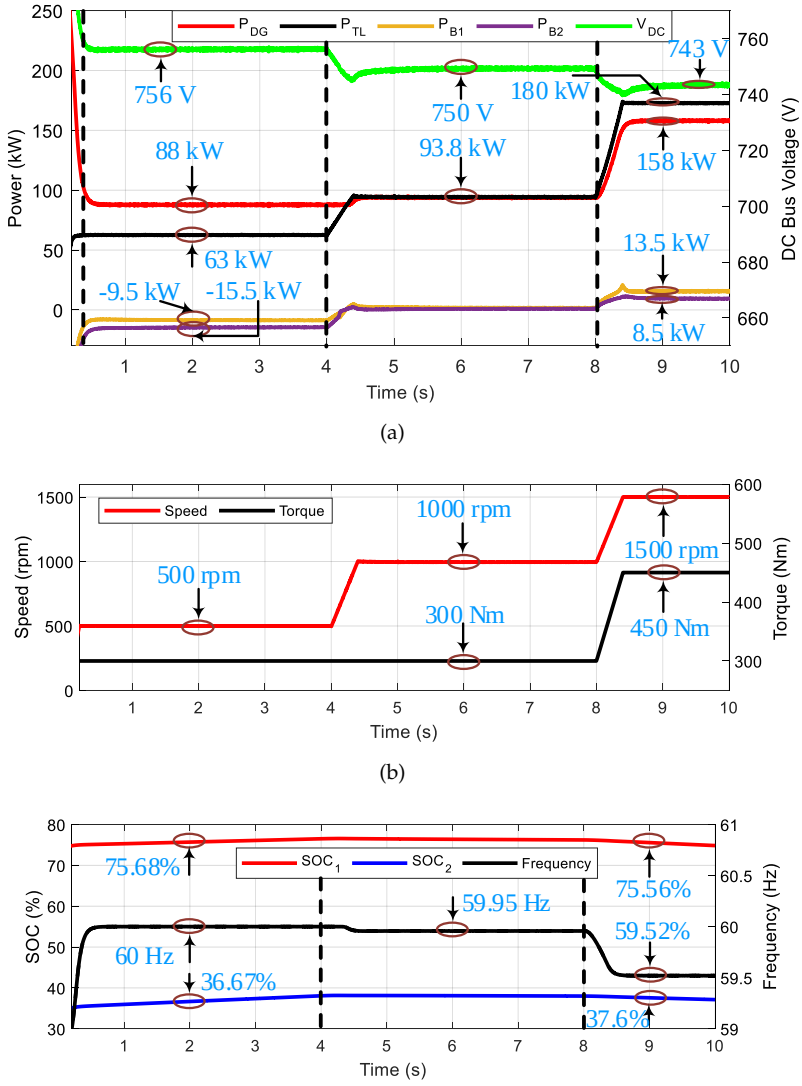

Figure. 3.8. Simulation results for high-loading scenario: (a) Sources and load power along with frequency, (b) Torque and speed of propulsion motor (c) state of charge of battery and DC bus voltage [7].

3.5.3 Case Study 3: All-Electric Port Operation

The third case study corresponds to AEPO knowing the fact that the absence of cold-ironing services at both ends leads to a need for an emission-free

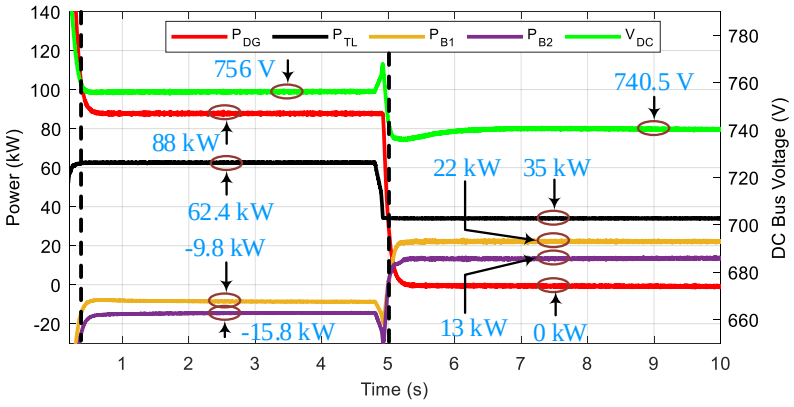

(a)

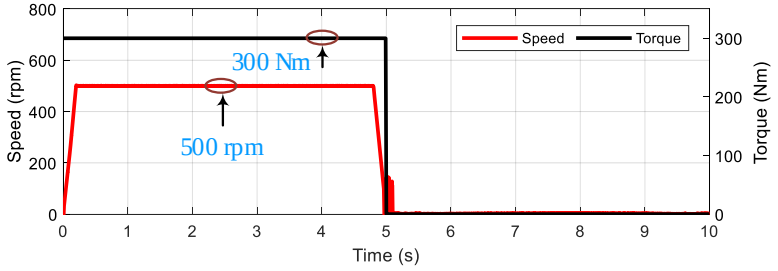

(b)

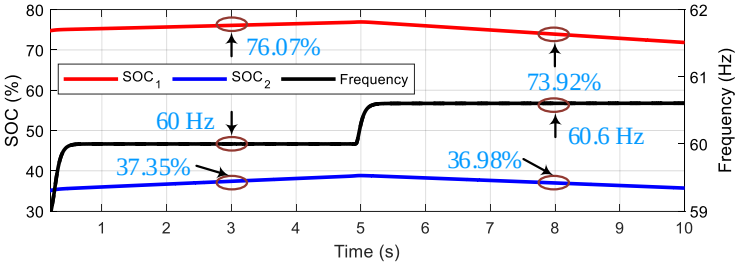

(c)

Figure. 3.9. Simulation results for all electric port operation scenario: (a) Sources and load power along with frequency, (b) Torque and speed of propulsion motor (c) state of charge of battery and DC bus voltage [7].

operation at ports. Instead of powering auxiliary loads through auxiliary generators or main generators, battery banks can be used. As hotel loads are far less than overall loading, moreover, the layover time of ferry is quite

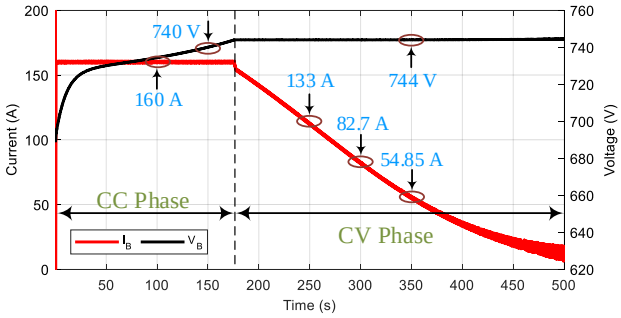

Figure. 3.10. CC-CV charging during onport operation [7].

shorter (5 mins), hence, supplying by battery banks can be easily an alternative approach. The transition from voyage mode to AEPO is depicted in Fig. 3.9. It can be observed from Fig. 3.9(a) that in the starting region, the ship was operating in a voyage mode (low-loading operation) thus power from generators is supplied to the load and battery bank. When the power of the propulsion motor drops to zero, instantly, the secondary loop operates bringing back frequency and voltage to the nominal value. This will help to smoothly transform from voyage mode to AEPO, thus the battery bank starts to power auxiliary load. The speed and torque of propulsion motor is illustrated in Fig. 3.9(b) verifying that after 5s during port operation speed and torque of propulsion motors drops to zero. The SOC of the battery bank in the starting region rises due to low-loading operation in the voyage mode whereas after 5s it starts dropping as the battery bank takes over the auxiliary load as verified from Fig. 3.9(c).

3.5.4 Charging During Onport Operation

This scenario implies charging mode such that during daytime port stays, the ship is charged with fast charging whereas during night time (longer stay at port) slow charging is performed. As shore connection with three-phase, AC supply is available, therefore, rectification following a DC-DC conversion stage are performed onboard. It can be observed from Fig. 3.10 that the battery bank is charged at a 1C rate, i.e., 160 A, which is a CC stage and will remain until battery voltage reaches the maximum value. The maximum battery voltage, in this case, is 744V, hence, upon reaching the maximum voltage, the CC stage is replaced with the CV stage and will continue until the battery is fully charged (0.05C).

3.5.5 Cold-ironing Facility

The fifth case study corresponds to providing a cold ironing facility upon port stays and the transition from AEPO mode to grid-connected mode. The conventional $P-Q$ control strategy is implemented in order to transform from one mode to another. It can be observed from Fig. 3.11(a) that until 4s, power is supplied to auxiliary loads from the onboard battery bank. At 4s, SMG is connected with the grid, hence, power supplied to auxiliary load from battery bank drops to zero whereas the grid takes over the auxiliary load. Further, along with supplying power to the auxiliary load, the grid starts to supply power (10 kW) at 5s and a step change of 10 kW at 7s to charge the battery bank. Additionally, it can be observed from Fig. 3.11(b) that at 2s, the synchronization process starts such that voltages of SMG and grid are synchronized before grid-connected operation. Further, it can be visualized that up till 4s SOC of the battery bank is falling illustrating auxiliary loads are supplied using onboard battery whereas from 4 s SOC of battery bank starts to rise indicating that power is being imported from the grid.

3.5.6 Ship-to-X operation

The last scenario corresponds to S2X operations, where battery banks of SMG can be utilized to support either DSO or TSO in terms of frequency services, load shifting, and so on. Hence, the references are either sent by DSO or TSO here whereas upon the availability of RES, excess power generated can be also be exported. In contrast to passenger cars that range up to 100 kWh only, battery banks of SMG vary from several kWh to MWh range, hence, a similar approach can be extended. It can be observed from Fig. 3.12(a) that up to 5s the reference signal is zero, hence no power is shared. At 5s and 7s, with a step response of 10 kW, the reference signal is sent, hence, SMG starts to share power where negative sign indicates that power is supplied by the SMG. It can further be inferred from Fig. 3.12(b) that at 2s, the synchronization process starts. Moreover, as power is being supplied, therefore, SOC of the battery banks falls.

3.6 Coordinated Control Scheme for Hybrid Energy Storage System

The modernized naval ships will be interfaced with electric weapons such as electromagnetic railguns, high energy lasers, high power radars, and electric propulsion systems [99]– [100]. Such loads are high power loads, which upon operation may lead to the instability of the SMG due to the ramp rate limitations of fossil fuel-based generation sources. Further, integration of

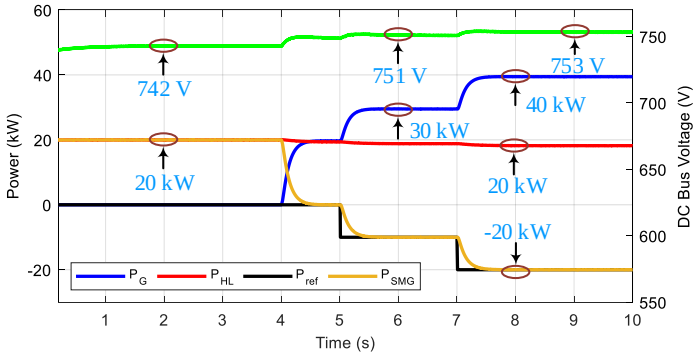

(a)

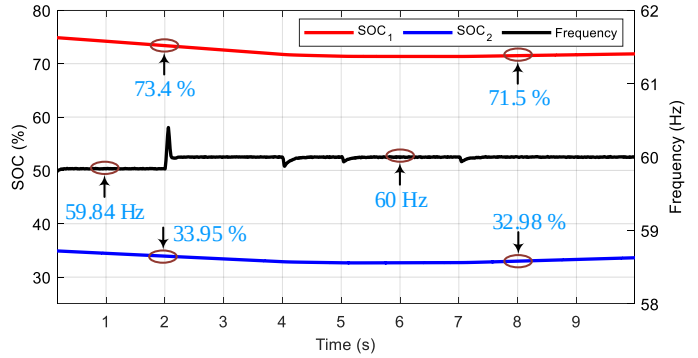

(b)

Figure. 3.11. Simulation results for cold-ironing scenario: (a) Sources and load power along with frequency, (b) Frequency and SOC of battery bank [7].

such loads will result in an increased amount of power requirement with limited available resources on board due to weight and space limitations. To tackle this problem, integration of ESS along with proper coordination between available resources is required. In addition, due to low cycle life, lower power density, and slow response of battery urge to the hybridization of two or more storage devices with complementary features. Therefore, a high power density device such as an ultra-capacitor is integrated to tackle sudden load fluctuations or to deal with pulsating load demands. The operation principle is based on load sharing between battery and ultra-capacitor using LPF.

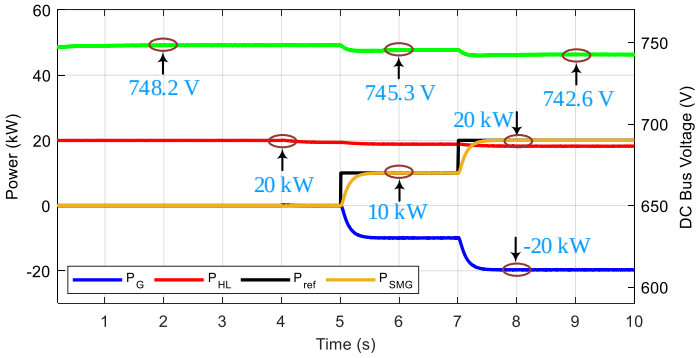

(a)

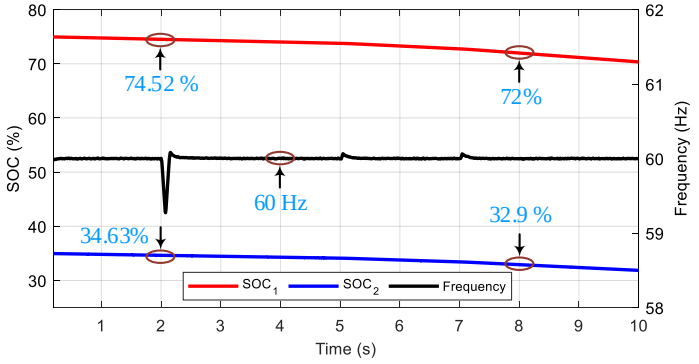

(b)

Figure. 3.12. Simulation results for S2X scenario: (a) Sources and load power along with reference power, (b) Frequency and SOC of battery [7].

3.7 DC Shipboard Microgrid Architecture with Hybrid Energy Strage System

In this section, the architecture taken into consideration is discussed, which comprises of four diesel generators, two at each side (starboard and port) as shown in Fig. 3.13. The generators are interfaced with the DC bus using an AFE converter bringing benefits in terms of low THD. Along with main sources as diesel generators, HESS comprising of the battery bank and ultra-capacitor with complementary features are integrated with the DC-Bus by the use of bi-directional DC-DC converting units. The parameters for the study taken into consideration are shown in Fig. 3.2.

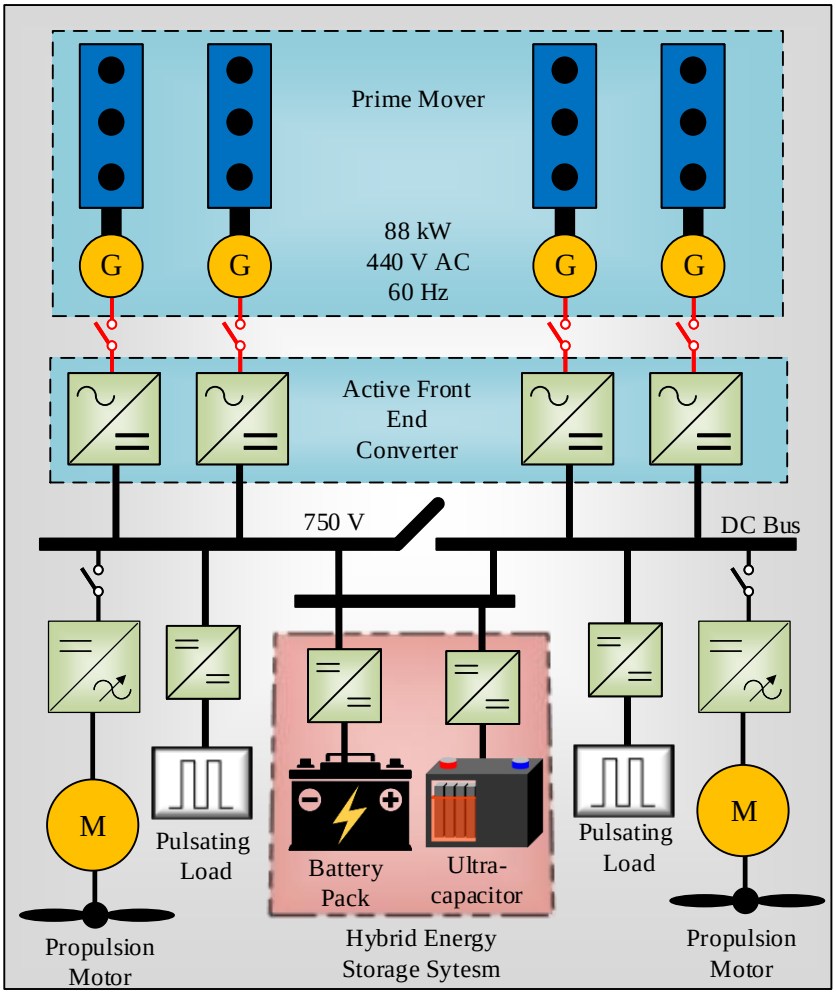

Figure. 3.13. DC Shipboard microgrid architecture with hybrid energy storage system [7].

3.7.1 Active Front End Converter Control

The conventional rectifiers are usually of 6-pulse and are being used in several industrial applications due to their simplicity and cost-effective nature [101]. They have a drawback that they produce harmonics into the grid ultimately resulting in losses and heat. To mitigate or reduce harmonics 12-pulse or 18-pulse based solutions are presented in the literature resulting in increased cost and footprints. Among other alternatives, passive and active filters are interfaced with increased cost and larger footprints. Alternatively, an AFE behaves as a controlled rectifier bringing benefits in terms of close to

Table 3.2. Parameters for the electric ferry.

Category	Parameters	Values
Diesel generators	Electric Power	2x88 kW (Starboard side) 2x88 kW (Port side)
	Nominal frequency	60 Hz
	RMS voltage	440 V
Battery Bank	Rated capacity	160 Ah
	Nominal voltage	400 V
Ultra-capacitor	Rated capacitance	1000 F
	Nominal voltage	500 V
Propulsion Motor	Rated power	2x112 kW
Voltage	DC-Bus voltage	750 V
Active Front End Converter	Inner Loop	K_{pi}=33, K_{ii}=666
	Outer Loop	K_{pv}=2, K_{iv}=400
	Input Filter	L_g= 0.6 mH, L_f=0.6mH C=10 μF
DC-DC Bi-directional Converter	Outer loop	Kpv_e=15, Kiv_e=400
	Inner loop (Battery Converter)	K_{pi_b} = 0.01816, K_{ii_b}=83.5
	Inner loop (Ultra-capacitor Converter)	K_{pi_c}=0.03725, K_{ii_c}=386.2
	Inductances	L_b =2 mH, L_c=1.8mH
	Switching frequency	F_{sw}=10kHz

unity power factor and low THD [102].

The AFE control is executed in a direct quadrature (DQ) frame, where the active (I_d) and reactive (I_q) components of the input three-phase current, which are separately controlled. The outer voltage loop allows the regulation of DC-side voltage by comparing DC side voltage (V_{DC}) with a reference voltage (750 V) followed by a PI compensator. Additionally, the outer loop allows the mitigation of load fluctuations. The referenced-axis current is produced by the outer loop compared with the inductor current (I_d). On the other hand, the q-axis reference is set to zero to ensure unity power factor. The overall control scheme for the AFE is shown in Fig. 3.14.

3.7.2 DC-DC Converter Control

To interface battery and ultra-capacitor with the DC bus, a boost converter is interfaced with each storage device to provide a steady state supply. The average model of boost converter can be defined by expression (3.15)–(3.18). When the switch is open the inductor current and capacitor voltage can be

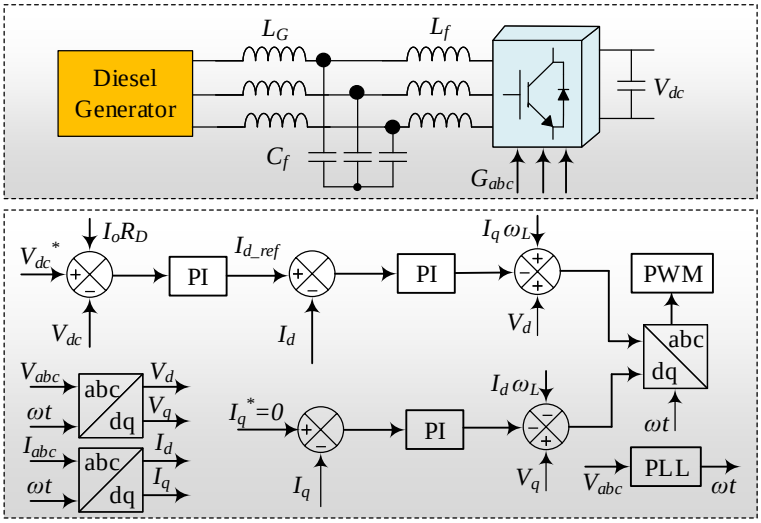

Figure. 3.14. Control scheme for active front end converter.

defined using (3.15)–(3.16).

$$L\frac{d}{dt}I_L(t) = \frac{V_{in}}{L} \tag{3.15}$$

$$C\frac{d}{dt}V_C(t) = -\frac{V_C}{RC} \tag{3.16}$$

The inductor current and capacitor voltage when the switch is closed can be defined using (3.17)–(3.18).

$$L\frac{d}{dt}I_L(t) = -\frac{V_C}{L} + \frac{V_{in}}{L} \tag{3.17}$$

$$C\frac{d}{dt}V_c(t) = -\frac{V_C}{RC} + \frac{I_L}{C} \tag{3.18}$$

The state space representation during switch off time will be:

$$\frac{d}{dt}\begin{bmatrix} I_L(t) \\ V_C(t) \end{bmatrix} = \begin{bmatrix} 0 & 0 \\ 0 & -\frac{1}{RC} \end{bmatrix}\begin{bmatrix} I_L(t) \\ V_C(t) \end{bmatrix} + \begin{bmatrix} \frac{1}{L} \\ 0 \end{bmatrix} V_{in} \tag{3.19}$$

The outputs of the converter are V_C and I_L. So,

$$y = \begin{bmatrix} 1 & 0 \\ 0 & 1 \end{bmatrix}\begin{bmatrix} I_L(t) \\ V_C(t) \end{bmatrix} \tag{3.20}$$

The state space representation during switch on time will be:

$$\frac{d}{dt}\begin{bmatrix} I_L(t) \\ V_C(t) \end{bmatrix} = \begin{bmatrix} 0 & -\frac{1}{L} \\ \frac{1}{C} & -\frac{1}{RC} \end{bmatrix}\begin{bmatrix} I_L(t) \\ V_C(t) \end{bmatrix} + \begin{bmatrix} \frac{1}{L} \\ 0 \end{bmatrix} V_{in} \tag{3.21}$$

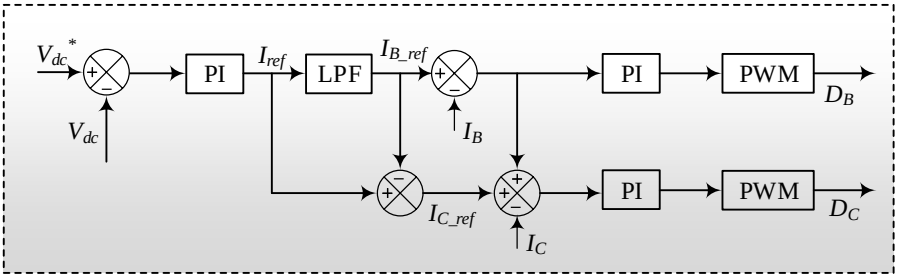

Figure. 3.15. Coordination control scheme for hybrid energy storage system.

The outputs of the converter are V_C and I_L. So,

$$y = \begin{bmatrix} 1 & 0 \\ 0 & 1 \end{bmatrix} \begin{bmatrix} I_L(t) \\ V_C(t) \end{bmatrix} \tag{3.22}$$

By applying state-space averaging, different possible transfer functions obtained can be represented as follows:

$$Gvd(s) = \frac{-LI_L(s) + V_C D^{'}}{LCs^2 + \frac{L}{R}s + D'^2} \tag{3.23}$$

$$G_{id}(s) = \frac{CV_C(s + \frac{1}{RC}) + I_L D^{'}}{LCs^2 + \frac{L}{R}s + D'^2} \tag{3.24}$$

$$G_{vi}(s) = \frac{-LI_L(s) + V_C D^{'}}{CV_C(s + \frac{1}{RC}) + I_L D^{'}} \tag{3.25}$$

where $G_{vd}(s)$ represents transfer function of voltage to duty cycle, $G_{id}(s)$ represents inductor current to duty cycle, and $G_{vi}(s)$ shows output voltage to inductor current transfer function.

The objective of the coordination control scheme for HESS is to minimize the stress on the battery thus aiding in increasing the lifetime of the battery. The control scheme allows ultra-capacitor to support fast transients, whereas slow transients are catered by the battery. To design the control parameters, the inner current loop for the battery converter is designed based on lower bandwidth ($2 * \pi * F_{sw}/12$) than ultra-capacitor ($2 * \pi * F_{sw}/9$) to allow ultra-capacitor to respond to transients before the battery. The transfer functions from duty to inductor current (G_{id}) along with the compensator for the inner loop is expressed in (3.26)– (3.27) for battery and ultra-capacitor respectively.

$$G_{id_b}(s) = \left(\frac{CV_C(s + \frac{1}{RC}) + I_L D_b^{'}}{LCs^2 + \frac{L}{R}s + D_b'^2} \right) \left(K_{pi_b} + \frac{K_{ii_b}}{s} \right) \tag{3.26}$$

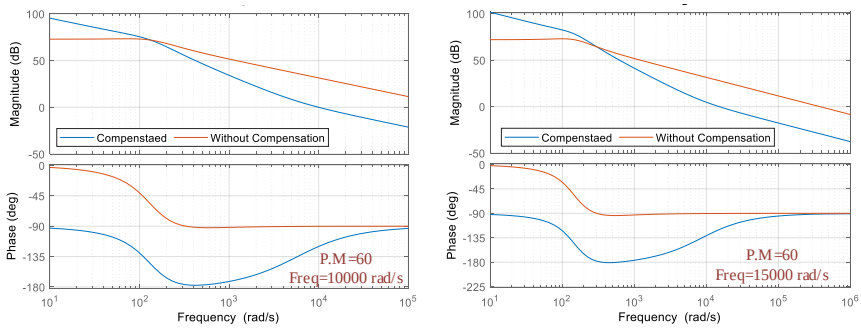

(a) (b)

Figure. 3.16. Open loop bode plot of inner loop, (a) Battery, (b) Ultra-capacitor.

$$G_{id_c}(s) = \left(\frac{CV_C(s + \frac{1}{RC}) + I_L D_c^{'}}{LCs^2 + \frac{L}{R}s + D_c^{'2}} \right) \left(K_{pi_c} + \frac{K_{ii_c}}{s} \right) \tag{3.27}$$

The inner loop parameters of compensator for battery are designed in a way to achieve a phase margin of 60 ° and frequency of 10000 rad/s as shown in Fig. 3.16(a), On the other hand, to have a faster transient response, compensator for ultra-capacitor are designed to achieve phase margin of 60 ° and frequency of 15000 rad/s as shown in Fig. 3.16(a),

3.8 Simulation Results

The parameters for the DC SMG with HESS shown in Fig. 3.13 are given in Table. 3.2. The architecture comprises two generators at each side (starboard and port) with their loads along with a HESS. To verify the efficacy of the control approach multiple case studies such as step-change in increase and decrease in the load and pulsed loads are taken into account.

3.8.1 Case Study A: Step Change in the Load

The first case study corresponds to when a fixed amount of power is supplied from the main source, i.e., diesel generator thus operating close to their optimal point and any change in the load demand, therefore, is catered by HESS. After every 1s, there is a step-change in the load to verify the response by the HESS. It can be verified from Fig. 3.17(a) that upon a sudden increase in load demand the transients are tackled by the ultra-capacitor whereas low-frequency components are given to the battery. Further, Fig. 3.17(b) shows

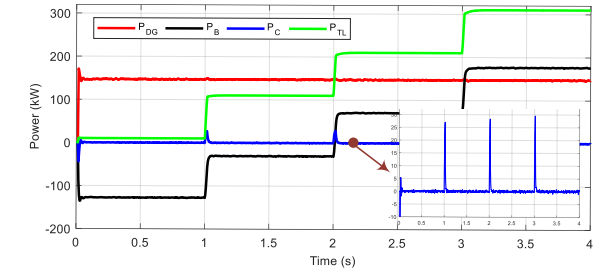

(a)

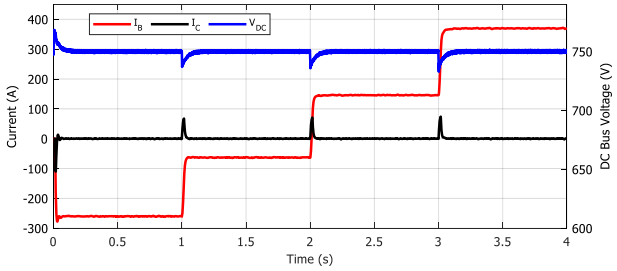

(b)

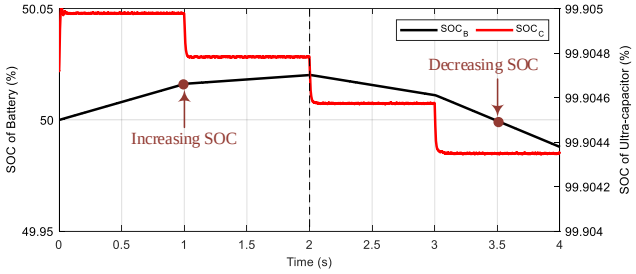

(c)

Figure. 3.17. Simulation results for sudden load change, (a) Power from sources and loads, (b) DC-bus voltage, current of ultra-capacitor and battery, (c) SOC of ultra-capacitor and battery.

the DC-bus voltage (V_{DC}) remains within the allowable deviation limit during the transient condition in SMGs, i.e., $\pm$ 10%. Moreover, as up till 2s load demand (P_{TL}) is less than the power produced by the diesel generator P_G, therefore, SOC of battery increases as verified from Fig. 3.17(c). In addition, as during transients ultra-capacitor contributes, hence, after every second, SOC of ultra-capacitor falls.

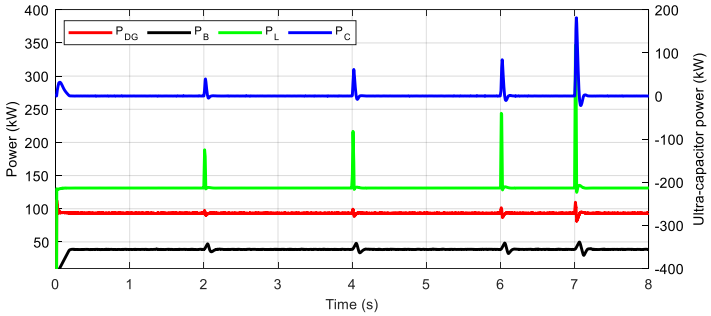

(a)

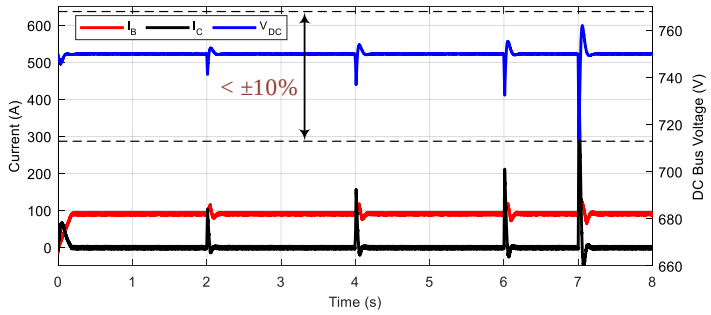

(b)

Figure. 3.18. Simulation results for pulsed load, (a) Power from sources and loads, (b) DC bus voltage, current of battery and ultra-capacitor.

3.8.2 Case Study B: Pulsating Load

The pulse load is interfaced to the DC-bus through the DC-DC converter as illustrated in Fig. 3.13. These loads such as electron-magnetic rail guns, high-power radars, and electromagnetic launch systems, will be part of future warships. As these loads draw several kW to MW power within ms-s, hence, can destabilize the microgrid [99]. Therefore, to tackle such pulsating loads integrating ESS devices (battery, ultra-capacitor, flywheel) is one of the possible solutions. The sole interfacing of the battery requires several kW to MW range battery banks, which may lead to increased stress as well. Further, C-rate charging and discharging limitations urge a need for a high power density storage device. Therefore, ultra-capacitor along with batteries are suitable candidates for future ships. In order to observe the impact on the DC bus voltage, several pulses with different power levels and pulse-width are taken into consideration. The pulse width in the case study is considered as 1ms with different power levels (100, 150, 200, 400 kW). It can be observed

from Fig. 3.18(a) that during pulsed load integration at 2, 4, 6, and 7s ultra-capacitor responds abruptly, thus powering the pulsed load and reducing the stress on the battery. Similarly, the current contribution of battery and ultra-capacitor showed in Fig. 3.18(b) illustrates the least and most contribution by the battery and ultra-capacitor respectively during transients or pulse load operation. In addition, it can be concluded that bus voltage remains within allowable limits.

3.9 Conclusion

The study has taken into account a hybrid electric ferry with a coordinated control strategy aiming at operating diesel generators within the specified range to minimize specific fuel consumption and reduce emissions. To achieve this, a bi-directional AC-DC converter is utilized by operating it using fixed and varying frequency operation during voyage mode. Moreover, the multi-mode control strategy helps to transit between different modes smoothly where during grid-connected operation conventional control scheme, i.e., P-f and Q-V is implemented. Further, S2X operation, where SMGs could be useful for exporting power back to the grid thus may help in frequency services, load shifting, storing power during low pricing and supplying during high pricing time, and so on. In addition, a coordination control scheme using a low-pass filter for a hybrid energy storage system is presented to tackle the pulsating loads and sudden load changes. Such an approach aids in minimizing stress on the battery and refraining from transients to propagate to the generator side.

Chapter 4

Shipboard-based Seaport Microgrid–Architecture and Control

This chapter summarizes the contribution made in the paper (Paper III) [103] and Paper IV [104]. A further detailed explanation along with results and outcomes can be found in the papers section.

4.1 Introduction

Cold-ironing is a process in which shore-side connection is provided to vessels at berth thus shutting down their auxiliary engines, therefore, bringing benefits in terms of minimizing emissions and noise pollution [105]. At present most of the seaports especially smaller ones are not equipped with cold-ironing features that provide power to the auxiliary loads of ships during their berth-in time. Such ports are generally local ports where mostly yachts, ferries, and smaller-sized cargo ships are berthed-in. Moreover, around 2400 inhabited Islands in the EU and UK territory exists that mainly belong to Italy, Denmark, Sweden, Germany, Greece, Spain, France, Estonia, and Portugal according to the European Parliament report published in 2021 [106]. These islands exist, which can have potentially their own ports and interfacing SMGs for providing col-ironing facilities could be part of such islands. Due to a vast number of Islands in the EU without any physical connection with the mainland, seaborne and airborne transportation plays a major role in dealing with the economies of such Islands of the EU. Among the aforementioned two sources of transportation of goods and passengers, there is a high dependency on ships due to their cost-effective nature. Such

sort of shipping is sometimes referred to as domestic shipping or short-sea shipping (SSS) [107]. According to the EU commission, SSS is defined as the transportation of goods from EU countries or territories to EU member countries, countries around the Baltic, Mediterranean, and Black sea areas where 1.8 billion tonnes of goods were transported in 2019 [107]– [108]. The surge in transportation through the sea will increase the number of marine vessels, which ultimately will pollute the environment if conventional fossil-fuel-based shipping along with ports are not retrofitted with RES and ESS. Due to the lack of availability of shore connection at the ports, auxiliary engines are kept online that are harmful to the environment especially for the inhabitants living closer to the port. However, at places where the grid is far from the seaport providing cold-ironing facilities from the grid is not considered to be a cost-effective solution. This chapter, therefore, addresses a novel solution to tackle this situation such that RES and ESS interfaced ships are utilized to provide cold-ironing facilities.

4.2 Architecture for Seaport Microgrid for Cold-ironing

The ships are interfaced with ESS (Lithium-ion), RES sources such as fuel cell stacks, and/or solar panels. Moreover, along with RES, some ships may have interfaced with diesel engines as well. Therefore, battery banks can be charged during the voyage during low-loading operation. The integration of RES and ESS interfaced SMGs together with the charging infrastructure placed at the port is termed as ships-based seaport microgrid (SBSM). The overall proposed architecture is shown in Fig. 4.1, which can fulfill the auxiliary load demands of an ICE-equipped ship along with charging batteries of electric ships upon deep discharge. Further, a cold-ironing facility on the basis of DC-distribution approach is utilized as most ESS and RES devices are DC interfaced that minimizing the conversion stages that occur in AC-based distribution and losses linked to these conversions. Such a type of novel architecture thus requires novel control strategies with autonomous and adaptive features.

4.3 Multi-mode Adaptive Control Strategy

Several ships particularly yachts and ferries are interfaced in parallel using charging infrastructure placed at the shore forming SBSM. The power-sharing methods in DC microgrids are categorized into centralized, master-slave, distributed, and decentralized approaches. In this study, power is shared among the peer ships based on adaptive decentralized droop control. Any contrast

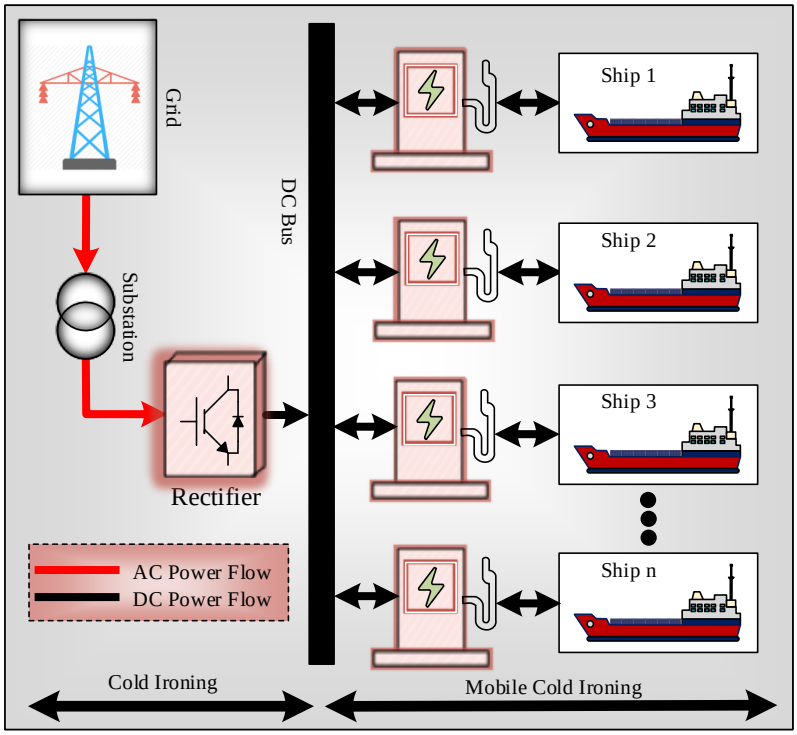

Figure. 4.1. Multi-ships power-sharing.

in the output voltage of SMGs will outcome in the circulating current to flow, therefore, to mitigate the circulating current to flow, a virtual resistance is integrated in the outer voltage-loop. The droop control in a DC-interfaced microgrid can be described as follows:

$$V_{\text{out}}{}^{*} = V_{\text{ref}} - I_{\text{out}} R_{\text{v}} \tag{4.1}$$

where $V_{out}{}^{*}$, V_{ref}, I_{out}, and R_v are the output voltage, reference voltage at no-load condition, output current, and the virtual resistance. To enhance the lifetime of batteries, optimal power-sharing, energy balancing, and to cope with unwanted power-sharing among several ships, modes are classified into six-modes based on the SOC of the battery and voltage of the DC-bus (V_{DC}) as shown in Fig. 4.2. These modes are referred to as variable current controlled charging mode, V-I droop modes, variable current controlled discharging mode, and extreme condition modes. The maximum allowable deviation in the voltage is set to be ± 5% of the reference voltage, i.e., V_{ref}, where V_{min}

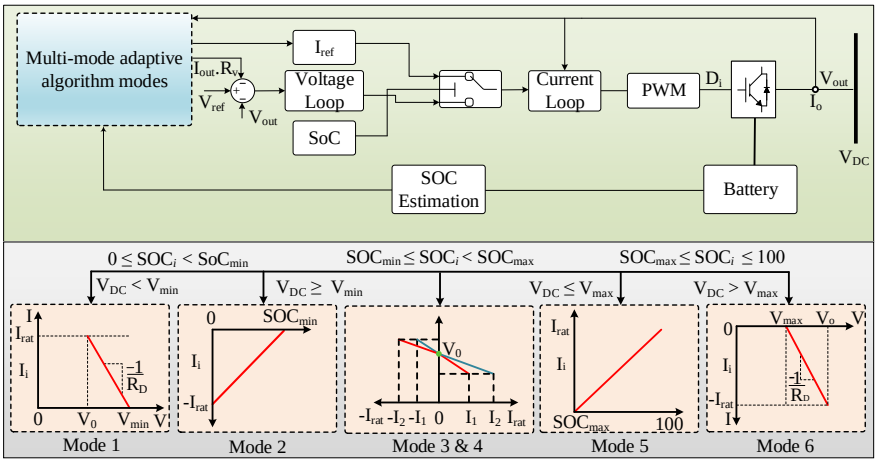

Figure. 4.2. Multi-mode adaptive algorithm.

refers to the minimum threshold limit whereas V_{max} refers to the maximum threshold limit.

The first mode is referred to as an extreme condition case in which generation sources such as PV and fuel cells are lacking and SOC of the battery bank of all SMGs falls below the minimum set threshold limit ($SOC_i < SOC_{min}$). Such a scenario will cause the DC-bus voltage to fall below V_{min} ($V_{DC} < V_{min}$), resulting in destabilizing the operation of the microgrid. To cope with this obstacle constant I-V droop method is attained, which limits power-sharing under such extreme conditions where reference current is calculated using (4.2) [104].

$$I_{\mathrm{j}}^{\mathrm{ref}} = \left(\frac{V_{\mathrm{min}} - V_{\mathrm{DC}}}{R_{\mathrm{v}}} \right), j = \{1, 2, ..., N\} \tag{4.2}$$

The second mode corresponds to variable current controlled charging mode illustrating that SOC of few SMGs is below the set minimum threshold limit ($0 \leq SOC_i < SOC_{min}$), where SOC_{min} represents minimum set threshold limit. Such a mode illustrates that the SOC of a few SMGs is deep discharged. Hence, SMG will start to consume power from the peer SMGs. In such a mode, DC bus voltage is less than ($V_{DC} \geq V_{min}$) illustrating that few SMGs are lacking in resources. Therefore, the reference current for such a scenario is calculated using (4.3) [104].

$$I_{\mathrm{j}}^{\mathrm{ref}} = I_{\mathrm{rat}} \left(\frac{SOC_{\mathrm{i}} - SOC_{\mathrm{min}}}{SOC_{\mathrm{min}}} \right), \{i, j\} = \{1, 2, ..., N\} \tag{4.3}$$

The third and fourth mode corresponds to V-I droop mode where SOC_i

of all SMGs are set above the minimum and maximum threshold limits ($SOC_{min} \leq SOC_i < SOC_{max}$, illustrating that each SMG is self-sufficient. Hence, there is no need to share power with the peer SMGs. The droop value of for charging and discharging modes are calculated using (4.4) and (4.5) respectively [104]. The double quadrant operation illustrates the extension of the traditional droop operation in which the first quadrant operation depicts the discharging-mode while the second quadrant shows the charging-mode.

On the other hand, if a diesel-equipped ship is berthed at the port and is required to power its auxiliary loads, each SMG starts to share following their SOC such that SMG with higher SOC shares the most, thus achieving proportional power-sharing.

$$R_{\text{charging}} = R_{\text{v}} \left(\alpha + \frac{SOC_{\text{i}} - SOC_{\text{min}}}{SOC_{\text{max}} - SOC_{\text{min}}} \right) \tag{4.4}$$

$$R_{\text{discharging}} = R_{\text{v}} \left(\beta - \frac{SOC_{\text{i}} - SOC_{\text{min}}}{SOC_{\text{max}} - SOC_{\text{min}}} \right) \tag{4.5}$$

where droop resistance is linearly varied from R_v to $2R_v$ such that $\alpha = 1$ and $\beta = 2$.

The fifth mode corresponds to variable current control discharging mode depicting that SOC of some of the SMGs rise above the maximum threshold limit $SOC_i \geq SOC_{max}$ outcomes in the DC-bus voltage rising above the reference value such that $V_{DC} \geq V_{ref}$. Hence, generation from RES can be utilized to charge the battery banks of peer SMGs. The reference current for such a case can be calculated using (4.6) [104].

$$I_{\text{j}}^{\text{ref}} = I_{\text{rat}} \left(\frac{SOC_{\text{i}} - SOC_{\text{max}}}{100 - SOC_{\text{max}}} \right), j = \{1, 2, ..., N\} \tag{4.6}$$

The sixth mode corresponds to an extreme condition mode when the SOC of every SMG are above the maximum set limit, i.e., $SOC_i > SOC_{max}$ resulting in an over voltage condition such that $V_{DC} > V_{max}$, which destabilizes the microgrid. To cope with such a situation, the constant I-V droop approach is used to limit power-sharing where reference current is calculated using (4.7) [104].

$$I_{\text{j}}^{\text{ref}} = \left(\frac{V_{\text{max}} - V_{\text{DC}}}{R_{\text{v}}} \right), j = \{1, 2, ..., N\} \tag{4.7}$$

Here, SOC of battery installed in each SMG is estimated using conventional Coulomb-counting approach as expressed in (4.8)

$$SOC(i)(t) = SOC(i)(t = 0) + \frac{1}{C_{\text{b}}} \int_0^t (V_{\text{in}}.I_{\text{i(in)}} - V_{\text{DC}}.I_{\text{i(o)}})dt \tag{4.8}$$

Table 4.1. Parameters taken into consideration in case studies.

Parameters	**Values**
Number of SMGs	4
Rated power of each converter	$2.2kW$
DC bus voltage	$220V$
Rated value of current	5A
Virtual resistance	1.9Ω
Minimum SOC limit	30%
Maximum SOC limit	80%
Inductance of each converter	$3.6mH$
Capacitance of DC bus	$3300\mu F$

where $SOC(i)(t = 0)$ represents initial SOC at time zero, C_b is capacity of battery bank (Wh), $I_{i(out)}$, $I_{i(in)}$ are the output current and the input current supplied, which is supplied by the RES (PV, fuel cell) onboard.

4.4 Simulation Results and Discussion

To implement the proposed adaptive control strategy for power-sharing between different SMGs interfaced with charging infrastructure placed onshore, we have taken several case studies that are performed in a SIMULINK environment along with its experimental verification in form of hardware-in-the-loop (HIL). Four SMGs equipped with ESS and/or RES-based sources are considered that are interconnected to each other using a charging station placed onshore, thus creating a DC bus. The parameters taken into consideration in this study are shown in Table. 4.1.

4.4.1 Case Study A

The first scenario corresponds to when each SMG is in the V-I droop mode, referring to Mode 4 such that SOC of all SMGs lies within the minimum and maximum set threshold limit, i.e., $SOC_{min} \leq SOC_i < SOC_{max}$. Such a scenario demonstrates that each SMG is self-sufficient and hence no power-sharing is needed, thus avoiding unnecessary losses and usage of battery, as each SMG can run its auxiliary loads indigenously. Therefore, when all SMGs are self-sufficient, the multi-mode control algorithm adapts to Mode 3 and Mode 4 as shown in Fig. 4.3, where DC bus voltage remains to the nominal value. The SOC of battery banks in this scenario is considered to be $SMG_{1(t=0)}$=35%, $SMG_{2(t=0)}$=50%, $SMG_{3(t=0)}$=65%, and $SMG_{4(t=0)}$=79%. It can be seen from

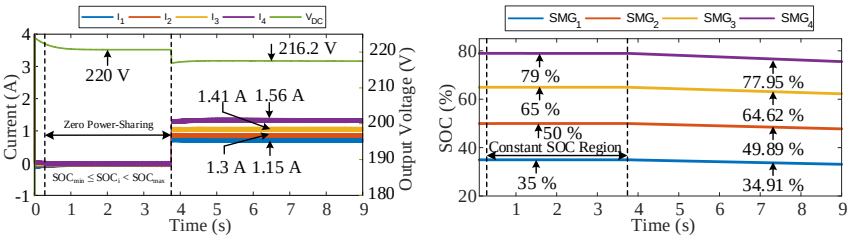

Figure. 4.3. Simulation results for case study A (a) Current sharing for each SMG and voltage of the DC-bus, (b) SOC of SMGS.

Fig. 4.3(a) that up till 3.75s SOC of SMGs are within the boundary limits due to which current sharing is zero and hence, SOC remains constant. At 3.75s, SMG equipped with diesel generator connects with the main bus and demands to power its auxiliary loads. Therefore, each SMG starts to share power in accordance with their SOC such that SMG with the lowest SOC (SMG_4) shares the least current as shown in Fig. 4.3(a). Owing to the highest current sharing of SMG_4, the SOC of SMG_4 falls the most as verified from Fig. 4.3(b).

4.4.2 Case Study B

The second case corresponds to when one of the SMG is in variable current-controlled charging mode (Mode 2) indicating that this SMG is lacking in resources, i.e., $0 \leq SOC_i < SOC_{min}$ whereas SOC of other SMGs, in this case, is considered to be within minimum and maximum set limits. To verify this case study, we have taken into account that the initial SOC of SMG_1 as 5% whereas the SOC of the rest of SMGs is set to be 50, 65, and 79% respectively. The current sharing of each SMG is illustrated in Fig. 4.4(a), where SMG_1 is absorbing while SMG_2 to SMG_4 are supplying the current. Further, it can be observed that owing to have the lowest and highest SOC of SMG_1 and SMG_4, the current sharing is highest (1.53A) and lowest (1.21A) respectively. In such a scenario, V_{DC} falls below the reference voltage, which keeps on increasing upon charging. Moreover, Fig. 4.4(b) illustrates that SOC of SMG_2 to SMG_4 decreases the least and the most respectively whereas SOC of SMG_1 keeps on increasing.

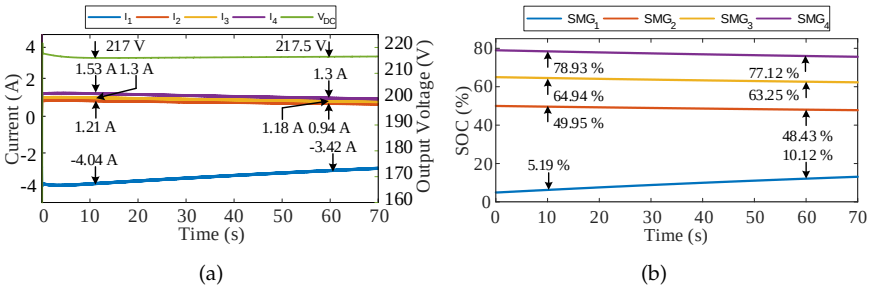

Figure. 4.4. Simulation results for case study B (a) Current sharing for each SMG and voltage of the DC-bus, (b) SOC of SMGS

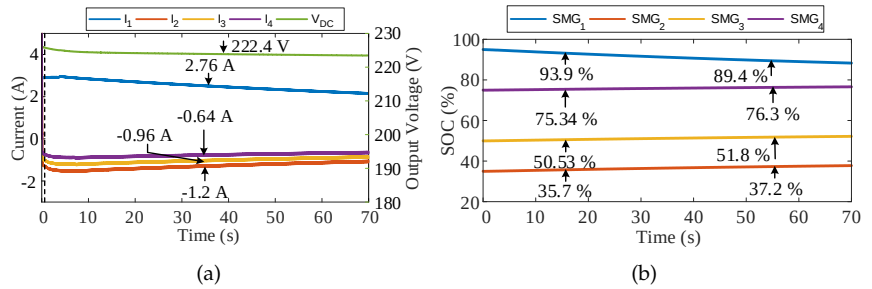

Figure. 4.5. Simulation results for case study C (a) Current sharing for each SMG and voltage of the DC-bus, (b) SOC of SMGS

4.4.3 Case Study C

The third case study illustrates when one of the SMGs is in variable current-controlled discharging scenario whereas SOC of rest of SMGs is within the range of set minimum and maximum threshold limits, referring to Mode 5 as illustrated in Fig. 4.5. The SOC of battery banks in this scenario is considered to be $SMG_{1(t=0)}$=95%, $SMG_{2(t=0)}$=35%, $SMG_{3(t=0)}$=50%, and $SMG_{4(t=0)}$=75%. It can be verified from Fig. 4.5(a) that SMG_1 starts to share power with peer SMGs resulting in a rise in the SOC. As a result, SMG with the lower SOC (SMG_2) will try to take in the highest current (1.2A) whereas SMG with the highest SOC (SMG_3) absorbs the least current (0.64A) where the negative sign indicates the battery is charging. Further, such a scenario with abundant resources causes bus voltage to rise above the nominal value as illustrated in Fig. 4.5(a). Moreover, it can be verified from Fig. 4.5(b) that δ_{SMG_3} (0.96%) is lowest while δ_{SMG_1} (1.5%) indicating the highest rise in SOC.

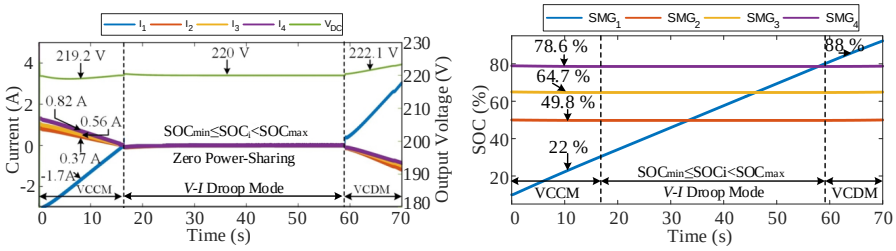

Figure. 4.6. Simulation results for case study D (a) Current sharing for each SMG and voltage of the DC bus, (b) SOC of SMGS

4.4.4 Case Study D

This case refers to inter-mode transition, in order to verify such a scenario the initial SOC of SMGs are assumed as: $SMG_{1(t=0)}$=10%, $SMG_{2(t=0)}$=50%, $SMG_{3(t=0)}$=65%, and $SMG_{4(t=0)}$=79%. As SMG_1 is operating in the start in variable current charging mode (Mode 2), hence, it will absorb power from peer SMGs. Further, excessive power generated by RES such as fuel cell or PV panels in this SMG is considered. Therefore, power absorbed by nearby SMGs and RES will result in increase in SOC and upon reaching the minimum threshold power-sharing will be zero. As at this insistent all SMGs are within the set minimum and maximum threshold limits i.e., $SOC_{min} \leq SOC_i < SOC_{max}$, hence avoiding unnecessary power sharing as shown in Fig. 4.6(a). In addition, RES in SMG_1 keeps on charging and as soon it reaches the maximum threshold limit ($SOC_i \geq SOC_{max}$), the mode 5 variable current discharging mode starts. The current will be share now in accordance with (4.7) such that SOC with higher SMG_i shares the most. The variation in SOC of each SMG_i in inter mode transition can be visualized from Fig. 4.6(b). It can be observed that SOC remains constant when SOC falls within the minimum and maximum threshold limits.

4.4.5 Case Study E

This case study illustrates two extreme condition scenarios when either all SMGs are deficient or abundant in resources corresponding to Mode 1 and Mode 6 respectively. Therefore, to stabilize the microgrid, constant *I-V* droop mode helps in restricting power-sharing thus limiting the bus voltage V_{DC} to lower and higher threshold limit as illustrated in Fig. 4.7. It can be visualized from Fig. 4.7(a) that SOC of all SMGs lies below the set minimum threshold limit ($SOC_i < SOC_{min}$). Hence, the DC-bus voltage is limited to lower limit

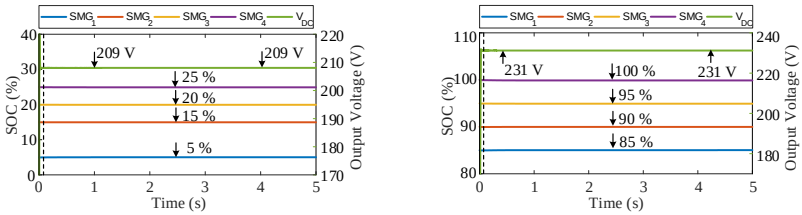

(a) (b)

Figure. 4.7. Simulation results for case study E (a) Current sharing for each SMG and voltage of the DC-bus, (b) SOC of SMGS

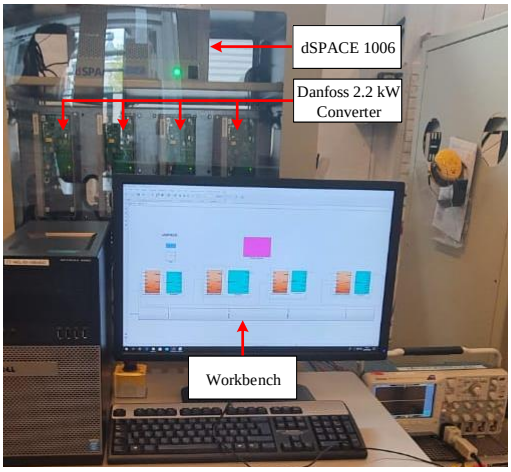

Figure. 4.8. Experimental setup.

(V_{min}) by limiting power-sharing. On the other hand, when SOC of all *SMGs* are above the set maximum threshold limit ($SOC_i > SOC_{max}$) as illustrated in Fig. 4.7(b), the bus voltage will be limited to higher threshold limit (V_{max}).

4.5 Experimental results

In order to support the proposed approach experimentally using HIL, dSPACE 1006 platform is utilized for a real time control as illustrated in Fig. 4.8.

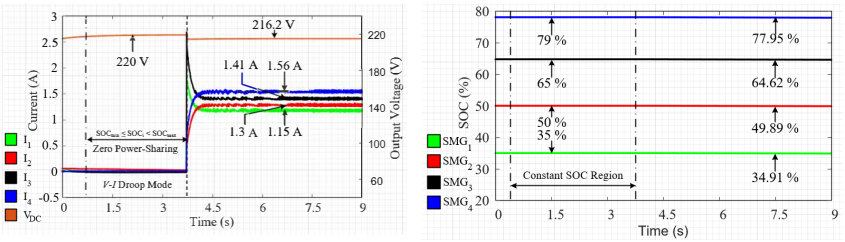

(a) (b)

Figure. 4.9. Experimental results for case study A (a) Current sharing for each SMG and voltage of the DC-bus, (b) SOC of SMGS

4.5.1 Case Study A

HIL results for a scenario when all SMGs lies within the minimum and maximum set threshold boundaries referring to Mode 4 with and without load can be visualized from Fig. 4.9. It can be seen from Fig. 4.9 that up till 3.7s there is zero power-sharing depicting that all SMGs are self-sufficient and within their boundary limits. As soon as a ship equipped with ICE docked at the port and connects with the microgrid in order to operate auxiliary loads onbaord. SMGs start sharing power in accordance to their SOCs such that SOC of SMG_1 shares the least current whereas SOC of SMG_4 shares the highest current. Due to the fact that there is zero power-sharing, hence, DC bus voltage remain at the nominal value as illustrated in Fig. 4.9(a). In addition, it can be verified from Fig. 4.9(b) that SOC remains constant in the starting region whereas in later region SOC of SMG_4 and SMG_1 drops the most and least respectively.

4.5.2 Case Study B

To verify the mode 2, where one SMG is deficient in its resources depicting that SOC of SMG is below the set minimum threshold limit. The initial SOC of SMGs are assumed as: $SMG_{1(t=0)}$=5%, $SMG_{2(t=0)}$=50%, $SMG_{3(t=0)}$=65%, and $SMG_{4(t=0)}$=79%. In such a scenario, peer SMGs with abundant resources shares power following their SOC as shown in Fig. 4.10(a) to the SMG with SOC lower than the threshold limit. The reference of current for such a case can be calculated using (4.2). In addition, bus voltage (V_{DC}) remains within allowable limit, i.e., $V_{DC} > V_{min}$ Additionally, it can be seen from Fig. 4.10(b) that δ_{SMG4} falls more i.e., 1.81 % in comparison with δ_{SMG2}, i.e., 1.5%.

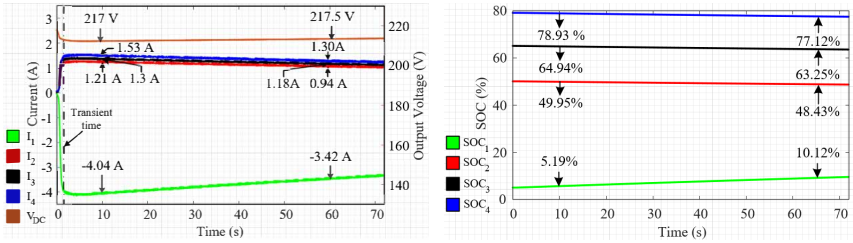

(a) (b)

Figure. 4.10. Experimental results for case study B (a) Current sharing for each SMG and voltage of the DC-bus, (b) SOC of SMGS

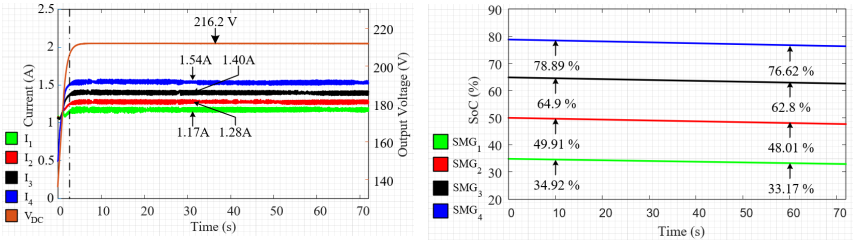

(a) (b)

Figure. 4.11. Experimental results for case study C (a) Current sharing for each SMG and voltage of the DC-bus, (b) SOC of SMGS

4.5.3 Case Study C

This case study shows the scenario where SMGs are providing mobile-cold-ironing features as illustrated in Fig. 4.9. In this scenario, all SMGs lies within minimum and maximum set threshold limit supplying power to an ICE-based ship to power its auxiliary load. The initial SOC of SMGs are assumed as: $SMG_{1(t=0)}$=35%, $SMG_{2(t=0)}$=50%, $SMG_{3(t=0)}$=65%, and $SMG_{4(t=0)}$=79%. It is verified from Fig. 4.11(a) that SMG_4 shares the highest current owing to have highest SOC where SMG_1 shares the least. Likewise, it can be observed from Fig. 4.11(b) that SOC of SMG_1 fall the least and SMG_4 falls the most.

4.6 Conclusion

In this chapter, a ships based seaport architecture and control of seaport microgrid is proposed for smaller seaports where electrifying ports through

national grid requires huge investment cost. As modernized ships are being equipped with RES and ESS devices for efficient and minimal emission along with DC-based architecture, therefore, DC-based architecture provides ease in the interface along with minimal conversion stages. Moreover, for state of charge balancing, power-sharing, and providing mobile-cold ironing facilities, a multi-mode decentralized droop control is proposed for proportional power-sharing. In addition, multi-mode droop control helps in avoiding unnecessary power-sharing thus avoiding losses involved in distribution when SMGs are self-sufficient.

Chapter 5

Conclusions and Future Works

The key contributions and outcomes of this Ph.D. study are summarized in this chapter. In addition, several recommendations are presented in terms of future study.

5.1 Conclusions

In the first chapter, shipboard microgrids (SMGs) are introduced together with a comparison with the terrestrial microgrids (TMGs). It is inferred that SMGs behave like a conventional TMG with a difference in terms of sources and loads. As loads in SMG dominates with highly dynamic loads such as propulsion motors and highly pulsating loads such as electromagnetic guns, radars, etc. On the other hand, sources in conventional SMGs are dominated by internal combustion engine (ICE)-based sources, which in modernized SMGs are being partially or fully replaced with ESS and/or RES. Moreover, challenges in conventional SMGs such as lack of cold-ironing facilities and charging infrastructure along with low-loading concerns of ICE base sources are discussed in this chapter.

In the second chapter, state-of-the-art for SMGs are presented where different architectures are classified based on distribution, network configuration, and propulsion system. It is inferred that conventional AC interfaced SMGs are being replaced/retrofitted with hybrid AC/DC-based distribution architecture. In contrast, newly build electric-ships are DC interfaced knowing the fact that most energy storage devices and RES are DC-driven. Moreover, the lack of reactive power compensation and ease in parallel connection are some of the other advantages of DC-based SMGs. In addition, this

chapter also provides different ESS being utilized or have the tendency to be used in the new generation SMGs. Currently, mostly either LFP and NMC based Lithium chemistries are being utilized in electric cars as well as in electric ships due to their high energy density, longer lifetime, higher cycles, and fast charging and discharging capabilities. Moreover, due to the involvement of highly fluctuating and pulsating loads urges a need for high power density devices such as flywheels and ultra-capacitors to tackle peak demands. Additionally, the benefits ESS brings to SMGs along with the different types of electric ships are part of this chapter. Besides, zero-emission shipping (100% battery-equipped), integrating ESS with conventional ICE-based sources brings several benefits such as the use of ESS during emergency purposes, regenerative braking, load leveling, spinning reserve, peak shaving, and so on. This chapter also presents coordination control schemes used for power-sharing in a decentralized manner.

In the third chapter, a multi-mode coordination control scheme is presented with the aim of minimizing fuel consumption by operating onboard generators within a specified operating range in a hybrid AC/DC architecture. The multi-mode control scheme helps to transit between islanded and grid-connected modes smoothly. With around 50 vehicle-to-grid successful projects around the world, this study also presents the Ship-to-X approach, where MWh range battery banks of SMGs can be used to export power to grid, nearby ships, and seaport. In addition coordination control scheme for hybrid energy storage system is presented that tackles the pulsating and sudden load changes, therefore aiding in reduced stress on battery banks, thus increasing its lifetime.

In the fourth chapter, a novel solution is presented to provide a cold-ironing facility using electric ships for smaller ports, particularly for remote islands. Additionally, a coordination control scheme with multi-mode features is presented to share power following their resources in a decentralized manner. Such an approach can be executed using a public-private partnership or through incentivizing owners of ship having battery-equipped ferries or yachts. This will bring fringe benefits in terms of minimizing emissions from the transportation-sector and also help in generating a sustainable solution involving greener ports, thus allowing ship owners to contribution to the blue growth. The proposed microgrid encompasses two cost components, a) infrastructure cost installed at the port, and b) shipboard microgrids cost. The cost of equipment for charging stations placed on the shore will be borne by the seaport itself and in return, the seaport may get benefits in terms of parking charges. One of the key benefits for the shipowner might be in terms of tax reductions/exemptions that are generally one-time or annually based taxes mostly paid while purchasing the ship. Other benefits that customers can avail of include a partial reduction in parking facilities charges at the seaport. Further, owing to having an emission-free ship the shipowner

will not have to pay any carbon tax. The shipowner will charge for selling its energy to their peers. For instance, if a shipowner has his yacht at the seaport and is equipped with PV panels, it will keep on generating power during the daytime, which if remain unused or not shared may get wasted and the shipowner will have to curtail PV panels. On the other hand, the shipowner may get benefited by supplying this energy to other peers and may earn an amount. Similarly, if the buyer owns a diesel-equipped ship and is required with a cold-ironing facility during the berth-in time, its auxiliary engine needs to be turned off otherwise he may have to pay a carbon tax. So, instead of paying in terms of tax, the shipowner may buy energy from peers. However various practical challenges including, technical challenges including smart-metering, economic feasibility along with an energy management system need to be addressed. The authors intend to extend their work in this direction in their future studies.

5.2 Future work

- The coordination scheme for multi-ships power-sharing in this study is limited to an islanded operation with primary control layer only. The future study will involve a hierarchical control scheme incorporating an energy management system at the tertiary level for the economic dispatch of multi-sources.
- The ships-based seaport microgrid proposed in the study is based on DC architecture. However, traditional ships are still equipped with AC-based distribution, therefore, hybrid AC/DC-based architecture may be used which can bring benefits in terms of space-saving onboard ships.
- In addition, integration of RES such as PV and fuel cell together with ESS in next-generation ships will help to support weaker grids particularly self-sustained islands disconnected from the mainland. The islands such as Ærø, that are equipped with RES can be supported by absorbing and supplying power during grid-connected on port operations using SMGs. Therefore, future study will explore SMG as a candidate for providing ancillary services such as peak shaving and frequency services to RES interfaced islands. Such an approach will help to improve stability and power quality of the grid and may bring profits for shipowners by absorbing surplus power during off peak hours and selling during peak hours.

Bibliography

[1] G. Rentier, H. Lelieveldt, and G. J. Kramer, "Varieties of coal-fired power phase-out across europe," *Energy Policy*, vol. 132, pp. 620–632, 2019.

[2] T. J. McCoy, "Electric ships past, present, and future [technology leaders]," *IEEE Electrification Magazine*, vol. 3, no. 2, pp. 4–11, 2015.

[3] T. Oetiker, "Share of transport greenhouse gas emissions," https://www.eea.europa.eu/data-and-maps/indicators/transport-emissions-of-greenhouse-gases/transport-emissions-of-greenhouse-gases-12.

[4] "Third imo ghg study 2014," https://www.imo.org/en/OurWork/Environment/Pages/Greenhouse-Gas-Studies-2014.aspx, 2014.

[5] "Fourth imo ghg study 2020," https://www.imo.org/en/OurWork/Environment/Pages/Greenhouse-Gas-Studies-2014.aspx, 2020.

[6] D. E. Olivares, A. Mehrizi-Sani, A. H. Etemadi, C. A. Cañizares, R. Iravani, M. Kazerani, A. H. Hajimiragha, O. Gomis-Bellmunt, M. Saeedifard, R. Palma-Behnke *et al.*, "Trends in microgrid control," *IEEE Transactions on smart grid*, vol. 5, no. 4, pp. 1905–1919, 2014.

[7] M. U. Mutarraf, Y. Guan, C.-L. Su, Y. Terriche, M. Nasir, J. C. Vasquez, and J. M. Guerrero, "Adaptive power management of hierarchical controlled hybrid shipboard microgrids," *IEEE Access*, vol. 10, pp. 21 397–21 411, 2022.

[8] E. Skjong, R. Volden, E. Rødskar, M. Molinas, T. A. Johansen, and J. Cunningham, "Past, present, and future challenges of the marine vessel's electrical power system," *IEEE Transactions on Transportation Electrification*, vol. 2, no. 4, pp. 522–537, 2016.

[9] B. Jabeck, "The impact of generator set underloading," https://www.cat.com/en_US/by-industry/electric-power/Articles/White-papers/the-impact-of-generator-set-underloading.html, 2003.

[10] T. Waris and C. Nayar, "Variable speed constant frequency diesel power conversion system using doubly fed induction generator (dfig)," in *2008 IEEE Power Electronics Specialists Conference*. IEEE, 2008, pp. 2728–2734.

[11] B. Zahedi and L. E. Norum, "Voltage regulation and power sharing control in ship lvdc power distribution systems," in *2013 15th European Conference on Power Electronics and Applications (EPE)*. IEEE, 2013, pp. 1–8.

[12] Z. Jin, L. Meng, J. C. Vasquez, and J. M. Guerrero, "Specialized hierarchical control strategy for dc distribution based shipboard microgrids: A combination of emerging dc shipboard power systems and microgrid technologies," in *IECON 2017-43rd Annual Conference of the IEEE Industrial Electronics Society*. IEEE, 2017, pp. 6820–6825.

[13] Z. Jin, L. Meng, J. M. Guerrero, and R. Han, "Hierarchical control design for a shipboard power system with dc distribution and energy storage aboard future more-electric ships," *IEEE Transactions on Industrial Informatics*, vol. 14, no. 2, pp. 703–714, 2017.

[14] X. Zhaoxia, Z. Tianli, L. Huaimin, J. M. Guerrero, C.-L. Su, and J. C. Vásquez, "Coordinated control of a hybrid-electric-ferry shipboard microgrid," *IEEE Transactions on Transportation Electrification*, vol. 5, no. 3, pp. 828–839, 2019.

[15] T. Van Vu, D. Gonsoulin, F. Diaz, C. S. Edrington, and T. El-Mezyani, "Predictive control for energy management in ship power systems under high-power ramp rate loads," *IEEE Transactions on Energy Conversion*, vol. 32, no. 2, pp. 788–797, 2017.

[16] N. B. B. Ahamad, J. M. Guerrero, C.-L. Su, J. C. Vasquez, and X. Zhaoxia, "Microgrids technologies in future seaports," in *2018 IEEE International Conference on Environment and Electrical Engineering and 2018 IEEE Industrial and Commercial Power Systems Europe (EEEIC/I&CPS Europe)*. IEEE, 2018, pp. 1–6.

[17] N. B. Ahamad, M. Othman, J. C. Vasquez, J. M. Guerrero, and C.-L. Su, "Optimal sizing and performance evaluation of a renewable energy based microgrid in future seaports," in *2018 IEEE international conference on industrial technology (ICIT)*. IEEE, 2018, pp. 1043–1048.

[18] S. G. Jayasinghe, L. Meegahapola, N. Fernando, Z. Jin, and J. M. Guerrero, "Review of ship microgrids: System architectures, storage technologies and power quality aspects," *inventions*, vol. 2, no. 1, p. 4, 2017.

[19] M.-H. Khooban, T. Dragicevic, F. Blaabjerg, and M. Delimar, "Shipboard microgrids: A novel approach to load frequency control," *IEEE Transactions on Sustainable Energy*, vol. 9, no. 2, pp. 843–852, 2017.

[20] K. Mahmud, M. S. Rahman, J. Ravishankar, M. J. Hossain, and J. M. Guerrero, "Real-time load and ancillary support for a remote island power system using electric boats," *IEEE Transactions on Industrial Informatics*, vol. 16, no. 3, pp. 1516–1528, 2019.

[21] J. G. Ciezki and R. W. Ashton, "Selection and stability issues associated with a navy shipboard dc zonal electric distribution system," *IEEE Transactions on power delivery*, vol. 15, no. 2, pp. 665–669, 2000.

[22] "Ieee recommended practice for electrical installations on shipboard— design," *IEEE, IEEE Std 45.1–2017*, 2017.

[23] Y. Terriche, C.-L. Su, M. U. Mutarraf, M. Mehrzadi, A. Lashab, J. M. Guerrero, and J. C. Vasquez, "Harmonics mitigation in hybrid ac/dc shipboard microgrids using fixed capacitor-thyristor controlled reactors," in *2020 IEEE International Conference on Environment and Electrical Engineering and 2020 IEEE Industrial and Commercial Power Systems Europe (EEEIC/I&CPS Europe)*. IEEE, 2020, pp. 1–6.

[24] Z. Jin, G. Sulligoi, R. Cuzner, L. Meng, J. C. Vasquez, and J. M. Guerrero, "Next-generation shipboard dc power system: Introduction smart grid and dc microgrid technologies into maritime electrical netowrks," *IEEE Electrification Magazine*, vol. 4, no. 2, pp. 45–57, 2016.

[25] H. E. Gelani, F. Dastgeer, M. Nasir, S. Khan, and J. M. Guerrero, "Ac vs. dc distribution efficiency: Are we on the right path?" *Energies*, vol. 14, no. 13, p. 4039, 2021.

[26] ABB, "Onboard dc grid–the step forward in power generation and propulsion," 2011.

[27] X. Liu, P. Wang, and P. C. Loh, "A hybrid ac/dc microgrid and its coordination control," *IEEE Transactions on smart grid*, vol. 2, no. 2, pp. 278–286, 2011.

[28] J. F. Hansen, J. O. Lindtjørn, K. Vanska, and O. Abb, "Onboard dc grid for enhanced dp operation in ships," in *Dynamic Positioning Conference, Houston*, 2011.

[29] G. Sulligoi, D. Bosich, A. Vicenzutti, and Y. Khersonsky, "Design of zonal electrical distribution systems for ships and oil platforms: Control systems and protections," *IEEE Transactions on Industry Applications*, vol. 56, no. 5, pp. 5656–5669, 2020.

[30] G. Sulligoi, A. Vicenzutti, and R. Menis, "All-electric ship design: From electrical propulsion to integrated electrical and electronic power systems," *IEEE Transactions on transportation electrification*, vol. 2, no. 4, pp. 507–521, 2016.

[31] N. Doerry, J. Amy, and C. Krolick, "History and the status of electric ship propulsion, integrated power systems, and future trends in the us navy," *Proceedings of the IEEE*, vol. 103, no. 12, pp. 2243–2251, 2015.

[32] T. J. McCoy, "Trends in ship electric propulsion," in *IEEE Power Engineering Society Summer Meeting,*, vol. 1. IEEE, 2002, pp. 343–346.

[33] R. Geertsma, R. Negenborn, K. Visser, and J. Hopman, "Design and control of hybrid power and propulsion systems for smart ships: A review of developments," *Applied Energy*, vol. 194, pp. 30–54, 2017.

[34] S.-Y. Kim, S. Choe, S. Ko, and S.-K. Sul, "A naval integrated power system with a battery energy storage system: Fuel efficiency, reliability, and quality of power." *IEEE electrification magazine*, vol. 3, no. 2, pp. 22–33, 2015.

[35] G. Castles, G. Reed, A. Bendre, and R. Pitsch, "Economic benefits of hybrid drive propulsion for naval ships," in *2009 IEEE electric ship technologies symposium*. IEEE, 2009, pp. 515–520.

[36] Y. Yuan, J. Wang, X. Yan, B. Shen, and T. Long, "A review of multi-energy hybrid power system for ships," *Renewable and Sustainable Energy Reviews*, vol. 132, p. 110081, 2020.

[37] Flexibility with hybrid marine propulsion systems. Accessed: May 31, 2022. [Online]. Available: https://www.man-es.com/marine/solutions/hybrid-marine-propulsion-systems

[38] M. C. Argyrou, P. Christodoulides, and S. A. Kalogirou, "Energy storage for electricity generation and related processes: Technologies appraisal and grid scale applications," *Renewable and Sustainable Energy Reviews*, vol. 94, pp. 804–821, 2018.

[39] M. U. Mutarraf, Y. Terriche, K. A. K. Niazi, J. C. Vasquez, and J. M. Guerrero, "Energy storage systems for shipboard microgrids—a review," *Energies*, vol. 11, no. 12, p. 3492, 2018.

[40] Energy storage technologies. Accessed: May 31, 2022. [Online]. Available: https://www.imperial.ac.uk/grantham/energy-storage/

[41] L. Farrier, P. Wu, and R. Bucknall, "Opportunities and constraints of electrical energy storage systems in ships." Low Carbon Shipping & Shipping in Changing Climates, 2017.

[42] B. Guellard, X. de Montgros, P. P. De La Barriere, G. Wolfensberger, and P. D'oliveira, "An overview of electric and solar boats market in france," in *2013 World Electric Vehicle Symposium and Exhibition (EVS27)*. IEEE, 2013, pp. 1–13.

[43] X.-G. Yang, T. Liu, and C.-Y. Wang, "Thermally modulated lithium iron phosphate batteries for mass-market electric vehicles," *Nature Energy*, vol. 6, no. 2, pp. 176–185, 2021.

[44] Y. Lu and J. Chen, "Prospects of organic electrode materials for practical lithium batteries," *Nature Reviews Chemistry*, vol. 4, no. 3, pp. 127–142, 2020.

[45] H. Ali, H. A. Khan, and M. G. Pecht, "Circular economy of li batteries: Technologies and trends," *Journal of Energy Storage*, vol. 40, p. 102690, 2021.

[46] M. Khodaparastan and A. Mohamed, "Flywheel vs. supercapacitor as wayside energy storage for electric rail transit systems," *Inventions*, vol. 4, no. 4, p. 62, 2019.

[47] Y. Tang and A. Khaligh, "On the feasibility of hybrid battery/ultracapacitor energy storage systems for next generation shipboard power systems," in *2010 IEEE Vehicle Power and Propulsion Conference*. IEEE, 2010, pp. 1–6.

[48] H. Chen, Z. Zhang, C. Guan, and H. Gao, "Optimization of sizing and frequency control in battery/supercapacitor hybrid energy storage system for fuel cell ship," *Energy*, vol. 197, p. 117285, 2020.

[49] J. Hou, J. Sun, and H. F. Hofmann, "Mitigating power fluctuations in electric ship propulsion with hybrid energy storage system: Design and analysis," *IEEE Journal of Oceanic Engineering*, vol. 43, no. 1, pp. 93–107, 2017.

[50] J. Hou, J. Sun, and H. Hofmann, "Battery/flywheel hybrid energy storage to mitigate load fluctuations in electric ship propulsion systems," in *2017 American Control Conference (ACC)*. IEEE, 2017, pp. 1296–1301.

[51] ——, "Control development and performance evaluation for battery/flywheel hybrid energy storage solutions to mitigate load fluctuations in all-electric ship propulsion systems," *Applied energy*, vol. 212, pp. 919–930, 2018.

[52] J. Hou, Z. Song, H. F. Hofmann, and J. Sun, "Control strategy for battery/flywheel hybrid energy storage in electric shipboard microgrids," *IEEE Transactions on Industrial Informatics*, vol. 17, no. 2, pp. 1089–1099, 2020.

[53] J. Arseneaux, "20 MW flywheel frequency regulation plant," Hazle Spindle LLC, Hazleton, PA (United States), Tech. Rep., 2015.

[54] Abb substations and wayside energy storage system support metro in poland. Accessed: May 31, 2022. [Online]. Available: https://new.abb.com/news/detail/46010/abb-substations-and-wayside-energy-storage-system-support-metro-in-poland

[55] Supercapacitor energy storage system for an all-electric ferry–case study. Accessed: May 31, 2022. [Online]. Available: https://www.nidec-industrial.com/document/supercapacitor-energy-storage-system-electric-ferry-case-study/

[56] E. V. Palconit and M. L. S. Abundo, "Electric ferry ecosystem for sustainable inter-island transport in the philippines: a prospective simulation for davao city–samal island route," *International Journal of Sustainable Energy*, vol. 38, no. 4, pp. 368–381, 2019.

[57] S. R. Sæther and E. Moe, "A green maritime shift: Lessons from the electrification of ferries in norway," *Energy Research & Social Science*, vol. 81, p. 102282, 2021.

[58] Rules for classification ships. Accessed: May 31, 2022. [Online]. Available: https://rules.dnv.com/docs/pdf/DNV/RU-SHIP/2015-10/DNVGL-RU-SHIP-Pt6Ch2.pdf

[59] C.-L. Su, J. M. Guerrero, and S.-H. Chen, "Happiness is a hybrid-electric: A diesel-burning boat finds new life with a direct-current microgrid," *IEEE Spectrum*, vol. 56, no. 8, pp. 42–47, 2019.

[60] M. U. Mutarraf, Y. Guan, C.-L. Su, L. Xu, , J. C. Vasquez, and J. M. Guerrero, "Electric cars, ships, and their charging infrastructure – a comprehensive review," *Sustainable Energy Technologies and Assessments.*, vol. 52, no. 102177, 2022.

[61] J. Yuan and V. Nian, "A preliminary evaluation of marinized offshore charging stations for future electric ships," 2020.

[62] G. Guidi, J. A. Suul, F. Jenset, and I. Sorfonn, "Wireless charging for ships: High-power inductive charging for battery electric and plug-in hybrid vessels," *IEEE Electrification Magazine*, vol. 5, no. 3, pp. 22–32, 2017.

[63] R. Bergqvist, M. Turesson, and A. Weddmark, "Sulphur emission control areas and transport strategies-the case of sweden and the forest industry," *European Transport Research Review*, vol. 7, no. 2, p. 10, 2015.

[64] L. Register, "Understanding exhaust gas treatment systems–guidance for ship owners and operators," *London: Lloyd's Register*, 2012.

[65] A. Innes and J. Monios, "Identifying the unique challenges of installing cold ironing at small and medium ports–the case of aberdeen," *Transportation Research Part D: Transport and Environment*, vol. 62, pp. 298–313, 2018.

[66] Shore power. Accessed: May 31, 2022. [Online]. Available: https://glomeep.imo.org/technology/shore-power/"

[67] D. Paul, V. Haddadian, B. Chavdarian, and K. Peterson, "Low-voltage shore connection power systems," in *2017 IEEE/IAS 53rd Industrial and Commercial Power Systems Technical Conference (I&CPS)*. IEEE, 2017, pp. 1–6.

[68] R. Bernacchi. Connecting low power consumption vessels to shore-to-ship power facilities. Accessed: May 31, 2022. [Online]. Available: https://search.abb.com/library/Download.aspx?DocumentID=9AKK107680A0195&LanguageCode=en&DocumentPartId=&Action=Launch&elqTrackId=b52ebc85b2664ccdaabc26fb1be2665c&elqaid=1667&elqat=2

[69] A. Rolán, P. Manteca, R. Oktar, and P. Siano, "Integration of cold ironing and renewable sources in the barcelona smart port," *IEEE Transactions on Industry Applications*, vol. 55, no. 6, pp. 7198–7206, 2019.

[70] Ellen ferry. Accessed: May 31, 2022. [Online]. Available: http://e-ferryproject.eu/

[71] E. A. Sciberras, B. Zahawi, D. J. Atkinson, A. Juandó, and A. Sarasquete, "Cold ironing and onshore generation for airborne emission reductions in ports," *Proceedings of the Institution of Mechanical Engineers, Part M: Journal of Engineering for the Maritime Environment*, vol. 230, no. 1, pp. 67–82, 2016.

[72] S. G. Jayasinghe, M. Al-Falahi, H. Enshaei, N. Fernando, and A. Tashakori, "Floating power platforms for mobile cold-ironing," in *2016 IEEE 2nd Annual Southern Power Electronics Conference (SPEC)*. IEEE, 2016, pp. 1–5.

[73] S. Fang, Y. Wang, B. Gou, and Y. Xu, "Toward future green maritime transportation: An overview of seaport microgrids and all-electric ships," *IEEE Transactions on Vehicular Technology*, vol. 69, no. 1, pp. 207–219, 2019.

[74] M. M. S. Khan and M. Faruque, "Management of hybrid energy storage systems for mvdc power system of all electric ship," in *2016 North American Power Symposium (NAPS)*. IEEE, 2016, pp. 1–6.

[75] M. M. S. Khan, M. O. Faruque, and A. Newaz, "Fuzzy logic based energy storage management system for mvdc power system of all electric ship," *IEEE Transactions on Energy Conversion*, vol. 32, no. 2, pp. 798–809, 2017.

[76] B. A. Kumar, R. Selvaraj, K. Desingu, T. R. Chelliah, and R. S. Upadhyayula, "A coordinated control strategy for a diesel-electric tugboat system for improved fuel economy," *IEEE Transactions on Industry Applications*, vol. 56, no. 5, pp. 5439–5451, 2020.

[77] Z. Zhou, M. B. Camara, and B. Dakyo, "Coordinated power control of variable-speed diesel generators and lithium-battery on a hybrid electric boat," *IEEE Transactions on Vehicular Technology*, vol. 66, no. 7, pp. 5775–5784, 2016.

[78] E. De Din, H. A. B. Siddique, M. Cupelli, A. Monti, and R. W. De Doncker, "Voltage control of parallel-connected dual-active bridge converters for shipboard applications," *IEEE Journal of Emerging and Selected Topics in Power Electronics*, vol. 6, no. 2, pp. 664–673, 2017.

[79] S. Faddel, A. A. Saad, M. El Hariri, and O. A. Mohammed, "Coordination of hybrid energy storage for ship power systems with pulsed loads," *IEEE Transactions on Industry Applications*, vol. 56, no. 2, pp. 1136–1145, 2019.

[80] S. K. Mazumder, M. Tahir, and K. Acharya, "Master–slave current-sharing control of a parallel dc–dc converter system over an rf communication interface," *IEEE Transactions on Industrial Electronics*, vol. 55, no. 1, pp. 59–66, 2008.

[81] M. Kamalesh, M. Vikashini, and S. Pradeep, "Precompensated master slave control of parallel dc-dc converter in dc-microgrid," in *2018 international conference on current trends towards converging technologies (ICCTCT)*. IEEE, 2018, pp. 1–5.

[82] T.-F. Wu, Y.-K. Chen, and Y.-H. Huang, "3c strategy for inverters in parallel operation achieving an equal current distribution," *IEEE Transactions on Industrial Electronics*, vol. 47, no. 2, pp. 273–281, 2000.

[83] J. M. Guerrero, J. Matas, L. G. de Vicuna, M. Castilla, and J. Miret, "Decentralized control for parallel operation of distributed generation inverters using resistive output impedance," *IEEE Transactions on industrial electronics*, vol. 54, no. 2, pp. 994–1004, 2007.

[84] J. M. Guerrero, J. C. Vasquez, J. Matas, L. G. De Vicuña, and M. Castilla, "Hierarchical control of droop-controlled ac and dc microgrids—a general approach toward standardization," *IEEE Transactions on industrial electronics*, vol. 58, no. 1, pp. 158–172, 2010.

[85] X. Lu, K. Sun, J. M. Guerrero, J. C. Vasquez, L. Huang, and R. Teodorescu, "Soc-based droop method for distributed energy storage in dc microgrid applications," in *2012 IEEE International Symposium on Industrial Electronics*. IEEE, 2012, pp. 1640–1645.

[86] X. Lu, K. Sun, J. M. Guerrero, J. C. Vasquez, and L. Huang, "State-of-charge balance using adaptive droop control for distributed energy storage systems in dc microgrid applications," *IEEE Transactions on Industrial electronics*, vol. 61, no. 6, pp. 2804–2815, 2013.

[87] M. Nasir, Z. Jin, H. A. Khan, N. A. Zaffar, J. C. Vasquez, and J. M. Guerrero, "A decentralized control architecture applied to dc nanogrid clusters for rural electrification in developing regions," *IEEE Transactions on Power Electronics*, vol. 34, no. 2, pp. 1773–1785, 2018.

[88] F. Gao, S. Bozhko, A. Costabeber, C. Patel, P. Wheeler, C. I. Hill, and G. Asher, "Comparative stability analysis of droop control approaches in voltage-source-converter-based dc microgrids," *IEEE Transactions on Power Electronics*, vol. 32, no. 3, pp. 2395–2415, 2016.

[89] Z. Jin, L. Meng, and J. M. Guerrero, "Comparative admittance-based analysis for different droop control approaches in dc microgrids," in *2017 IEEE Second International Conference on DC Microgrids (ICDCM)*. IEEE, 2017, pp. 515–522.

[90] M. Nasir, M. Anees, H. Abbas Khan, and J. M. Guerrero, "Dual-loop control strategy applied to the cluster of multiple nanogrids for rural electrification applications," *IET Smart Grid*, vol. 2, no. 3, pp. 327–335, 2019.

[91] F. Petruzziello, P. Ziogas, and G. Joos, "A novel approach to paralleling of power converter units with true redundancy," in *21st Annual IEEE Conference on Power Electronics Specialists*. IEEE, 1990, pp. 808–813.

[92] L.-Y. Lu and C.-C. Chu, "Consensus-based droop control synthesis for multiple dics in isolated micro-grids," *IEEE Transactions on Power Systems*, vol. 30, no. 5, pp. 2243–2256, 2014.

[93] N. Salgado-Herrera, O. Anaya-Lara, D. Campos-Gaona, A. Medina-Rios, R. Tapia-Sanchez, and J. Rodriguez-Rodriguez, "Active front-end converter applied for the thd reduction in power systems," in *2018 IEEE Power & Energy Society General Meeting (PESGM)*. IEEE, 2018, pp. 1–5.

[94] G. Sulligoi, S. Castellan, M. Aizza, D. Bosich, L. Piva, and G. Lipardi, "Active front-end for shaft power generation and voltage control in fremm frigates integrated power system: Modeling and validation," in *International Symposium on Power Electronics Power Electronics, Electrical Drives, Automation and Motion*. IEEE, 2012, pp. 452–457.

[95] American Bureau of Shipping, Rules for building and classing Part 4 Vessel systems and machinery. (10.02.2021). [Online]. Available: http://www.optiloading.be/willem/assorted/rules.pdf

[96] "Ieee recommended practice for electrical installations on shipboard–design," *IEEE Std 45.1-2017*, pp. 1–198, 2017.

[97] V2G Global roadtrip: Around the world in 50 project. (10.02.2021). [Online]. Available: https://innovation.ukpowernetworks.co.uk/wp-content/uploads/2018/12/V2G-Global-Roadtrip-Around-the-World-in-50-Projects.pdf

[98] C. Gschwendtner, S. R. Sinsel, and A. Stephan, "Vehicle-to-x (v2x) implementation: An overview of predominate trial configurations and technical, social and regulatory challenges," *Renewable and Sustainable Energy Reviews*, vol. 145, p. 110977, 2021.

[99] V. Salehi, B. Mirafzal, and O. Mohammed, "Pulse-load effects on ship power system stability," in *IECON 2010-36th Annual Conference on IEEE Industrial Electronics Society*. IEEE, 2010, pp. 3353–3358.

[100] R. E. Hebner, J. D. Herbst, and A. L. Gattozzi, "Pulsed power loads support and efficiency improvement on navy ships," *Naval Engineers Journal*, vol. 122, no. 4, pp. 23–32, 2010.

[101] L. Morán, J. Espinoza, M. Ortíz, J. Rodríguez, and J. Dixon, "Practical problems associated with the operation of asds based on active front end converters in power distribution systems," in *Conference Record of the 2004 IEEE Industry Applications Conference, 2004. 39th IAS Annual Meeting.*, vol. 4. IEEE, 2004, pp. 2568–2572.

[102] J. R. Rodríguez, J. Pontt, R. Huerta, G. Alzamora, N. Becker, S. Kouro, P. Cortés, and P. Lezana, "Resonances in a high-power active-front-end rectifier system," *IEEE Transactions on industrial electronics*, vol. 52, no. 2, pp. 482–488, 2005.

[103] M. U. Mutarraf, Y. Terriche, M. Nasir, Y. Guan, C.-L. Su, J. C. Vasquez, and J. M. Guerrero, "A decentralized control scheme for adaptive power-sharing in ships based seaport microgrid." in *IECON 2020 The 46th Annual Conference of the IEEE Industrial Electronics Society*. IEEE, 2020, pp. 3126–3131.

[104] M. U. Mutarraf, Y. Terriche, M. Nasir, Y. Guan, C.-L. Su, J. C. Vasquez, and J. M. Guerrero, "A communication-less multi-mode control approach for adaptive power-sharing in ships-based seaport microgrid," *IEEE Transactions on Transportation Electrification*, 2021.

[105] T. P. Zis, "Prospects of cold ironing as an emissions reduction option," *Transportation Research Part A: Policy and Practice*, vol. 119, pp. 82–95, 2019.

[106] D. Haase and A. Maier, "Islands of the european union: State of play and future challenges," *Study for the REGI Committee, March*, 2021.

[107] Maritime transport statistics–short sea shipping of goods. Accessed: May 31, 2022. [Online]. Available: https://ec.europa.eu/eurostat/statistics-explained/index.php?title=Maritime_transport_statistics_-_short_sea_shipping_of_goods

[108] A. Christodoulou and J. Woxenius, "Sustainable short sea shipping," 2019.

Part II

Papers

Paper I

Energy Storage Systems for Shipboard Microgrids—A Review

Muhammad Umair Mutarraf, Yacine Terriche, Kamran Ali Khan Niazi, Juan C. Vasquez and Josep M. Guerrero

The paper has been published in the
Energies Vol. 11(12), 3492, 2018.

Paper II

Control of Hybrid Diesel/PV/Battery/Ultra-Capacitor Systems for Future Shipboard Microgrids

Muhammad Umair Mutarraf, Yacine Terriche, Kamran Ali Khan Niazi, Fawad Khan, Juan C. Vasquez and Josep M. Guerrero

The paper has been published in the
Energies Vol. 12(18), 3460, 2019.

Paper III

A Decentralized Control Scheme for Adaptive Power-Sharing in Ships based Seaport Microgrid.

Muhammad Umair Mutarraf, Yacine Terriche, Mashood Nasir, Yajuan Guan, Chun-Lien Su, Juan C Vasquez, and Josep M Guerrero

The paper has been published in the
IECON 2020 The 46th Annual Conference of the IEEE Industrial Electronics Society, pp. 3126-3131, 2020.

Paper IV

A Communication-less Multi-mode Control Approach for Adaptive Power-Sharing in Ships-based Seaport Microgrid

Muhammad Umair Mutarraf, Yacine Terriche, Mashood Nasir, Yajuan Guan, Chun-Lien Su, Juan C Vasquez, and Josep M Guerrero

The paper has been published in the
IEEE Transactions on Transportation Electrification Vol. 7(4), pp. 3070–3082, 2021.

Paper V

Adaptive Power Management of Hierarchical Controlled Hybrid Shipboard Microgrids

Muhammad Umair Mutarraf, Yajuan Guan, Chun-Lien Su, Yacine Terriche, Mashood Nasir, Juan C Vasquez, and Josep M. Guerrero

The paper has been published in the
IEEE Access Vol. 10, pp. 21397–21411, 2022.

Paper VI

Electric Cars, Ships, and their Charging Infrastructure – A Comprehensive Review

Muhammad Umair Mutarraf, Yajuan Guan, Luona Xu,
Chun-Lien Su, Juan C Vasquez, and Josep M. Guerrero

The paper has been published in the
Sustainable Energy Technologies and Assessments Vol. 52, 102177, 2022.

ISSN (online): 2446-1636
ISBN (online): 978-87-7573-889-2

AALBORG UNIVERSITY PRESS